VILNIUS UNIVERSITY
CENTER FOR PHYSICAL SCIENCES AND TECHNOLOGY

Aura
KISIELIŪTĖ

Scanning electrochemical microscopy for the investigation of biosensors

DOCTORAL DISSERTATION

Natural sciences,
Chemistry (N 003)

VILNIUS 2021

This dissertation was written between 2016 and 2020 in Vilnius University, Faculty of Chemistry and Geosciences. The research was supported by Research Council of Lithuania.

Academic supervisor:
Prof. habil. dr. Arūnas Ramanavičius (Vilnius University, Natural sciences, chemistry – N 003).
Academic consultant:
Dr. Inga Morkvėnaitė-Vilkončienė (Vilnius Gediminas Technical university, Technology, materials engineering – T 008).

This doctoral dissertation will be defended in a public meeting of the Dissertation Defence Panel:
Chairman − prof. habil. dr. Albertas Malinauskas (Center for Physical Sciences and Technology, Natural Sciences, chemistry – N 003).
Members:
Dr. Lina Mikoliūnaitė (Center for Physical Sciences and Technology, Natural Sciences, chemistry – N 003);
Dr. Urtė Samukaitė-Bubnienė (Center for Physical Sciences and Technology, Natural Sciences, chemistry – N 003)
Dr. Tomas Tamulevicius (Kauno Technologijos universitetas, technologijos mokslai, medžiagų inžinerija – T 008)
Dr. Vitali Syritski (Talinn University of Technology, Natural Sciences, chemistry – N 003).

The dissertation shall be defended at a public meeting of the Dissertation Defence Panel at November 26th 2021 14:00 at the Inorganic Chemistry Auditorium of the Faculty of Chemistry and Geosciences, Vilnius University. Address: Naugarduko str. 24, LT-03225, Vilnius, Lithuania, tel. (8 5) 219 3108; e-mail: info@chgf.vu.lt

The text of this dissertation can be accessed at the libraries of (Vilnius University and FTMC), as well as on the website of Vilnius University: www.vu.lt/lt/naujienos/ivykiu-kalendorius

VILNIAUS UNIVERSITETAS
FIZINIŲ IR TECHNOLOGIJOS MOKSLŲ CENTRAS

Aura
KISIELIŪTĖ

Skenuojančios elektrocheminės mikroskopijos taikymas biologinių jutiklių tyrimuose

DAKTARO DISERTACIJA

Gamtos mokslai,
Chemija (N 003)

VILNIUS 2021

LIST OF ORIGINAL PAPERS

Paper 1 A. Ramanavicius, I. Morkvenaite-Vilkonciene, A. Kisieliute, J. Petroniene, A. Ramanaviciene. Scanning electrochemical microscopy based evaluation of influence of pH on bioelectrochemical activity of yeast cells − *Saccharomyces cerevisiae,* Colloids and Surfaces B: Biointerfaces. 2017 Jan 1;149:1-6.

Paper 2 A. Kisieliute, A. Popov, R. M. Apetrei, G. Cârâc, I. Morkvenaite-Vilkonciene, A. Ramanaviciene, A. Ramanavicius, Towards microbial biofuel cells: Improvement of charge transfer by self-modification of microoganisms with conducting polymer–Polypyrrole, Chemical Engineering Journal. 2019 Jan 15;356:1014-21

Paper 3 I. Morkvenaite-Vilkonciene, A. Ramanaviciene, A. Kisieliute, V. Bucinskas, A. Ramanavicius, Scanning electrochemical microscopy in the development of enzymatic sensors and immunosensors, Biosensors and Bioelectronics. 2019 Sep 15;141:111411.

AUTHOR 'S CONTRIBUTION TO ORIGINAL PAPERS

Paper 1   Carried out the amperometric experiments, recorded the bioelectrochemical activity of yeast cells, analysed the results, designed the figures, prepared the literature review and the manuscript.

Paper 2   Carried out the SECM experiments, recorded the electrochemical activity of *A. Niger* cells, analysed the results, designed the figure, prepared the literature review and the manuscript.

Paper 3   Analysed and reviewed the research papers, prepared the literature review and manuscript

TABLE OF CONTENTS

LIST OF ABBREVIATIONS

$[Fe(CN)_6]^{3-}$ – ferricyanide ion

$[Fe(CN)_6]^{4-}$ – ferrocyanide ion

AFM – atomic force microscopy

Ag/AgCl(KCl$_{3M}$) – silver wire electrode, coated with silver chloride in 3 M KCl

AN/*A. niger* - *Aspergillus niger*

CE – counter electrode

CFE – carbon felt electrode

CV – cyclic voltammetry

DCPIP – 2,6-dichlorophenolindophenol

ECC- electrochemical cell

EDC – 1-ethyl-3-(3-dimethylaminopropyl) carbodiimide hydrochloride

FB – feedback mode

FeMeOH – ferrocene methanol

GC - generation-collection mode

GOx – glucose oxidase

GR – graphite rod electrode

HRP - horseradish peroxidase

i_{max} – maximal current value

Δi – the difference between maximum and minimum current values

KF - potassium ferricyanide/$K_3[Fe(CN)_6]$

$K_M(app.)$ – apparent Michaelis constant

MFC – microbial fuel cells

Med$_{ox}$/Med$_{red}$ – oxidized/reduced form of a redox mediator

MWCNT – multi-walled carbon nanotubes

NADH -nicotinamide adenine dinucleotide

NHS - N-hydroxysuccinimide

Ox – oxidized form

pBQ – p-benzoquinone

PBS – phosphate buffer saline

PD – 1,10-phenantroline-5,6-dione

Py - pyrrole

Ppy – polypyrrole

PQ – 9,10 phenantrenequinone

RE – reference electrode

Red – reduced form

RG - ratio between the radius of the insulating glass sheet and the metal wire

RS/*Rhizoctonia* sp.– *Rhizoctonia* species

S. cerevisiae – Saccharomyces cerevisiae

SECM – scanning electrochemical microscopy

SEM – scanning electron microscopy

SG-TC – substrate generation – tip collection

UME – ultramicroelectrode (diameter up to 25 μm)

WE – working electrode

YPD - yeast extract peptone dextrose

INTRODUCTION

Scanning electrochemical microscopy (SECM) is a technique, which enables the visualization of local electrochemical activity of various surfaces [1]. The SECM is based on electrochemical measurements registered by an ultramicroelectrode (UME), which can be positioned accurately in the x y z planes and perform area scans of a space close to the surface of interest that could contain catalytic, redox or other electrochemically active sites. In such experiments the UME is usually connected as a working electrode in an electrochemical setup, and the current, registered by a potentiostat, depends on the local concentration of the electroactive species and applied potential. The main advantage of SECM is that this technique can be applied for in situ studies without any damage to the system of interest. In addition, the SECM can be used for high-resolution imaging of local chemical reactions and topography of cells [2–4], enzymes [5,6], corroding materials [7,8].

The SECM is also a powerful tool for the investigation of surfaces modified with bio-materials, which could be applied in the design of biosensors [9], biofuel cells [10], immunoassays [11].

Electrochemical enzyme biosensors have been widely researched and are commercialy available for clinical, industrustrial, agriculture and environmental applications. They are sensitive and highly bioselective. On the other hand, microbial biosensors are more economical and can be used in toxicity or bioavailability measurements. The analyte is monitored by being a substrate or an inhibitor in the respiration and metabolic functions of the viable cell [12]. Various microbial biosensor designs are being studied to increase their potential for future employement.

Microbial fuel cells (MFC) developed as a very attractive source of electrical energy that can convert the chemical energy into an electrical current and generate electricity even from diluted solutions of biofuels by biochemical redox processes [13,14]. This advantage opens the way to apply MFC for simultaneous generation of electrical current and waste water treatment. However, the main problem of MFC efficiency still persists, due to charge transfer, therefore some researches are still aiming to develop novel techniques for the improvement of MFC performance. For example, the application of some conductive materials (e.g. carbon nanotubes, conducting polymers, etc.) and/or immobilization of cells in complex matrices can improve the charge transfer in MFC. In addition, the usage of more efficient redox mediators, which would be less toxic, and the encapsulation of cells in biocompatible electrically conducting polymer matrix could be employed to increase the stability and the efficiency of MFC.

The interest for the development of electrochemical immunoassays has recently emerged, because these methods can be successfully used as an alternative to the well-known and widely applied enzyme-linked immunosorbent assay (ELISA). In the sandwich ELISA format, the enzyme, which is present on the surface in the form of an antibody-enzyme conjugate, can be detected using the scanning electrochemical microscope. The redox and enzymatic reactions can be successfully adapted for the detection of antigens after affinity interactions with the antibodies labelled with enzymes at the localized surface areas [15,16].

The increasing attention towards electrochemical methods could be explained by the lower consumption of the chemical reagents, faster analysis, the ability to sensitively determine the analyte, and the possibility to miniaturize the electrochemical systems.

The aim of this study was to examine the different effects of varying modifications to the bioelectrochemical activity for whole cell biosensors and immune sensors by means of SECM.

The objectives of this study:

1. To investigate the electrochemical effects of redox mediators and to determine optimal parameters for chronoamperometric and SECM experiments involving whole living *Saccharomyces cerevisiae* cells in an electrochemical cell.

2. To evaluate the bioelectrochemical effects of in situ polymerized polypyrrole for *Saccharomyces cerevisiae* cells with scanning electrochemial microscopy.

3. To inspect the bioelectrochemical effects of multi-walled carbon nanotubes and pyrrole for *Saccharomyces cerevisiae* cells with cyclic voltammetry.

4. To explore the bioelectrochemical effects of in situ polymerized polypyrrole for whole living cells of *Aspergillus niger* and *Rhizoctonia* species.

5. To find optimal parameters for detecting human growth hormone in the formation of an immune sensor with glucose oxidase as a label by scanning electrochemical microscopy and to examine the formation of an immune complex with the antibodies against human growth hormone labelled with the glucose oxidase by a mathematical model.

SCIENTIFIC NOVELTY

The *in situ* microorganism-assisted polymerization with pyrrole (Py) is a new method of modification of living cells in a conductive material, which electrochemical properties have yet to be carefully examined. The microorganism-assisted formation of polypyrrole could be applied for the advancement of electrochemical performance of microbial fuel cells and/or cell-based biosensors. In this research, this type of modification was tested with living *Aspergillus niger*, *Rhizoctonia* sp. and *Saccharomyces cerevisae* cells by two electrochemical techniques: amperometric measurements of a modified electrode in the electrochemical cell (ECC) and amperometric measurements over immobilized cells with scanning electrochemical microscopy. The alteration of *S. cerevisiae* cells with polypyrrole and/or multi-walled carbon nanotubes (MWCNT) was also combined to investigate the changes in the charge transfer on a carbon felt electrode (CFE). The improved charge transfer could be used in the development of MFC and biosensor electrode design.

There is a plethora of studies examining various strategies for the development of immunoassays, one of which are the electrochemical immunoassays which can have the advantages of being faster, more economical and simpler. Our research demonstrated a viable methodology for studying the aspects of an immunoassay: labeling, immobilization, conditions for electrochemical visualization. The SECM substrate generation – tip collection (SG-TC) mode with the potassium ferricyanide (KF) as the redox mediator for the detection of human growth antigen in a non-competitive sandwich mode with the glucose oxidase (GOx) labelled human growth antibody determined qualitative and quantitative results. Developments in this area will undoubtedly further enhance the degree of sensitivity achievable in analysis.

STATEMENTS FOR DEFENSE:

1. The highest current values from the bioelectrochemical activity of *Saccharomyces cerevisiae* cells can be registered in a double redox mediator system with 9,10-phenanthrenequinone and potassium ferricyanide compared to other lipophilic redox mediators or a single redox mediator.

2. The modification of *Saccharomyces cerevisiae* cells with varying concentrations of pyrrole in the incubation solution for 24 hours can lower the electron transfer when the cells are immobilized on an insulating surface and measured with scanning electrochemical microscopy in the double redox mediator system of 9,10-phenentrenequinone and potassium ferricyanide.

3. The modification of *Saccharomyces cerevisiae* cells with multi-walled carbon nanotubes and/or pyrrole can increase the electron transfer when the cells are entrapped in a conducting carbon felt electrode and measured with cyclic voltammetry.

4. The microorganism-assisted formation of polypyrrole with the *Aspergillus niger* cells and *Rhizoctonia* species cells can increase the electron transfer when measured amperometrically.

5. The human growth antigen can be detected in a non-competitive sandwich method with the glucose oxidase labelled human growth antibody by scanning electrochemical microscopy substrate generation – tip collection mode and potassium ferricyanide as the redox mediator. The results could be evaluated quantitatively using a mathematical model

1 LITERATURE REVIEW

1.1 Scanning electrochemical microscopy

Scanning electrochemical microscopy (SECM) was introduced by Professor Allen J. Bard, who developed the technique and theory in 1989 [1]. It is a scanning probe microscopy technique like atomic force microscopy (AFM) [15] and scanning tunneling microscopy (STM) [17], which provides information about the electrochemical activity of the conducting, semi-conducting, insulating surfaces that are immersed in a solution. SECM is a powerful surface characterization technique, which allows the electrochemical profiling of the surfaces with sub-micrometer resolution [18]. By probing an immersed surface of a substrate in a solution, the concentration profiles in the diffusion layer can be registered.

The probe in SECM experiments is an ultramicroelectrode [19] positioned by the piezo-electric motors that can scan in all three x, y and z directions. The faradaic current registered at the UME near the surface characterizes the electrochemical processes in a solution. SECM similarly to AFM can measure surface topography, however it has a limited lateral resolution due to the electrode probe being bigger. Nevertheless, the resolution can be notably improved in SECM by nanoelectrodes which have diameters in nanometer dimensions [20]. Unfortunately, even then the resolution of AFM or STM cannot be achieved. Regardless, SECM has several advantages over other techniques: it can visualize the local chemical or biochemical activity of immobilized samples on a surface, ion fluxes through pores, monitor the living biological cell activity, the electrochemical modification of substrates, etc, furthermore, compared to the other microscopic techniques such as scanning electron microscopy (SEM) or fluorescence microscopy, a tedious pretreatment of the biological sample is not required, the object of interest can simply be immersed in a redox mediator solution and since the probing is a non-destructive process, the experiment can be repeated [18]. What is more, the sample under investigation can be fitted to a mathematical model and the kinetic parameters calculated. Various biological processes have been observed by the SECM: electroosmotic flow of ions through the skin [21], redox activity of cancer cells [22], photosynthetic electron transport of plant cells [23]. Lastly, SECM can be adapted to serve as a quality control tool for the biosensor fabrication.

The biological samples are not visualized directly by the SECM, rather the redox processes in which the biological samples are involved. When SECM is used to image an enzyme, which is immobilized on a surface, the

mechanism and the behavior of the enzyme's products, co-factors, substrates are imaged, not the enzyme itself. This technique gives additional information which helps to improve the understanding of the images, obtained by other probing techniques. For better research advancement, scientists have been trying to combine SECM with other techniques (e.g. AFM [24], electrochemical impedance spectroscopy [25]).

1.1.1 Set-up

The SECM device consists of several main parts: a computer, a high resolution positioning system, an electrochemical cell, an electrochemical measuring instrument (e.g. potentiostat). The electrochemical cell usually consists of a three electrode system: a working electrode (WE) which is usually the UME, a reference electrode (RE) (e.g. $Ag/AgCl(KCl_{3M})$), an auxiliary electrode (e.g. platinum wire) and a sample, which is usually immobilized (e.g. on a Petri dish) in a solution containing redox mediators and an electrolyte. At the start of an experiment, the redox mediator is usually present in one form only (reduced or oxidized). The potentiostat is used to control and set the potential of the WE and to register the current. If the electrode is polarized at a certain potential and oxidation or reduction of the redox mediator occurs, a diffusion-limited current at the UME will be detected.

The positioning system consssists of high-precision positioning elements (e.g. piezoelectric), which can be driven mechanically in three dimensions (x,y,z) at a nanometer scale. The position of the UME, scanning parameters and the data-acquisition system is controlled by the computer interface. By operating particular computer programs (e.g. SECM or NOVA), real-time data from approach curves, horizontal/array scans, cyclic voltammograms can be visualized.

1.1.2 Ultramicroelectrodes

The UME are used as probes to scan the surface of interest by SECM. They vary in shapes, materials and sizes. The tip size of an UME should be smaller than the diffusion layer in a solution containing the active species. The most popular geometries of UMEs are: disk shaped [26], cylindrical, conical, ring or band electrodes. Scientists develop ways of fabricating smaller electrode tips with also well-defined geometries for the improved lateral resolution. An UME tipically consists of a metal wire (e.g. gold, platinum) sealed in an insulating material (e.g. a glass tube). The wire is electrically connected to a

connection wire usually made out of copper at one end and the other end is open and immersed in a solution (Fig. 1). Usually the geometry of the UME is a planar disk microelectrode, which has a general expression for the radial diffusion:

$$i_{T=\infty} = 4n_eFDCr \tag{1}$$

Where n_e is the number of electrons involved in the electrode process, F is the Faraday constant (96 485 C mol^{-1}), D is the diffusion coefficient (cm^2 s^{-1}), C is the concentration of the electroactive species (mol cm^{-3}), and r is the radius of the disk-shaped electrode (cm).

The recorded signal is commonly a current from the reduction/oxidation reactions at the UME tip, but potentiometric studies can also be applied. Small concentration changes can be detected, because the UME can measure currents in the order of picoamperes (pA). Compared to macroelectrodes, UMEs are insensitive to convections and reach the steady-state quickly, after the application of a potential step. That is why, ultramicroelectrodes can be considered as steady-state systems when moving through the solution. When the UME reaches a steady-state current, it is implied that the measured current is regulated by the diffusion of the electroactive species to the electrode.

In bulk solutions, when the electrode's tip is far away from the surface, the size of the insulating sheet surrounding the active electrode area does not affect the hemispherical diffusion of the electroactive species. The size of the insulating layer becomes important only when the tip approaches the substrate within a tip radius. The insulating sheet of the electrode is usually sharpened to a pencil like shape for better sensitivity (Fig. 1). This way it is easier to approach the sample within a few microns distance. As the UME approaches the substrate surface, it becomes very sensitive to the changes in the concentration profile. The blocking of the diffusion of the electroactive species to the active area of the electrode by the insulating sheet becomes progressively important within shorter distances. The ratio of the radius of the insulating sheet to the radius of a metal wire is defined by the RG value. Values below RG 10 are very desired for the best results, due to minimal hampering effects, when the glass sheet of the electrode tip is not ideally perpendicular to the surface.

UME have several advantages in electrochemical studies: they can be used for the electrochemical measurements in non-polar solvents and high-resistance electrolytes, they can be used in the measurements of very large rate constants of the heterogenous electron transfer at the electrode/electrolyte interface, they allow measurements in a very short time scale. Due to the small

size of the electrodes, they can be used for biological system sensing (e.g. for single cells, synapses), and as probes for high-resolution imaging.
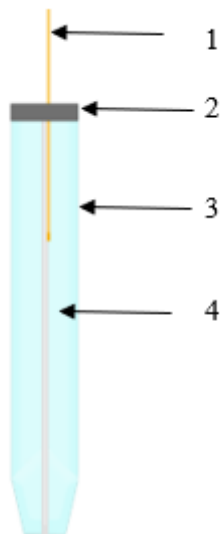
Fig.1. Schematic representation of an ultramicroelectrode: 1 – metal wire, 2 – insulating sheath, 3 – connecting wire, 4 -sealing epoxy.

1.1.3 Operation modes

The most common SECM operational modes include: positive/negative feedback mode, tip generation - substrate collection mode, and substrate generation-tip collection mode, redox competition mode. The feedback mode is the most common, because it is used to determine the tip to substrate/surface distance, to evaluate kinetic parameters, while substrate generation-tip collection mode is frequently used in the visualization of active samples (e.g. enzymes).

Feedback mode

The feedback mode can be used in a solution containing a redox mediator or without one (by measuring the concentration of dissolved oxygen). The sample under investigation and the tip of the electrode have to be immersed in a solution. Further the tip has to be set to a potential sufficient enough to oxidize/reduce an electroactive species (e.g. redox mediator, oxygen) at a diffusion-limiting rate. When the electrode is positioned far away from the surface, the current measured at the tip corresponds to the hemispherical

steady-state diffusion layer controlled by the mass transfer to the electrode. The current can be calculated by the equation 1.

As the electrode approaches a surface, the current can change in two ways (Fig. 2). If the electrode approaches an insulating surface (e.g. glass), a part of the diffusion layer will be hindered by the surface, resulting in a decrease of the current. When the tip comes in contact with the surface, the diffusion is completely blocked, and the current ideally will approach a value of 0. Due to the decrease in the steady state current, when approaching the surface of an insulator, the term - negative feedback is used [27].

The dependence of the current on the tip-to-substrate distance is called an approach curve. On the other hand, if a conductive/electrochemically active surface is approached, which was at a Nernstain potential sufficient enough to reduce M_{ox}, the redox mediator is recycled. Therefore, the tip records an increasing concentration of M_{red} as it approaches the substrate. The UME current, with the decreasing distance to the surface, would increase compared to the steady state current when the UME was far away from the surface. The flux of the M_{red} to the electrode tip is the sum of the diffusion of M_{red} from the bulk solution under physically hindered conditions also the flux of M_{red} - from the species that are regenerated at the surface. The regeneration may occure due to the interaction of the redox mediator with an oxidoreductase enzyme, the redox centre in an immobilized cell, or the electrochemical reaction at another electrode surface. The blocking of the hemispherical diffusion by the substrate takes place, but it is outweighted by the regeneration reaction. The term „positive feedback" is used to describe the increase of the UME current with the decreasing distance to a conductor [27]. The degree of feedback is notably influenced by the distance of the tip-to-sample and the ratio between the microelectrode diameter and the active area diameter - RG.
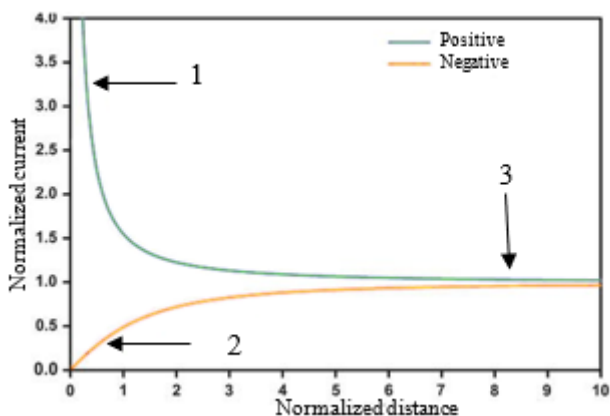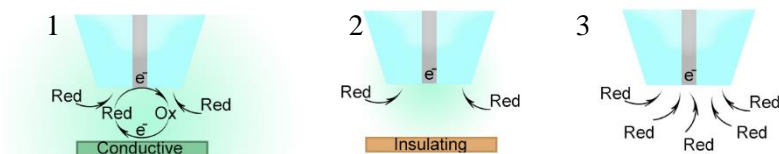
Fig. 2. Schematic representation of the feedback mode. 1 – positive feedback, 2 - negative feedback, 3 - steady state

Generation/Collection mode

The generation/collection mode at the start of the experiment contains no detectable redox species, in contrast to the feedback mode. The redox species are generated only at an active site of the sample and are collected by the electrode tip or vice versa. There are 2 types of generation/collection modes: Tip Generation - Sample Collection (TG-SC) mode and Sample Generation - Tip Collection (SG-TC) mode.

The investigation of immobilized enzymes or the activity of a living cells are the common examples of SG-TC mode, where the electrode's tip is used to collect and study the diffusion of released metabolites [26]. In this mode, the electrochemically active species are generated by the substrate and diffuse to the UME where they are detected. In an ideal SG-TC experiment, the diffusion layer of the sample would not be disturbed by the UME. Nevertheless, as the tip moves, the convection fluxes are induced, hindering the diffusion of ions to the sample. Therefore, in order to achieve a minimal disturbance to a concentration profile and a better resolution, nanometer-sized electrodes should be used [6] to avoid possible feedback problems.

TG/SC is the other type of mode, where the electrode tip generates species, which then diffuse to the sample and undergo the electrochemical reactions. This mode is generally used in studying the homogeneous reaction kinetics (e.g. decomposition studies). For example, if the tip is oxidizing species M_{red} at a certain distance from the substrate at a mass transfer rate, at the same time, the substrate electrode is poised at the reverse reduction reaction, where it is regenerating M_{red}. In the case where M_{ox} decomposes or reacts with a passive compound in the solution, the current approach curve will be influenced by the positive feedback signal from the regeneration reaction. The collection efficiency is better when the tip is in a close proximity to the sample. Therefore, all species electrogenerated at the electrode tip are collected at the

surface of the sample. The TG/SC mode is suitable for analyzing kinetics of the interfacial redox species [28].
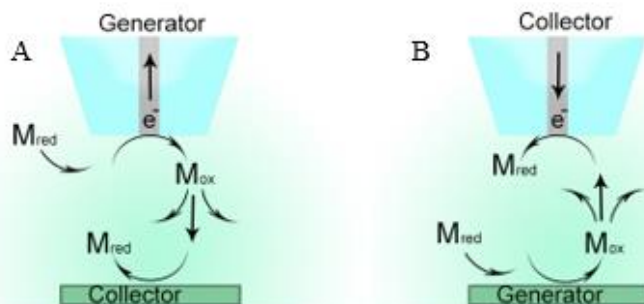
Fig. 3. A Tip generation – substrate collection mode, **B** Substrate generation – tip collection mode

Advantages/Disadvantages

A decision about the mode for studying biological systems has to be made before setting up an experiment. Usually, the negative feedback mode is applied to evaluate the distance from the tip to the surface and to localize biological samples. Limited information about the biological activity of the substrate can be achieved from these experiments.

Usually, the choice is between the generation collection (GC) mode and the positive feedback mode [29]. The electrode's probe serves as a passive sensor, which does not disturb the local concentrations in the GC measurements. However, this differs from the feedback experiments where the tip-generated species are actively involved in the surface reactions. Due to the fact that the GC mode is independent of the substrate process, it can use different selective probes (e.g. amperometric, ion-selective, enzyme-modified etc.). The GC experiments are controlled by the mass transport of the biological specimen and, unlike in the feedback experiment, they do not localize the reaction under the electrode. However, lower analyte concentrations can be detected in the GC mode, because it does not have a significant background current from the dissolved redox mediator in the solution.

On the other hand, high lateral resolution is produced in the feedback mode, due to the UME tip being the only source of the reactant. However, when using the feedback mode, some aspects are worth notice: 1) the redox mediator can affect the sample's behavior (e.g. inhibit) or it can react with the

sample product; 2) a limited sensitivity of the feedback mode due to the species, which are regenerated at the substrate must be detected against the species of the redox mediator, which is already diffusing from the bulk solution to the tip under the hindered diffusion conditions; 3) the conductive modified surfaces like gold are hard to visualize with the positive feedback mode because the surface and the immobilized sample contribute to the positive feedback signal. However, these issues can be resolved with the generation collection mode. For example, the tip of the electrode could be used only as a detector. In such a way, it would provide a high detection sensitivity (minimal background current) and would allow the visualization of the substrates immobilized on the active surface.

It is necessary to underline the importance of deciding whether image resolution or detection limits are more important while making a decision which SECM mode has to be used in the particular experiment.

Imaging of cells

Unlike other probing techniques, SECM can be used to image living samples under in vivo conditions, without tedious preparation. With the ability to examine substrates non-invasely, SECM presents itself as a unique technique for studying intracellular processes with high spatial resolution [30]. Studies show the use of the hydrophilic redox mediator with a high formal redox potential is an effective strategy to study the interactions of other redox mediators with the eukaryote cell redox processes [31–33], examine the photosynthetic in vivo activity of various leaf structures by probing the oxygen reduction concentration profiles [23]. Since then, a substantial amount of research has been made for SECM technique refinement, biological system investigation. One of the most common techniques is based on the dissolved oxygen concentration profile depletion in the medium due to respiration.

Enzyme imaging

SECM is a valuable technique in the enzymatic studies: research of the enzyme activity are performed and the catalytic rates calculated [34]. The patterning of the enzymes on surfaces and long scanning distances make the technique an attractive option for enzyme activity assays.

Feedback or the generation collection mode SECM can be used to visualize the activity of immobilized enzymes in a buffer solution. In the feedback mode, the cofactor or electron acceptor of the enzyme is replaced by a redox mediator. The redox mediator form (oxidized or reduced), which is needed to

sustain the enzymatic reaction, is maintained by applying a proper potential to the electrode's tip. When the electrode is positioned above the immobilized enzyme, the redox mediator is regenerated by the enzymatic reactions and therefore there is an increase in the current [32].

The generation collection mode has been also used for the visualization of the enzyme activity. The product of the enzymatic reaction, which is electrochemically active, can be detected at the UME tip. Several enzymes have been investigated in the GC mode of SECM [32].

1.2   Bioelectrochemistry

Bioelectrochemistry combines electrochemistry with a biological object by studying the transport of electrons/protons and redox enzyme reactions. The field of bioelectrochemistry has grown considerably in the areas of biological, environmental, medical, energy, food industry and engineering over the past century. Many scientists strive for creating cheaper, more environmentally friendlier biosensors and/or biofuel cells with higher accuracy, precision, lower limit detection, efficiency and longer shelf life. These devices are used in drug discovery, clinical diagnostics, environmental control, food and beverage analysis, energy consumption and more.

1.2.1   Biosensors

Biosensors are analytical devices incorporating a biological recognition element (such as enzymes, whole intact cells, tissue, antibodies, DNA, transport proteins or receptors) either closely connected to, or integrated within a physicochemical transducer (e.g. electrochemical, optical, thermal) [35] (Fig. 4). Biosensors in which the physicochemical transducer is an electrochemical transduction element (electrode) have been defined as electrochemical biosensors [36] The biorecognition system provides the sensor with high analyte selectivity. The classification of the electrochemical biosensors is based on the recognition system, which they contain (e.g. enzyme/microbial sensors, imunosensors), or is based on the mode of the signal transduction (amperometric, potentiometric, field effect, conductivity sensors). The most popular biosensors are the amperometric ones, which measure the current at a constant potential resulting from the electrochemical oxidation/reduction of electroactive species. The current is directly correlated to the electroactive species concentration of its production or consumption rate within the adjacent bio-catalytic layer. The biosensors usually employ

molecules that can undergo redox reactions with cellular components. These types of molecules are called redox mediators [37].

The microbial biosensors are based on microorganisms (e.g. bacteria, cells etc.) being in a close contact with a transducer that converts the biochemical signal into the electrochemical signal. The oxygen consumption by the aerobically respiring cell (fungi, bacteria, plant, animal) is a frequent technique used to monitor catabolism [38]. The amperometric microbial biosensors are used to detect the oxygen consumption by the catabolizing cells and to monitor the cellular response to a specific analyte [39]. For real-time analysis of the oxygen consumption and for a quick biochemical characterization of organisms, the oxygen probes are used to measure and to analyze the change in the oxygen concentration over a period of time [40]. Due to low solubility of the oxygen in a water this method provides a limited response range to the extracellular catabolites. However, this disadvantage can be overcome by using the artificial redox mediators. The advantage of the redox mediator is based on the fact that it can be present in the cell at much higher concentrations compared to the oxygen. This leads to the possibility for increasing the concentration of cells in the sensor and, hence, for improving the linear response [39]. The catabolism in bacteria was monitored by replacing oxygen with the redox mediators, which captured electrons from a redox molecule in the electron transport chain [41]. The oxidized redox mediators are reduced by their interaction with the reduced electron transport chain molecules. Consequently, the accumulated redox mediator can be quantified by the electrochemical methods such as amperometry, coulometry, voltammetry [42]. It was reported that the mediated electrochemical detection of the yeast cell catabolism could be achieved in a system comprising either of a single hydrophilic redox mediator [43] or a double system comprising of a hydrophilic and lipophilic redox mediator [44].

The lipophilic redox mediator is usually used because of possibility to permeate the cell's membrane and to access the intracellular redox sites. On the opposite side, the hydrophilic redox mediators can only interact with molecules that are extracellularly produced during the catabolism. For this reason, a double redox mediator system is usually applied for the eukaryotes, whereas single hydrophilic systems are used with bacterial cells, which have the electron transport chain enzymes in the cell membrane. A double redox mediator system comprising of the lipophilic and hydrophilic redox mediators enables the intracellular redox systems to be accessed. The lipophilic redox mediators can cross the cell membrane and interact with the intracellular redox systems being accessed. The lipophilic redox mediators can cross the cell membrane and interact with intracellular redox centers, become reduced and

diffuse. Otherwise they are transported out of the cell to transfer electrons to the hydrophilic reporter redox mediator. In practice, the lipophilic redox mediators usually cannot be used as the sole redox mediator because the low aqueous solubility limits the redox mediator concentration and hence the magnitude of the signal [33]. The amperometric microbial biosensors could measure a variety of compounds: alcohols [45], phenolic compounds, sugars [46].

Sample	Biorecognition	Transducer	Electronic system
• Blood/Urine/Saliva • Food • Water • Cells	• Microorganisms • Antibodies • Enzymes • DNA	• Electrochemical • Gravimetrical • Optical • Piezoelectric	• Signal amplifier • Data processing • Display
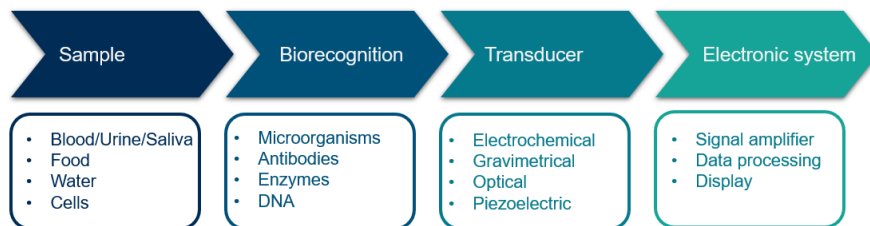
Fig. 4. Principal scheme of a biosensor

Saccharomyces cerevisiae

Saccharomyces cerevisiae (yeast) are simple eukaryotic cells that serve as a model organism for many eukaryotes (including human cells) for studying fundamental cellular processes (e.g., the cell cycle, cell division, DNA replication, recombination, and metabolism [47–49]). *S. cerevisiae* have provided researchers valuable information about individual human gene functions, which are responsible for some medical disorders e.g., cancer [50,51]. Yeast cells can be used as a model system for investigating the toxicity of compounds [52,53], which affect the cell's viability and could be evaluated using the Hill's function [54]. The cells are used for detecting a variety of compounds, including: glucose, toxicity, hormone biosensors [55–57]. Most electrochemically detectable reactions in the cells are associated to the activity of redox enzymes or oxidation related processes [39,58]. These processes occur inside the cell - cytoplasm, organelles (e.g. mitochondria) and are protected by the cell's wall. During the oxidation of organic compounds (e.g. glucose), many reduced compounds are formed (e.g. NADH, NADPH, $FADH_2$, cytochromes, quinones) in the cytosplam and mitochondria, these compounds are the potential sources of electrons. Reactions in the mitochondria generate many reduced compounds, mostly are formed in the Krebs cycle reactions. These compounds are used in various reactions as a source of electrons (reducers) for the cell. The accumulated electrons can be transmitted to the anode using electron transfer mediators and reaction kinetics can be evaluated [59–61]. A combination of lipophilic/hydrophilic redox

mediators are applied in order to establish an electron transfer from the redox enzymes inside living cells to the electrode. Hydrophilic redox mediators are soluble in the aqueous environment of the electrochemical cell but they do not cross the cell's membrane [39]. The different behaviors of three lipophilic redox mediators including 2-methyl-1,4-naphthalenedione (menadione), 2,6-dichlorophenolindo-phenol (DCPIP) and N,N,N,N-tetramethyl-p-phenylenediamine (TMPD) in probing the redox activity of the yeast cells were studied [62]. The results showed that the menadione/ferricyanide system enabled *S. cerevisiae* to switch to a nearly complete respiratory (aerobic) metabolism and with the DCPIP/ferricyanide or the TMPD/ferricyanide the yeast cells maintained anaerobic fermentation as a predominant mode. In addition, a publication showed great results with 9,10-phenentrenequinone (PQ) and potassium ferricyanide application in a double redox mediator system for SECM-based evaluations of immobilized yeast cells [59].

Aspergillus niger

Aspergillus niger is one of the most valuable microorganisms in biotechnology. It is a filamentous fungi and is used to prepare: citric acid, gluconic acid, also used for enzyme production: glucoamylase, pectinases, alpha-galactosidase in the industry [63–65]. *A. niger* is mainly used for glucose oxidase extraction for biosensor design, because of its affinity to β-D-glucose [66].

Rhizoctonia sp.

Rhizoctonia is an anamorphic saprotrophic fungus, which is composed of hyphae, sclerotia, but does not form spores [67]. It is widely studied in biology and ecology [68].

Conductive materials

For the development of charge transfer in biosensors, which use cells or enzymes, various modifications can be made: immobilization of the biorecognition object in a conductive polymer [69], modification with nanoparticles [70] or genetically modifying the cells [71]. Polypyrrole can be used in the development and modification of bioelectrochemical devices, due to possessing many valuable attributes: electrical conductivity, biocompatibility, redox and catalytic activity, it is eco-friendly, thermally

stable, and can conserve biological integrity [72]. Multi-walled carbon nanotubes (MWCNT) can also be applied for improved electrochemical detection of biomolecules [73]. They have many advantages: high stability, superior biocompatiblity, high surface energy, strong signal amplification [74].

1.2.2   Microbial Fuel Cells

Microbial fuel cells (MFC) are bioelectrochemical systems which generate an electric current by using microorganisms that convert the chemical energy of some organic compounds/inorganic materials [13,75] into an electrical current by biochemical redox processes that are involved in the metabolism of the microorganisms [76]. MFC have drawn significant attention because they can produce electric energy from organic compounds, which are mostly present in waste water and in waste generated by the food industry. The metabolic reactions of microorganisms joined with the oxidation/ reduction processes generate an electron flow from the anode towards the cathode [77] in the MFC.

 MFC have some advantages over conventional fuel cells and even over enzymatic fuel cells [10]. Firstly, for the reason that whole living microorganisms are used, which have a variety of redox enzymes acting in a cascade-manner, therefore the chemical energy of multiple substrates can be very efficiently converted into an electrical currrent. Secondly, MFC based on intact microorganisms provide optimal environmental conditions for the action of most enzymes, which are present in living cells.

In order to design highly efficient MFC, special attention should be paid to the development of both electrodes: the anode and the cathode. Both electrodes should be highly conductive, establish efficient electrical wiring with enzymatic processes that are running in microorganisms, possess good biocompatibility towards selected microorganisms, and have sufficient chemical and mechanical stability [78]. Typically, the charge transfer is the rate-limiting process during MFC operation. However, despite of numerous attempts, the most of the microbial fuel cells suffer from one significant and common disadvantage – low current density, which is mainly resulted by the complicated charge transfer between the microbial cells and the electrodes [79]. The facilitation of charge transfer from a microorganism to an electrode can significantly improve the overall performance of MFC. The main obstacle, which determines low charge transfer efficiency, is caused by the high electrical resistance of the cell walls of microorganisms [80]. Therefore, the

power output density of MFC is still too low for efficient practical applications.

Thus, in order to increase the current density, new strategies, which can reduce the electrical resistance of cell walls of microorganisms whilst preserving their biological function, should be developed. The application of some conductive materials (e.g., carbon nanotubes, conducting polymers, etc.) and/or immobilization of cells in complex matrices can improve the charge transfer in MFC. In addition, the usage of more efficient redox mediators, which would be less toxic, and the encapsulation of cells in biocompatible electrically conducting polymer matrix can be employed to increase the stability and the efficiency of MFC. MFC efficiency mostly relies on the number of charge transfer processes occurring in the chain reactions and/or charge transfer processes between the fuel and the electrode. The slowest and, therefore, the rate-limiting process in this chain is slow charge transfer through the membrane and the cell wall of microorganisms. Charge transfer from the natural metabolic redox-chain of microorganisms can be accelerated by the modulation of interactions between microorganisms, redox-redox mediators and electrodes [81]. In such cases, adaptations/ modifications of the electrode materials and structures are required to increase the efficiency of charge transfer and the uptake of substrates. One straightforward approach is to increase the population of the so-called 'exo-electrogens' on the anode. On the other hand, the charge transfer efficiency between microorganisms and the electrode can be improved by redox mediators such as ferricyanide, etc. Charge then can be transferred faster between the reaction site and the electrode through the diffusion of redox mediators, which are repeatedly cycled. Therefore, the better contact between components will enhance the efficiency of MFC. In addition, the improvement of electrical conductivity on the cell wall and the increase of the cell's surface area decreases the electron and mass transfer resistance and increases electrochemical connection between the electrode and redox processes, which are occurring in the cell.

Various methods have been developed to improve electrodes of MFC, including the modification of the surface of the conducting part of the electrode, heat treatment, nanostructure fabrication, and incorporation within nanomaterials and polymers. In this context, it was demonstrated that the modification of the anode with a conducting polymer could enhance the biocompatibility of the electrode. Furthermore, conducting polymers can increase the charge transfer to the anode improving the performance of MFC. Therefore, recently some electrodes of the MFC have been modified with polypyrrole (Ppy) [82], polyaniline [83], multi-walled carbon nanotubes [84] and some other π-π conjugated conducting materials [85]. Multiple synergistic

effects have been observed after the incorporation of cells within conducting polymer-based composite materials [86], which have improved the performance of bioelectronic devices.

The conducting polymer – polypyrrole was applied in many recent research, because it has been considered to have relatively good biocompatibility with mammalian organisms [87], living cells [88,89] and microorganisms [90]. Although it is worth to mention that by basic encapsulation of cells within a polymer film, nutrient transfer from dissolved substrates in the extracellular medium to intracellular medium can be hindered, which is resulting in a decrease of bio-catalytic activity and charge-generation efficiency. Therefore, advanced methods for synthesis of conducting polymers are required.

The recently studied in situ self-encapsulation of living cells with polypyrrole is very efficient [91], which can advance the electrochemical connection between redox processes occurring in the cell's cytoplasm and the electrode. The recent development of an in situ 'green' synthesis of conducting polymers, within the microorganism cell wall has gained researcher curiosity whether it could be applied for the advancement of bioelectrochemical properties, which are required for electrochemical devices [91]. There are some expectations that Ppy can improve the charge transfer rate through both cell's membranes and the cell wall. Moreover, Ppy is biocompatible with many types of living cells [88,89].

Therefore, the selection of biocompatible reagents and chemicals for the modification of various structures is an important issue in the development of biomedical devices [92,93]. It was determined that, in the polymerization reaction, the used pyrrole did not induce any inhibition on the growth of Streptomyces spp. and allowed innovative biocatalytic synthesis of hollow Ppy microspheres, which can be applied in the design of bio-mimetic materials and bio-electronics [94].

1.2.3   Electrochemical Immunoassays

Scanning Electrochemical Microscopy (SECM) is a well-known electrochemical technique which can be used for in situ imaging enzyme-modified surfaces without any damage to their surface [34,95,96]. The electrochemical measurements are performed in a 3D space by an ultramicroelectrode, close to a catalytic, redox or other electrochemically active surface of interest. The redox and enzymatic reactions can be successfully adapted for the detection of antigens after affinity interactions with antibodies labelled with enzymes at the localized surface areas [16]. The

most commonly used enzyme as a label in immunoassays is the horseradish peroxidase (HRP) [11,97–99]. Also, there are a few publications where alkaline phosphatase was successfully applied [100,101]. Enzymes, which are used as labels for antibodies, are eco-friendly, electrochemically detectable- by registering the substrate/product of the enzymatic reaction or various redox mediators, and enhancing the analytical signal after the immune complex formation. The determination of electrochemical activity of glucose oxidase by SECM was firstly performed in 1992 [102]. However, there is no data about the application of GOx in the development of immunoassays based on SECM. Despite the fact that GOx is very often used in the development of enzymatic glucose biosensors, to this day it has not been applied in the development of immunoassays measured by SECM.

The interest for the development of electrochemical immunoassays has recently emerged, because these methods can be successfully used as an alternative to the well-known and widely applied enzyme-linked immunosorbent assay (ELISA), where the optical density of an enzymatic reaction product is registered. In the sandwich ELISA format, the capture antibody, which is immobilised on the solid substrate, selectively interacts with the analyte and then the detection antibody, which is labelled with an enzyme, binds forming the antibody/analyte/antibody-enzyme complex on the surface. The amount of the bound antibody-enzyme conjugate can be evaluated electrochemically. The increasing attention towards electrochemical methods can be explained by the lower consumption of the chemical reagents, faster analysis, the ability to sensitively determine the analyte, and the possibility to miniaturize the electrochemical systems. Although the concept of ELISA has been reported at 1971 [103] and has made many improvements to be one of the primary analytical immunoassays in the industries of medicine, food and the environment, the electrochemical immunoassay may be developed in a way that can surpass it. In the sandwich ELISA format, the enzyme, which is present on the surface in the form of an antibody-enzyme conjugate, could be detected using the scanning electrochemical microscope.

SECM can work in different modes, however, the most sensitive and providing the least negative impact to the system of interest is the substrate generation – tip collection method (GC-SECM). In this mode, the UME can be placed at a higher distance from the surface of interest, compared to the other modes, because the reaction on the surface occurs independently of the UME presence/absence [102,104], In this mode, the redox mediator is generated by the sample to be collected by the probe. The measurement occurs while the probe is moving through the diffusion layer of the sample. For the

quantification analysis, the structures on the surface should be microscopic in order to achieve a steady state diffusion layer.

In 1995 imaging of immobilized capture antibody layers after the interaction with an antigen-alkaline phosphatase conjugate was performed amperometrically by GC-SECM by Wittstock [100]. The detecting antibody-HRP conjugates used in the sandwich immunoassay format were detected by two SECM modes: FB-SECM and GC-SECM [105]. The applicability of SECM in a dual immunoassay was also proved by Shiku and Yasukawa [11,105]. Simultaneous detection of four tumor markers by protein microarrays using a detecting antibody labelled with HRP was successfully performed using the GC-SECM [106]. Additionally, the applicability of GC-SECM for qualitative and quantitative determination of antibiotics in a direct competitive immunoassay format where the antibiotic and its labelled analogue competed for the capture antibody was showed [99] Antibody-HRP conjugates can be successfully detected using the electrochemical impedance spectroscopy combined with SECM [107]).

2   MATERIALS AND METHODS

2.1   Chemicals and materials

Phosphate buffer solution (PBS) was made by dissolving premade tablets (0.14 M NaCl, 0.0027 M KCl, and 0.01 M phosphate buffer pH 7.4) (Carl Roth (Karlsruhe, Germany)), in deionized water; Redox mediators such as 9,10-phenanthrenequinone (PQ), 1,10-phenanthroline-5,6-dione (PD), menadione (MD), p-Benzoquinone (pBQ), 2,6-dichlorophenolindophenol sodium salt hydrate (DCPIP), phenazine methosulfate (PMS) were dissolved in ethanol to yield a 5 mM concentration, potassium ferricyanide was dissolved in a phosphate buffer solution to a final concentration of 0.25 M and were applied for electrochemical studies; Poly-L-lysine 0.1% was used for cell immobilization on the surface of a Petri dish or a graphite rod (3.0 mm diameter, 150 mm length, 99.999% purity, low density); all the above mentioned materials were obtained from Sigma Aldrich (St. Luis, USA). D-(+)-Glucose (Carl Roth GmbH&Co (Karlsruhe, Germany)) was used as a fuel inducing the bioelectrochemical activity of cells and glucose oxidase, it was dissolved in PBS to a 1 M concentration and left at least 24 h before use to allow glucose to mutarotate. Ethanol, which was used for the preparation of concentrated initial solution redox mediators was purchased from Spiritus Vilnensis (Vilnius, Lithuania), and the polycarbonate membrane for the electrode preparation (Pore size 3 μm) – from Merck Millipore (Carrigtwohill, Ireland). All reagents were of high purity. All water-based solutions were prepared using deionized water, which was purified with a water purification system Adrona SIA (Riga, Latvia). All the solutions were stored in a lightproof container at 4 °C temperature.

Recombinant human growth hormone from *Escherichia coli* (hGH), monoclonal anti-human growth hormone IgG2B antibodies (m-anti-hGH) from a mouse and polyclonal anti-human growth hormone IgG antibodies (p-anti-hGH) from a goat were obtained from R&D Systems. Glucose oxidase conjugation kit–Lightning-Link® was purchased from Abcam. 1-ethyl-3-(3-dimethylaminopropyl) carbodiimide (EDC), N-hydrosuccinimide (NHS), 11-mercaptoundecanoic acid (11-MUA), were bought from Sigma Aldrich of the highest analytical quality. PBS tablets (0.14 M NaCl, 0.0027 M KCl, and 0.01 M phosphate buffer pH 7.4), sulfuric acid (H_2SO_4) and potassium chloride (KCl) were purchased from Carl Roth. Acetone and isopropyl alcohol were received from Sigma Aldrich.

2.2   Preparation of the electrochemical cell

Scanning electrochemical microscope from Sensolytics (Bochum, Germany) was used for cell experiments and a homebuilt SECM consisting of three closed-loop piezo actuators (PI HERA, P625.1CD piezos and LVPZT Amplifier E-509 C3A, Physik Instrumente, Karlsruhe, Germany) mounted on an inverted optical microscope (Eclipse TS100, Nikon, Düsseldorf, Germany) and an analogue potentiostat (µP3, M. Schramm, Heinrich Heine University of Düsseldorf, Germany). was used for immune sensor experiments. The woking electrode was the UME- a disk-shaped Pt electrode with a 25 µm diameter. The platinum wire (diameter 25 µm, purity 99.99 %) was sealed in an 85 mm length and a 2 mm diameter borosilicate glass tube; The Rg value was measured by the optical microscope and was determined to be about 10. Before the start of all the measurements, the UME was cleaned with a 95 % ethanol solution and deionized water, afterwards it was polished with polishing paper (grain size of 0.3 µm) and washed with the PBS, pH 7. The electrode's quality was evaluated by cyclic voltammetry. For the experiments including cells, a three electrode system was used with the UME as a working electrode, $Ag/AgCl(KCl_{3M})$ as a reference electrode and the platinum (Pt) wire as a counter electrode. For the immune sensor experiments, a double electrode system was used with the UME as the working electrode and the silver wire coated by AgCl was exploited as a pseudo reference electrode.

2.3   Cultivation of *Saccharomyces cerevisiae*

A wild type strain of the yeast *Saccharomyces cerevisiae* was obtained from the Center of Physical Sciences and Technology (Lithuania). The yeast cells were maintained on the agar slants containing (g L^{-1}): peptone 20, yeast extract 10, glucose 20 and agar 15, at 4 °C. The yeast cultures for the experiment were grown in 10 mL yeast extract peptone dextrose (YPD) broth in the test tubes containing 2% glucose, 2% peptone, 1% yeast extract and rotated at 150 rpm for 20-24 h at 28 °C. The cells were then harvested by the centrifugation progress at 3 g for 3 minutes and later washed three times with 0.1 M PBS, pH 7. The wet cell mass was weighed and suspended in PBS to a concentration of 0.33/0.5 g mL^{-1}.

2.4 *S. cerevisiae* cell modification with Ppy and/or MWCNT

After the *Saccharomyces cerevisiae* cells had been cultivated, a suspension of 0.5 g mL^{-1} was prepared and could be used for the modification of the cells. For the modification, a 5 mL Eppendorf tube was taken and used for the different modification solutions (Table 1). The mixtures were left in a 30°C incubator and shaken for 24 hours. Lastly, the cells were collected by centrifugation at 3 g for 3 min and washed 3 times with the PBS and a 0.5 g mL^{-1} suspension prepared.

Table 1. Solution mixtures for varying modifications of *S.cerevisiae*

Sample	PBS, μL	Y, μL	Glc, μL	KF(red), μL	Py, μL	MWCNT, μL
0.1 M Ppy	1186.16	200	400	200	13.84	0
0.30 M Ppy	1158.5	200	400	200	41.5	0
0.50 M Ppy	1130.8	200	400	200	69.2	0
0.1 mg mL^{-1} MWCNT	1360	200	400	0	0	40
0.05 mg mL^{-1} MWCNT	1180	200	400	0	0	20
(II) 1 mg mL^{-1} MWCNT + 0.3 M Py	1118.5	200	400	200	41.5	40
(I) 0.5 mg mL^{-1} MWCNT + 0.1 M Py	1138.5	200	400	200	41.5	20

2.5 *S. cerevisiae* cell immobilization on a Petri dish

The surface of the Petri dish was cleaned with an ethanol dampened cotton ball, later 0.5 μL of poly-L-lysine was placed in the center and left to dry. Afterwards 0.5 μL of yeast suspension was placed on top of the dried poly-L-lysine and also left to dry. The experiments were carried out after the cells had dried, afterwards the cells were washed three times by the buffer solution to ensure that the cells were immobilized.

2.6   *S. cerevisiae cell* immobilization on a carbon felt electrode

Firstly, the carbon felt electrode (CFE) was cut out to a diameter of 1.5 cm, then cleansed in an ethanol solution for 10 minutes in a sonicated bath, later it was cleansed in a solution of PBS and a lower percentage of ethanol for another 10 minutes. The process was repeated 6 times with the lowering concentrations of 96/80/60/40/20/0% of ethanol, each time for 10 minutes in an ultrasonic bath. This was done to remove the impurities and to clean the electrode. Later on, the damp CFE was placed in an instrument which could create a vacuum on which a suspension of 1 mL was injected, after waiting for a minute for the suspension to pass through, the vacuum was turned on so that the water from the suspension would be extracted and the yeast entrapped in the material of the CFE.

2.7   Cultivation of *Aspergillus niger* and *Rhizoctonia* sp

Aspergillus niger and *Rhizoctonia* sp. cells were provided by Microbial Cultures Collection of the Bioaliment Research Center, Faculty of Food Science and Engineering of 'Dunarea de Jos' University of Galati, Romania. Stock cultures were preserved by cryoconservation in 20% glycerol at -70°C. Cells from subcultures were activated on agar medium and inoculated into 100 mL flasks of broth containing 6% sucrose, 0.1% KH_2PO_4, 0.05% $MgSO_4$ x $7H_2O$, 0.6% $NaNO_3$, 0.05% KCl, 0.001% $FeSO_4$ x $7H_2O$ with the pH adjusted at 5. Flasks were incubated at 27ºC on an orbital shaker at 180 rpm. Due to submerged fermentation conditions, spore germination and vegetative hyphae aggregation into spherical dense agglomerates called (bio)-pellets was noticed starting with day 3 signifying that the microorganisms reached exponential growth phase. Pyrrole monomer (30 mM) was added into the culture in the 6th day of growth and kept in the same cultivation conditions for another 4 days. Subsequently, pellets were removed from growth liquid medium by centrifugation at 10 g for 10 min and washed with phosphate buffer solution (1 M, pH 9) and the procedure repeated twice.

2.8   Immobilization of *Aspergillus niger* and *Rhizoctonia* sp. pyrrole modified cells on the graphite rod electrode

A solution of 1,10-phenanthroline-5,6-dione (PD) 0.05 M was prepared in acetonitrile. Graphite rods were cut and polished by fine emery paper. The surface of the carbon electrodes was rinsed with distilled water and dried at room temperature. Afterwards a droplet of 0.05 M 4.5 μL PD was placed on

the electrode's surface (GR/PD) and left to dry. Suspensions of Py-modified *Aspergillus niger* (AN:Py) and *Rhizoctonia* sp. (RS:Py) were used for the modification of GR/PD electrodes. Approximately a 0.5 mg pellet of each suspension of cells (*A. niger* and *Rhizoctonia.* sp.) was deposited on the GR/PD surface. Afterwards, a polycarbonate membrane with a pore size of 3 μm was attached to the electrode's surface by a silicone tube to avoid cells from detaching into the solution. A silicone tube was used to seal the lateral surface of the electrode to assure an equal working surface area of cell-modified GR/PD electrodes (GR/PD/[AN:Py] and GR/PD/[RD:Py]) during electrochemical measurements.

2.9 *Aspergillus niger* cell immobilization on a Petri dish

For the immobilization of the cells, the surface of a Petri dish was cleaned with an ethanol dampened cotton ball, later a 0.5 μL droplet of poly-L-lysine was placed in the center of the Petri dish and left to dry. Afterwards a 1.5 mg pellet of *A. niger* cells was placed on top of the dried poly-L-lysine patch. After the deposited droplets of the cell pellet had dried, the Petri dish was then inverted on a 5 mL beaker with 2.5 mL of glutaraldehyde inside and left in the vapor of the glutaraldehyde to cross-link on the surface of the cells for 10 min. The specimen of cells, which were immobilized on poly-L-lysine from the bottom and with glutaraldehyde on top, was then immediately used for SECM experiments.

2.10 SECM measurements

After the ECC was prepared and the three electrodes immersed, electrochemical measurements of samples were performed using a potentiostat PGSTAT 30/Autolab from EcoChemie and software from Sensolytics. The UME was used to determine the distance to the surface of interest: the surface of a sample or an insulator. When approaching an insulating surface, negative feedback mode was used at -0.6 V vs Ag/AgCl(KCl$_{3M}$). When approaching a sample to determine the highest current value of the redox process, the GC-SECM mode was used at $+0.4$ V. The UME speed was set to 10 μm s^{-1} in z-direction when far away and 1 μm s^{-1}, when near the surface. After the surface was analyzed and the distance determined, the UME-based probe was positioned at varying distances from the surface and x-direction horizontal plane scans were performed using generation-collection mode of SECM with KF ($+0.4$ V) and

feedback mode with ferrocenemethanol (+0.45 V), the step speed was 10 $\mu m\ s^{-1}$ and the step size 5 μm.

2.11   Chronoamperometric measurements

Chronoamperometric measurements were made in an ECC while constantly stirred with the three electrode system mentioned previously. The concentration of yeast cells in the PBS was 6.7 mg mL^{-1} and the potassium ferricyanide was used as a hydrophilic redox mediator, which was transferring the charge between the UME and the second lipophilic redox mediator (PQ, MD, pBQ, PD or DCPIP, PMS). The potential was set to +0.4 V vs Ag/AgCl(KCl$_{3M}$) and the current values were recorded every second.

2.12   Amperometric measurements

The system was based on a modified graphite electrode, which served as a working electrode at a constant potential amperometry mode at +0.3 V vs Ag/AgCl(KCl$_{3M}$). All experiments were stirred in PBS, in the presence of 10 μM KF. The electrochemical evaluation of the analytical signal was performed with varying concentrations of glucose in the range of 5–300 mM.

2.13   Optical microscopy imaging

The morphological analyses of cell cultures were performed using an optical microscope (OLYMPUS BX51 (Tokyo, Japan)). Tiny 0.5 μL droplets of 100 times diluted cell suspensions were placed on glass slides, covered with glass coverslips, and placed under the microscope. The microscope was set to x400 magnification under a bright-field view and an automatic exposure.

2.14   SEM imaging

The surface morphology of *Saccharomyces cerevisiae* cells was evaluated by scanning electron microscopy (SEM) (Hitachi TM 3000, Tokyo, Japan), and the SEM imaging of *Aspergillus niger* cell cultures were performed by Helios Nanolab 650 FEI company (Eindhoven, The Netherlands). Tiny 0.5 μL droplets of 100 times diluted cell suspensions were placed on conductive carbon adhesion tapes, left to dry and placed in the vacuum chamber of the SEM and the samples analyzed.

2.15 AFM measurements

The surface roughness of modified *Saccharomyces cerevisiae* cells was evaluated by atomic force microscope (AFM) (Bioscope Catalyst (Bruker, USA)). The cells were entrapped in a polycarbonate membrane of a pore size of 3 µm and the topography images were achieved by using peak force tapping mode (0.3 Hz) in a solution.

2.16 Calculations of Michaelis-Menten kinetics

Hyperbolic dependency between amperometric signals and the glucose concentration was observed, and it was in good agreement with Michaelis-Menten kinetics. Therefore, the calculation of kinetics parameters such as the maximal current (I_{max}) and the apparent Michaelis constant (K_{Mapp}.), of $y=ax/(b+x)$, was applied where a and b parameters of the hyperbolic function correspondingly represented I_{max} and K_{Mapp}.

2.17 Labelling of p-anti-hGH antibody with glucose oxidase

Conjugation kit was used to label p-anti-hGH with GOx as stated in the instruction manual. Firstly, 1.8 µL of modifying reagent was added to a solution containing 18 µL of 0.5 µg mL^{-1} p-anti-hGH and then gently mixed by pipetting. Furthermore, 18 µl of the mixture was taken and poured over 10 µg of lyophilized GOx. The solution was gently mixed by pipetting and the container was then sealed and stored for 3 h in the dark. Lastly, 1.8 µL of a quencher reagent was added and the mixture and was kept for another 30 min. The final concentration of the p-anti-hGH-GOx conjugate was 0.3 µg L^{-1} and the solution was kept in the fridge at +4°C until further use.

2.18 Preparation of gold micro-discs on a glass slide

Glass slides were firstly cleaned by washing in acetone and isopropyl alcohol, afterwards dried at 120°C on a hotplate. The cleaned and dried slides were coated by an adhesion promoter Ti-prime and later, by spin coating, a 5 µm thin reversed image photoresistor TI35E was obtained. After the coating, a standard optical lithography procedure was executed by forming 30/50 µm diameter circles that were 0.3/1 mm distance apart. After the lithography, 15 nm chrome and 35 nm gold layers were deposited by thermal evaporation and the gold was lifted off by a procedure in the acetone. The last step

consisted of cleaning the slides with gold micro-disc structures by washing in isopropyl alcohol and deionized water.

2.19 Au-micro-disc surface preparation for hGH antibody/antigen immobilization

The glass slide with gold (Au) micro-discs was firstly cleaned with water and ethanol and then sealed in the electrochemical cell (gold side up). The ECC had a well of around $\varnothing = 5$ mm and could retain a solution of around ~200 μL. The different solutions of immobilization were poured inside of the well. The surface with Au micro-discs was cleaned again, only this time inside the ECC with methanol for 10 min and 2 min with hexane. Firstly, the self-assembling monolayer (SAM) was formed on the Au by pouring 1 mM 11-MUA methanol solution inside the ECC well and leaving it for around 18 h to form strong Au-thiolate bonds. Secondly, after the given period of time, the SAM was cleaned by lightly washing it with methanol and hexane again. The next step involved mixing 50 μL of 0.4 M EDC with 50 μL of 0.1 M NHS and pouring the mixture over the surface of 11-MUA SAM for 20 min. Afterwards, the surface was washed with 10 mM PBS, pH 7.4. The last step activated the carboxyl groups of 11-MUA SAM present on the Au micro-discs and prepared the surface for the covalent immobilization of proteins.

2.20 Immobilization of m-anti-hGH on the pre-modified gold micro-discs

For the covalent immobilization of m-anti-hGH, the steps were as follows: 50 μL of 100 nM m-anti-hGH solution was transferred onto the surface and kept for 30 min, after the interaction with the activated carboxyl groups, the solution was collected and the surface was rinsed 3 times with 10 mM PBS pH 7.4. For the deactivation of the remaining active functional groups, the modified surface was left in a 10 mM PBS, pH 7.4 solution for 1 h.

2.21 m-anti-hGH/hGH/p-anti-hGH-GOx complex formation on the pre-modified gold-discs

Firstly, the interaction of m-anti-hGH covalently immobilized on gold micro-discs with a concentration of 100 nM hGH and 50 μL was carried out for 30 min. After the rinsing of the surface by 10 mM PBS, pH 7.4 for 3 times, 50 μL of hGH 40 nM solution was introduced and left to bind specifically to

the m-anti-hGH for 30 min. Afterwards, the surface was cleaned with 10 mM PBS, pH 7.4 and left for the active groups to deactivate for 1 hour and later washed for another 3 times. Finally, a solution containing 100 nM p-anti-hGH 50 μL was poured and left for another 30 min. After rinsing 3 times with 10 mM PBS, pH 7.4, the surface with the formed m-anti-hGH/hGH/p-anti-hGH complex was ready for the analysis by SECM.

2.22 Immobilization of hGH or p-anti-hGH-GOx on the pre-modified gold micro-discs for the control experiments

For the optimization of the experiment protocol and for the confirmation of the obtained results registering m-anti-hGH/hGH/p-anti-hGH-GOx complex formation, control experiments using surfaces with covalently immobilized hGH or p-anti-hGH were performed. Subsequently, after the activation of 11-MUA functional groups on SAM, 50 μL of 40 nM hGH or 50 μL of 10/100 nM p-anti-hGH-GOx solution was poured into the ECC well and kept for 30 min, afterwards the solution was collected, the surface washed and the active groups deactivated by leaving the pre-modified surface in a 10 mM PBS, pH 7.4 solution for 1 h. Finally, the surface was rinsed with 10 mM PBS, pH 7.4 for 3 times and the ECC was prepared for the electrochemical experiments with the SECM.

2.23 Electrochemical experiments for hGH

If the electrode appeared to be adequate, SECM approach curves in negative feedback mode were registered to determine the distance to the surface. By positioning the electrode close to the active area (Au micro-disc), setting the potential to –0.3 V and observing the current signal changes, it could be concluded at which point the electrode was in closest proximity to the insulating surface of the glass. Then the electrode was retracted 5 μm in z- direction (vertical distance to the surface), positioned 50 μm from the gold micro-disc in x and y directions and the SECM was set for an array scan at +0.3 V potential vs Ag/AgCl, the scan step of 10 μm with the area of 100x100 μm in a 10 mM PBS, pH 7.4 solution with 0.1 M KCl and 5 mM KF Lastly, after the area scan was completed, several horizontal scans were performed at varying heights of 5/10/25/50 μm. After all the mentioned experiments were completed, the electrode was then polished and cleaned again and the experiments repeated with a different solution (solution containing KF with/without glucose).

2.24 Evaluation of the immune complex formation by a mathematical model

The attempt to quantify the flux of the redox species of each surface after the addition of glucose was made. Firstly, an extraction from the 3D SECM image was made of a cross-section over the active area. The resulting profile was then evaluated by fitting the mathematical model to the data: generation collection line scan over disc pore (eq. 1, 2) [108] and the concentration of $K_4[Fe(CN)_6]$ was obtained.

$$i_T = i_{offset} + 4nFD(K_4FeCN_6)r_T[K_4FeCN_6]_s\zeta \qquad (1)$$

$$\zeta = \frac{2}{\pi}arctan\left(\frac{\sqrt{2}r_s}{\sqrt{\left(\Delta x^2 + d^2 - r_s^2 - \sqrt{(\Delta x^2 + d^2 - r_s^2)^2 + 4d^2r_s^2}\right)}}\right) \qquad (2)$$

In this equation i_T is the current at a certain position, i_{offset} is the current offset, n is the number of electrons transported per redox mediator molecule to the electrode. In our case n=1 (equation 1), F is the Faraday constant 96485C, $D(K_4[Fe(CN)_6]) = 3.09 \times 10^{-6}$ cm^2/s is the diffusion constant of the redox mediator, r_T is the radius of the UME tip, $[K_4[Fe(CN)_6]]_s$ is the surface concentration of the substrate, r_s is the radius of the surface (30 µm), Δx is the position from the center, d is the distance to the surface (checked through an inverted optical microscope as well as the approaching procedures in negative feedback both to hold a value of 5 µm), ζ is a dimensionless factor describing the decrease of $K_4[Fe(CN)_6]$ concentration as a function of the lateral distance Δx and the vertical distance from the center of the disc at $(x_0, d=0)$.

Additionally, calculation of the generation rate (J) flux of the redox mediator coming from the active enzyme area (Eq 3) could be calculated [109], by assuming a uniform and consistent flux (Ω) of $K_4[Fe(CN)_6]$.

$$\Omega = 4D(K_4[Fe(CN)_6])r_s[K_4[Fe(CN)_6]] \qquad (3)$$

$$J = \frac{\Omega}{\pi r_s^2} \qquad (4)$$

3 RESULTS AND DISCUSSION

3.1 Bioelectrochemical activity of *Saccharomyces cerevisiae*

The schematic representation of a double redox mediator system, which was applied in thie amperometric measurements of *Saccharomyces cerevisiae*, is shown in Fig. 5. Redox mediators acted as electron carriers in a chain of reactions, which linked intracellular activity with the medium outside the cell, resulting in a current that was registered by the UME (Fig. 5). The lipophilic redox mediators penetrated the cell's membrane and shuttled the electrons to ferricyanide/ferrocyanide-based system from NAD^+ and $NADP^+$ dependent flavoproteins, sulfur-iron proteins, quinones, cytochromes, and some other compounds, which were participating in the metabolism-related redox processes in the cell [6]. A double redox mediator system was employed for quantitative analysis, this system was based on a lipophilic redox mediator (e.g., PQ/MD/pBQ/DCPIP/PD/PMS) and a hydrophilic redox mediator − KF, which acted as an extracellular electron acceptor [110]. This type of system could be called a 'second generation biosensor', which employed artificial redox mediators with reversible electron transfer properties and were used as freely-diffusing electron transfer shuttles [62]. The accumulated concentration of the microbially reduced redox mediator was directly proportional to the rate of metabolism. The microorganism's redox activity was intertwined with respiration via the electron transport chain therefore, by analyzing the metabolic state of the living cell, it could be used as an indication of toxicity [12,111].
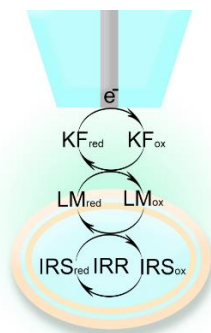

Fig. 5. The double redox mediator system with *Saccharomyces cerevisiae* cell; KF_{red}/KF_{ox} – reduced/oxidized forms of potassium ferricyanide, LM_{red}/LM_{ox} – oxidized/reduced forms of the lipophilic mediator, IRR-intracellular redox reactions, IRS_{red}/IRS_{ox} – reduced/oxidized forms of intracellular redox species, e- - electrons.

3.1.1　　Chronoamperometric measurements

Firstly, to determine the most efficient lipophilic redox mediator, the ECC was set up as described in the methods section 2.2 and the efficiency of six different compounds (PQ, MD, pBQ, DCPIP, PD, PMS) (100 μM), were compared in the presence of ferricyanide (5 mM) in PBS (Fig. 6A) (method section 2.11). These compounds were lipophilic and were able to act as intracellular redox mediators in the charge transfer chain (Fig. 5) of yeast cells (6.7 mg mL^{-1}) After 10 min of constant stirring in the ECC, the UME current at +0.4 V vs Ag/AgCl(KCl$_{3M}$), measured with PQ displayed the highest current (i_T(PQ) = 8.10 nA), when compared to the other evaluated lipophilic redox mediators. Even though, MD is used more frequently than PQ in the bioelectrochemical research papers about yeasts [62,112], the registered current was lower (i_T(MD) = 6.65 nA), with the lowest currents recorded with PD (i_T(PD) = 0.07 nA) and PMS (i_T(PMS) = 0.03 nA). For the aforementioned reasons, for our subsequent experiments, PQ was chosen as our lipophilic redox mediator as it recorded the highest currents.

Secondly, the effect of components was analyzed on the measured electrical current in the double redox mediator system after 10 min of incubation in the ECC (Fig. 6B). In the presence of *Saccharomyces cerevisiae* (6.7 mg mL^{-1}) and potassium ferricyanide (5 mM) (i_T(KF) = 0.20 nA), even with the addition of glucose (10 mM) (i_T(KF+Glc) = 0.21 nA) the solutions displayed the weakest UME signal. This confirms that if potassium ferricyanide is used as a redox mediator it is not very efficient by itself, since it cannot cross the cell's membrane. Later the double redox mediator system was tested out, the simultaneous application of two redox mediators − KF (5 mM) and PQ (100 μM). Two redox mediators with different properties enabled to register an increased (about x15) current by the UME (i_T(KF+PQ) = 3.53 nA), even if no glucose was added to the solution, the cells were active and therefore could transfer the charge towards the UME. What is more, by adding 10 mM of glucose to the above-mentioned system, the UME current significantly increased (i_T(KF+PQ+Glc) = 6.61 nA). It was evident that in order to achieve higher currents, a double redox mediator system was necessary with the addition of glucose.
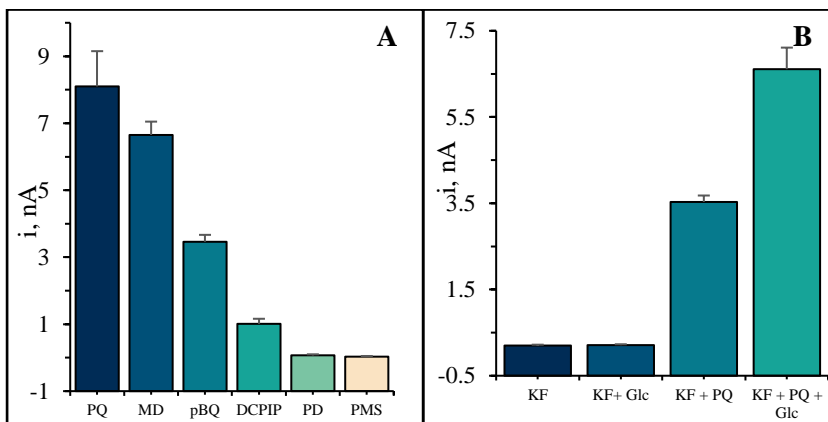
Fig. 6. A Current dependency on varying lipophilic redox mediators; **B** Current dependency on varying solution compositions.

Thirdly, an investigation was conducted to link the increases in the electrical signal to the presence of yeast cells. In order to achieve that, two chronoamperograms were registered with the subsequent additions of reagents (Table 2) (Fig 3A). A solution of PBS was firstly stirred in an ECC and after one minute of reaching the steady state, the *S. cerevisiae* cells were added ($i_T(Y) = 0.38$ nA), control experiments were also made without the cells ($i_T(-) = 0.13$ nA). Afterwards, KF was injected into the ECC, nevertheless there was almost no difference in the current ($i_T(Y+KF) = 0.39$ nA) ($i_T(KF) = 0.12$ nA). After another 60 seconds, PQ was introduced into the solution and the current had increased significantly and continued to rise slowly in the solution with *S. cerevisiae* ($i_T(Y+KF+PQ) = 1.07$ nA), whereas in the control experiments, the current remaines the same ($i_T(KF+PQ) = 0.12$ nA). At the fourth minute glucose was added and later on, the current rose a lot faster and at the 10th minute had reached $i_T(Y+KF+PQ+Glc) = 4.59$ nA, compared to $i_T(KF+PQ+Glc) = 0.26$ nA in the control experiments.

Lastly, a similar test was fabricated to find out the bioelectrochemical activity of the *S. cerevisiae* in a 2-hour time period. The concentrations were the same as in the previous experiments, and the reagent additions were carried out in a similar manner as in table 2. From the chronoamperogram (Fig. 7A) a semi-steady state was reached at around the 15th minute. After approximately 30 minutes, the electrical signal started to decline gradually, unless glucose was additionally added.

Table 2 Injection time of the varying reagents into the ECC

t,s	Solution	Final concentration in the electrochemical cell
0	PBS	0.1 M
60	Y	6.7 mg 10 mL^{-1} (none in the control)
120	KF	5 mM
180	PQ	100 µM
240	Glc	10 mM
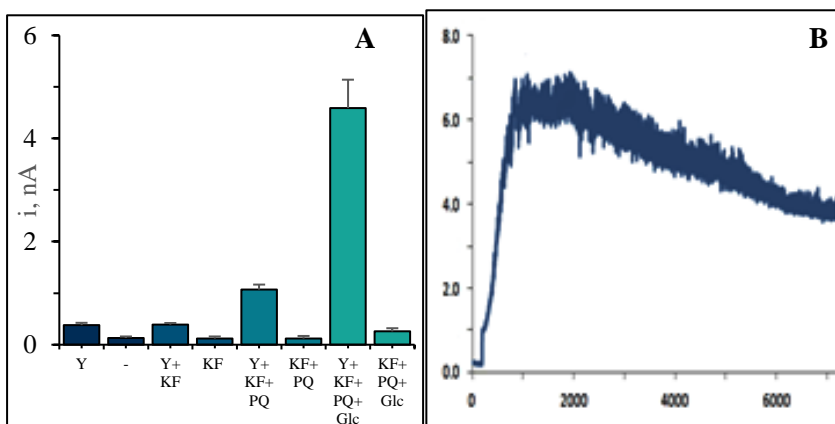
Fig. 7. A Current dependency on the addition of various reagents to the electrochemical cell. **B** Chronoamperogram of *S. cerevisiae* bioelectrochemical activity

From these chronoamperometric measurements a conclusion was made that the simultaneous application of two redox mediators – Potassium ferricyanide and 9,10- Phenanthrenequinone with the addition of glucose in the PBS, recorded the highest current values for *Saccharomyces cerevisiae* cells.

3.1.2   SECM measurements

For our latter experiments, SECM was used with the purpose of evaluating the metabolic activity of immobilized *S. cerevisiae* cells, since the influence of different parameters in our previous amperometric measurements was investigated (Fig.6-7). The cells were immobilized as described in the method section 2.5. After the immobilization was completed, the buffer solution was poured in the ECC and the three-electrodes for the experiments with SECM

were immersed. Firstly, an approach curve (z-direction) was registered in order to evaluate the distance to the surface of the cells (Fig. 8A) (method section 2.10). The measured UME oxidation current at +0.4 V was related to the concentration of potassium ferrocyanide due to the cell's metabolic activity and the distance to the cells. As the approach to the surface of the *S. cerevisiae* was made, the electrical current increased, until the maximum of about $i_T(0) = 3$ nA was reached and further advance towards the surface would risk contaminating the electrode as it would be in contact with the cells. From the position where the maximum current was reached, the electrode was retracted by 20 μm and scanned horizontally over the immobilized area. The same was repeated with the distances from the surface at 50 and 100 μm (Fig. 8B). As it was anticipated, the further from the surface - the lower the current values and the higher the background current values ($\Delta i(20) = 0.13$ nA, $\Delta i(50) = 0.12$ nA, $\Delta i(100) = 0.10$ nA). At the distance of 20 μm the metabolic activity was the most prominent, the registered electrical currents were high, and there was almost no probability to contaminate the electrode's tip. Thus, for further research, a distance of 20 μm was chosen as it was found that this distance proved to be optimal for SECM investigations over immobilized cell surfaces.
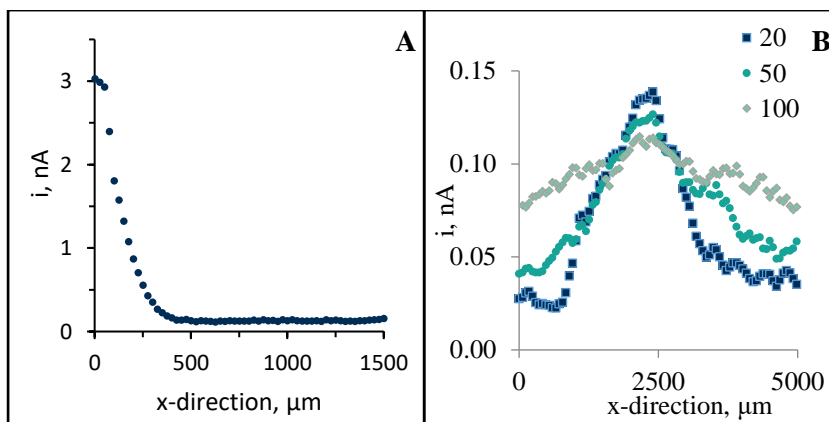

Fig. 8. A The approach curve of the UME to the surface of the immobilized *S. cerevisiae* in the GC mode of SECM; **B** Horizontal scans over the immobilized *S. cerevisiae* at varying heights of 20/50/100 μm.

Next, a sample for visualizing the metabolic activity of *S. cerevisiae* in an array scan was prepared. Firstly, an approach curve to the surface of the cells was registered and later, the horizontal scan in order to position the sample in the center was recorded (Fig. 9A). Lastly, an area scan over the

surface of the immobilized yeast cells was recorded. A specific map of yeast metabolic activity is presented in Figure 9B. From this graph, the localization of the immobilized yeast cells could be determined and the electrochemical activity map could be derived. It was determined that over the immobilized *S. cerevisiae* cells at a 20 µm distance, the current was $\Delta i = 0.41$ nA.
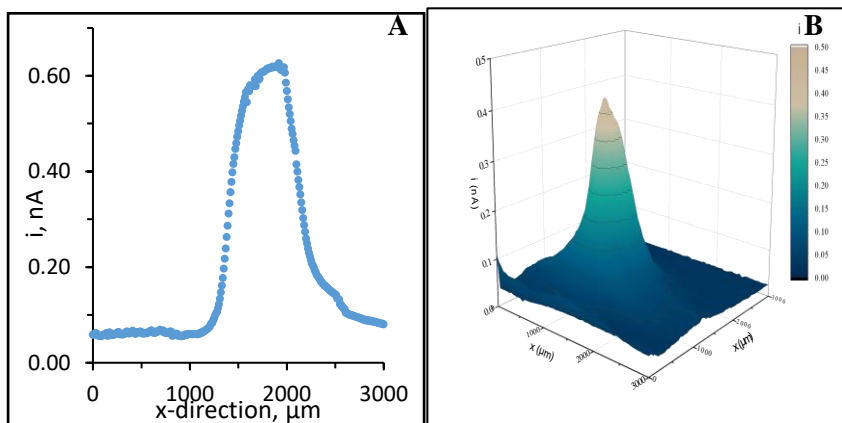

Fig. 9. A horizontal scan at the x-direction over the immobilized yeast cells; **B** Array scan over the immobilized yeast cells.

3.2 Modification of *Saccharomyces cerevisiae* cells with polypyrrole and/or carbon nanotubes

In order to improve bioelectrochemical devices for biosensors and/or MFC, a new modification technique for cell electron transfer was experimented. The polymerization of pyrrole and/or multi-walled carbon nanotubes were used for experiments with the *Saccharomyces cerevisiae* cells. Due to the polymer and the nanotubes being electrically conductive, it was relevant to examine whether they influence the electron flux towards the electrode.

The one-step *in situ* environmentally friendly method was reported recently in literature [91,113,114] addressing many concerns and having preferred parameters (e.g. electrical onductivity, biocompatibility), however it required further investigation for applications to the anode in biosensors or MFC.

The carbon nanotubes (CNT) were also used for the modification of the cells. The multi-walled carbon nanotubes facilitate electron transfer and exhibit lower cytotoxicity than single-walled carbon nanotubes [90,115], thus being an object of interest for bioelectrochemical systems. The MWCNT or other conductive nano-particles together with conductive polymers could be

48

applied for modification of the electrode's surface [116], cell modification or cell/enzyme incorporation into a conductive matrix [117,118]. Thus, the electrochemical impact of the modification with polypyrrole and/or MWCNT would have on our system was analyzed.

The biochemical in situ (oxidative polymerization) method was used for the polymerization of the pyrrole (method section 2.4). The polymerization reaction was catalyzed with $K_3[Fe(CN)_6]$, which formed from the *Saccharomyces cerevisiae* cell plasma membrane oxido-reductases or other oxidative (high positive redox potential) compounds that oxidized the initial $K_4[Fe(CN)_6]$ in the medium. The polymer affected the cell differently: the inner membrane structure was destabilized due to the polymer, however, the outer β-glucan layer bonded with the polymer, and the overall layer stiffness increased [114] (Fig. 10).
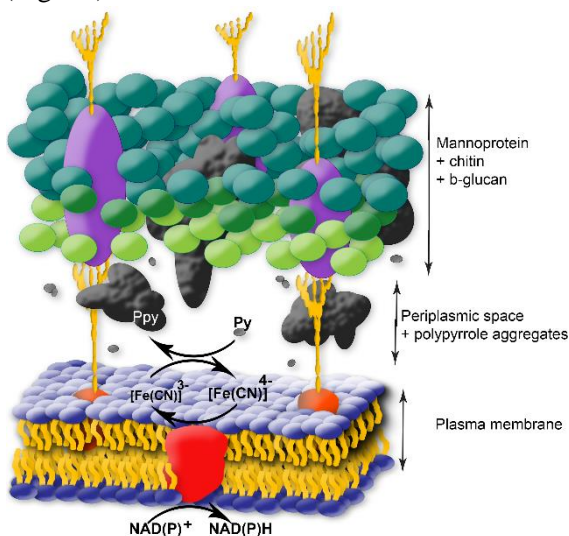

Fig. 10. The bioelectrochemical polymerization of pyrrole inside the *Saccharomyces cerevisiae* cell's wall.

3.2.1   Imaging of the polypyrrole modified cells

To visualize the differences between the Py modified cells and the unmodified yeast cells, which were used as a control, some optical microscope images were made (Fig. 11) (method section 2.13). In the micrographs the control group was mostly uniform in shape and almost transparent (Fig. 8A). The other group - the Py modified cells, however, were very distinguishable: the cell wall was darker with some clusters of polypyrrole in between the cells (Fig. 11B). The optical microscope was a decent tool for distinguishing the

two cell groups, also by visualizing that the Ppy formed mostly around the cells, increased the thickness of the cell's wall and formed a few agglomerates in the extracellular medium. However, for a more detailed evaluation of the modification effects, SEM and AFM were used.
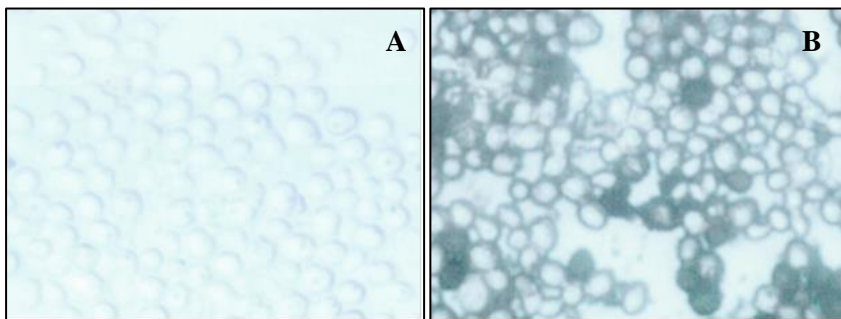

Fig. 11. Optical microscope micrograph of *Saccharomyces cerevisiae* cells **A** control group; **B** 0.3 M Py modified cell group.

In order to obtain more data about the polypyrrole modification, atomic force microscopy was applied, as it provided more insight about the physical properties, e.g. surface roughness and a higher resolution of the images (method section 2.15). 4 types of varying cell modifications: 0.05/0.1/0.3/0.5 M Py also a control group were chosen to see the differences in the morphology of the cell wall. For the AFM measurements polycarbonate membranes containing small pores for cell entrapment were used, so the cells would not move throughout the scanning process. The polymerization formed polypyrrole agglomerates which varied in size, shape and their placement was disordered when compared to the control cells which were flat and smooth (Fig. 12). The roughness of the modified cell surface was calculated using the AFM data for all the cell types for additional information. The data is provided in Table 3: R_q is the root mean square average of height deviation taken from the mean image data plane, R_a is the arithmetic average of the absolute values of the surface height deviations measured from the mean plane and the maximum roughness depth, (R_{max}) is the largest single roughness depth within the evaluation length. From the results in Table 3 an observation was made that the roughness of the 0.05/0.1 M Py ($R_a(0.05) = 0.21$, $R_a(0.1) = 0.22$) cell group was lower than the control cell group ($R_a(0M) = 0.48$). On the other hand, the cells which were modified with higher polypyrrole concentrations had a greater surface roughness: the 0.3 M Py cell group had $R_a(0.3) = 0.70$ surface roughness and for the 0.5 M Py cell group – around 3 times bigger values ($R_a(0.5) = 1.19$).
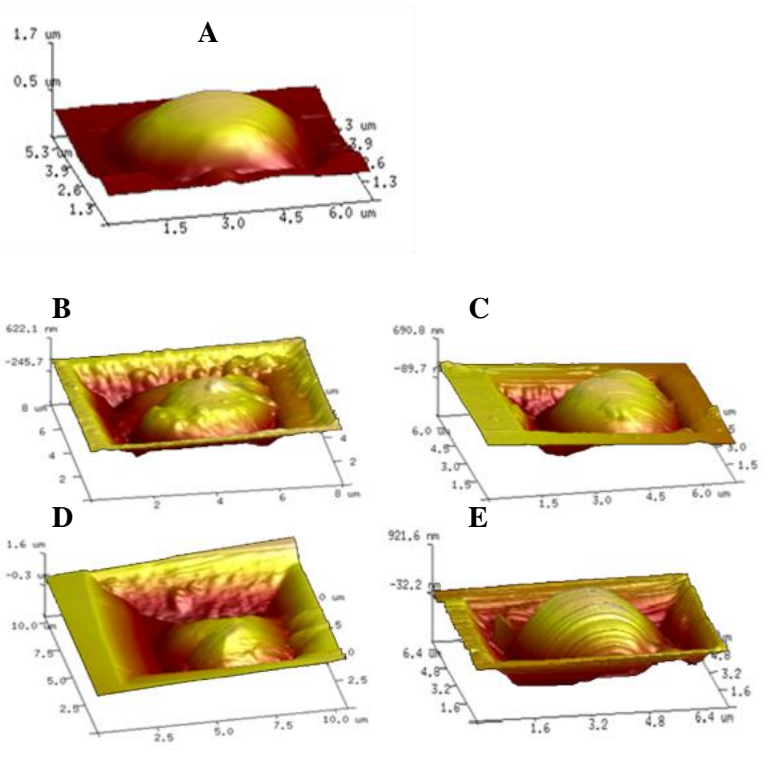
Fig. 12. AFM micrographs of *Saccharomyces cerevisae* cells **A** control **B** 0.05 M Py **C** 0.1 M Py **D** 0.3 M Py **E** 0.5 M Py.

Table 3 Surface roughness values dependence on pyrrole concentration, obtained from the AFM images

	0 M	0.05 M	0.1 M	0.3 M	0.5 M
R_q	0.56	0.27	0.31	0.93	1.50
R_a	0.48	0.21	0.22	0.70	1.19
R_{max}	1.76	2.62	8.15	24.2	13.0

It was determined that the more pyrrole was in the incubation solution, the higher the chance that it would form larger and denser polymer structures. The R_{max} value increased with the concentration of pyrrole, the cells may have become more rigid as the polymer affectes the cell's wall structure and stiffness.

3.2.2 SECM measurements of the polypyrrole modified cells

Later on, the UME current dependencies of the modified *Saccharomyces cerevisiae* on the pyrrole incubation solution that had varied in concentrations were studied (Fig. 13A). This was achieved by approaching the immobilized yeast surface with the generation-collection mode of the SECM. As the concentration of the Py incubated solution increased, the current signals decreased. The cells, incubated at a pyrrole concentration of 0.1 M produced only half of the current signal ($i_T(0.1) = 0.17$ nA) compared to the control group ($i_T(C) = 0.3$ nA), with the 0.3 M py $i_T(0.3) = 0.12$ nA current was measured, and $i_T(0.5) = 0.4$ nA current with the 0.5 M Py modified group. At the second step of the investigation, the horizontal scans were made over the cells to evaluate the differences by SECM. Just like in the previous measurements, the cell viability dropped accordingly to the increasing pyrrole concentration in the incubation medium (Fig. 13B).

The UME over the control group registered a current almost 25% higher ($\Delta i(C) = 0.19$ nA) than the 0.1 M Py modified cell group ($\Delta i(0.1) = 0.15$ nA), 3 times bigger than the 0.03 M Py group ($\Delta i(0.3) = 0.06$ nA) and almost 10 times larger than the 0.5 M Ppy group ($\Delta i(0.5) = 0.02$ nA). The Py seemed to affect the cell's viability, probably by disrupting the transfer of compounds or nutrients through the cell's wall [91] .
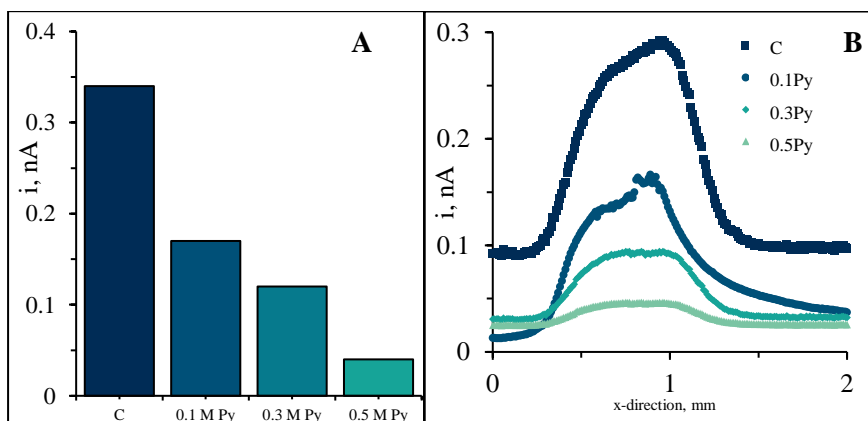

Fig. 13. Current dependence on the pretreated cells by incubating in varying pyrrole solutions, registered by **A** approaching the immobilized modified yeast surface at the GC SECM; **B** recording horizontal scans over the immobilized yeast cell groups.

3.2.3 Imaging of the *Saccharomyces cerevisiae* cells modified with polypyrrole and multi-walled carbon nanotubes

The pretreatment of cells was altered by incubating them not just in a pyrrole solution, but also with MWCNT (method section 2.4). The MWCNT did not penetrate the cell's wall, rather they attached to their surface electrostatically, by van der Waals and hydrophobic interactions. MWCNT are somewhat cytotoxic [119], however, in low concentrations, the cells remain viable. The charge transfer was expected to enhance with the MWCNT by serving as a link between the electrode and the cells modified with Py, potentially eliminating the need for a hydrophilic redox mediator. For this reason, different types of modification solutions were tested in which the cells were incubated. From the photographs taken via a camera, the difference in color of the incubation solution and the cells after centrifugation the following day of incubation was detected (Fig 14). Pyrrole is a colorless substance, however, when it polymerizes – it becomes green in low (0.1 M) and dark in high (0.5 M) concentrations. If the carbon nanotubes are added, the suspension becomes almost black (0.5 and 1 mg 10 mL^{-1}). After centrifugation, the polypyrrole modified cells looked uniformly darkened regardless of the concentration, however, the cells with the MWCNT had formed black conglomerates.
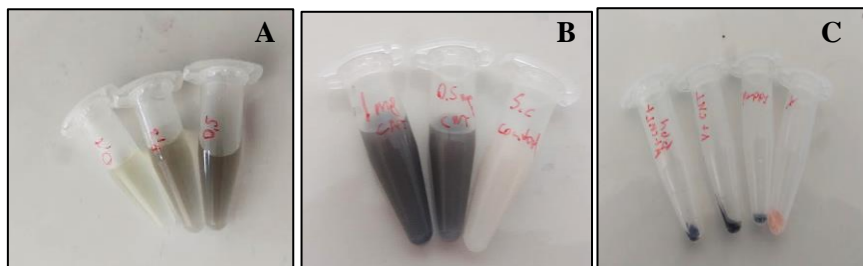

Fig. 14. Pictures of varying suspensions for cell modifications after 24 hours **A** 0.1/0.3/0.5 M pyrrole; **B** 0/0.5/1 mg 10 mL^{-1} MWCNT; **C** after centrifugation of the modified cells with the MWCNT and Ppy.

For better evaluation, the cells were examined using the scanning electron microscope (method section 2.14) From the SEM micrographs (Fig. 15), no significant difference was seen between A, B, and C: the cells looked deflated (this was due to the cells being dry and placed in a vacuum). However, in Figure 15C the cells retained their shape as a result of the formed polypyrrole inside the cell's wall. By visual analysis, it was determined that the

modification with 0.3 M Py changes the morphology of the cell in a way that the cell's wall becomes more rigid, though 0.05 M Ppy was insufficient to reach the stability of the cell wall. The MWCNT modified cell group displayed almost no significant differences compared to the control group, since the nanotubes on the cell's surface were not visible in this magnification and they did not alter the cell's mechanical properties.
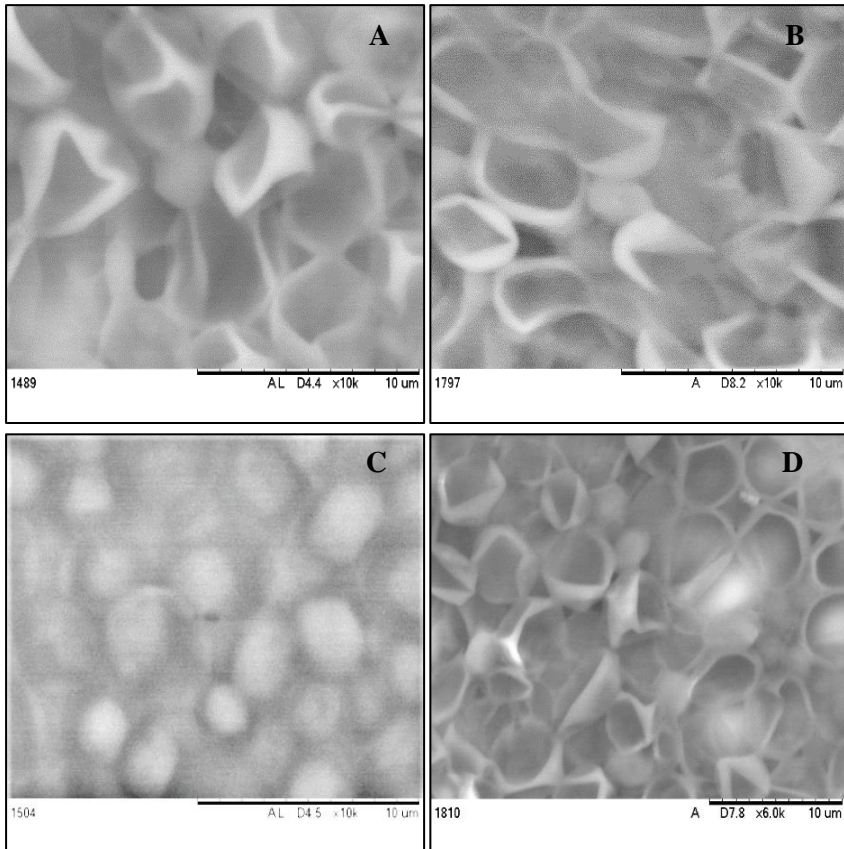

Fig. 15. SEM micrographs of **A** the control *Saccharomyces cerevisiae* cell group; **B** the modified cell group with 0.05 M pyrrole; **C** the modified cell group with 0.3 M of pyrrole; **D** the modified cell group with MWCNT 1 mg 10 mL^{-1}.

3.2.4 Cyclic Voltammetry with the carbon felt electrode and the *Saccharomyces cerevisiae* cells modified with the polypyrrole and multi-walled carbon nanotubes

For further investigation, the cells were entrapped in the carbon felt electrically conductive electrode, in the hopes of a favorable charge transfer connection to the electrode. The cells were entrapped between the mesh (method section 2.6), therefore no additional substances were needed to immobilize them. The ECC included a three-electrode system with the CFE ⌀= 1.5 cm, pierced through with a steel rod as the working electrode, a Calomel electrode as the reference electrode, and a steel wire as the counter electrode. Cyclic voltammograms were registered with 5 mV s^{-1} speed. The setup was used to compare the different effects of the incubation solutions and to test the new immobilization technique. Cyclic Voltammetry was used to better perceive the redox processes occurring in the ECC. The different reagents were introduced one by one into the phosphate buffer saline solution (firstly 40 uM PQ, secondly - 10 mM Glc, lastly- 2,5 mM KF). This sequence was chosen to compare the redox mediator systems Figures 16-19A - single lipophilic (PQ) redox mediator system, Figures 16-19B with the double redox mediator system PQ and KF. The cyclic voltammetry curves were scanned 3 times after the addition of a compound and the last cycle is shown in the diagrams.

First of all, a comparison was made about the polypyrrole's influence on the system by varying its concentrations from 0.1 to 0.3 M Py (Fig.16A, B). There was almost no difference between the groups in the solution containing one lipophilic redox mediator: they both showed a low profile i_T <0.02 mA (Fig. 16A). On the other hand, when KF was added to the solution (Fig. 16B), the shape of the cyclic voltammetry curve changed drastically: the 0.3 Py modification group had an oxidative peak at around 0.22 V with the current rising to $i_T(0.3) = 1,62$ mA and the 0.1 M Py modified cell group recorded an oxidative peak at around 0.47 V with $i_T(0.1) = 0.75$ mA. This was a promising outcome, because earlier experiments with the SECM and chronoamperometry suggested that the modification reduces the charge transfer, yet by entrapping the cells in a conductive material, the modification with pyrrole demonstrated a better charge transfer by increasing the pyrrole concentration in the incubation medium.
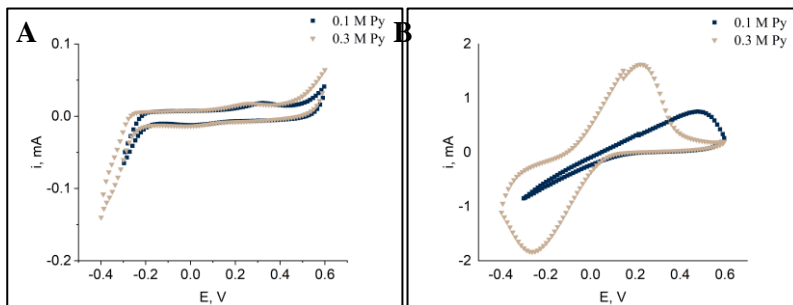
Fig. 16. Cyclic voltammetry curves of cells modified with 0.1/0.3 M Polypyrrole **A** in a solution of PQ and Glc; **B** in a solution of PQ, Glc, KF.

Secondly, the same setups were tested out with the 0.5 and 1 mg 10 mL^{-1} of MWCNT modified cell groups (Fig. 17). From the graphs it could be seen, that the solution with only the lipophilic redox mediator also did not show any differences between the two cell groups (Fig. 17A). The shape of the cyclic voltammetry curve illustrates that the surface of the electrode increased, this was due to the attached MWCNT on the cell's surface, increasing the cumulative surface area of the electrode. Other than that, the graph did not display any oxidative response due to the metabolic activity of yeast in the -0.4 – 0.6 V potential range (the current was around 0.06 mA). But as soon as potassium ferricyanide was added (Fig. 17B), the oxidation peak of KF appeared at 0.24 V with $i_T(0.5) = 1.85$ mA and $i_T(1) = 1.2$ mA for the modified cells with 0.5 mg 10 mL^{-1} and 1 mg 10 mL^{-1} of MWCNT respectively.
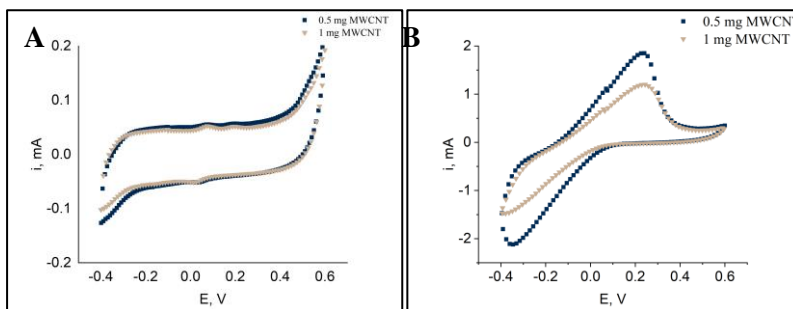
Fig. 17. Cyclic voltammetry curves of cells modified with 0.5/1 mg 10 mL^{-1} MWCNT; **A** in a solution of PQ and Glc; **B** in a solution of PQ, Glc, KF.

For our third type of cell modification, incubation with Py and MWCNT with varying concentrations (Table 1) was assessed. I incubation solution contained 0.5 mg 10 mL^{-1} MWCNT and 0.1 M Ppy while II contained 1 mg 10 mL^{-1} MWCNT and 0.3 M Py (Fig. 18). The redox processes were

visible with just the lipophilic redox mediator (Fig. 18A) in the ECC with an oxidative peak registered at about 0.24 V with $i_T(I) = 0.10$ mA for the I cell modification type and $i_T(II) = 0.13$ mA for the II cell type. As for the solution that contained the double redox mediator system (Fig. 18B), the oxidation peak was at around 0.25 V $i_T(I) = 0.91$ mA for the (I) cell modification type and $i_T(II) = 0.46$ mA for the (II) cell group.
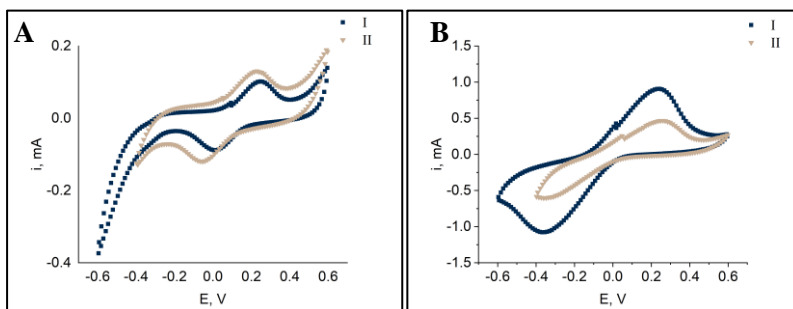

Fig. 18. Cyclic voltammetry curves of cells modified with I and II incubation solutions; **A** in a solution of PQ and Glc; **B** in a solution of PQ, Glc, KF.

Lastly, for the comparison between the modification types, the cell groups that registered the highest oxidation peaks were chosen, because they exhibited the best metabolic activity. In Figure 19A the single redox mediator – PQ containing graphs were depicted and from these results, the variance between the bioelectrochemical activity was visualized: the cell group which was modified with the I solution stood out the most. In the potential range of –0.4 - 0.6 V this type of cell group had a distinguished oxidation peak at 0.24 V $i_T(I) = 0.10$ mA. This may have been caused by a conductive chain formed where it shuttled the electrons from PQ to the Ppy aggregates and later to the MWCNT and from them - to the CFE. Because neither the Ppy nor the MWCNT exhibited the same effect when incubated separately. Also, these results are consistent between the varying concentrations of I and II cell groups (Fig. 18A). In contrast, in Figure 19B – the double redox mediator system comprising of PQ and KF demonstrated the best results with the modification with 0.5 mg mL^{-1} MWCNT ($i_T(0.5) = 1.85$ mA) compared to 0.3 M Py ($i_T(0.3) = 1.62$ mA) and $i_T(I) = 0.91$ mA for the I cell group. Also worth mentioning, that the oxidative peaks were mostly identical at around 0.25 V with the exception of the control group.
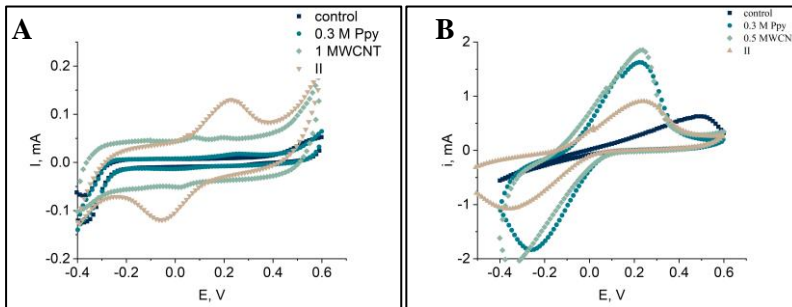
Fig. 19. Cyclic voltammetry curves of different modified cell groups; **A** in a solution of PQ and Glc; **B** in a solution of PQ, Glc, KF.

The results from Figure 19 confirmed that the electron transfer occurs several times better using the double redox mediator system, when compared to the single redox mediator system. The addition of KF to the I modification group, increased the i_T 9 times (from 0.10 mA to 0.91 mA). The highest current value $i_{max} = 1.85$ mA of the double redox mediator system was observed with the 0.5 mg mL^{-1} MWCNT cell group and was about 30 times lower than using only the lipophilic redox mediator. So even though a hypothesis was made that a charge transfer between the Ppy and the MWCNT was observed, the electrical currents were several times lower compared to the double redox mediator system and the cells, modified with just polypyrrole or just the MWCNT. In addition, the polypyrrole-modified cells displayed one of the highest current values in the double redox mediator system, that is why for our next step, it was decided to further develop and examine modifications using the polypyrrole.

3.3 *Aspergillus niger* and *Rhizoctonia* sp. modifications with the polypyrrole

For the next set of experiments different types of cells – *Aspergillus niger* and *Rhizoctonia* sp. were chosen and modified with polypyrrole (Fig. 20). The encapsulation of the fungi cells was accomplished at the Center for Physical Sciences and Technology located inVilnius by a colleague from Romania and given for further electrochemical evaluation [90]. The fungi strains *A. niger* and *Rhizoctonia* sp. were selected due to their ability to produce oxidoreductases, which can initiate the oxidative synthesis of polypyrrole from pyrrole monomers [120]. *Aspergillus niger* (AN) is a type of filamentous fungi, widely researched for intracellular glucose oxidase production [121], while Rizhoctonia sp. (RS) has been characterized as a good producer of extracellular β- fructofuranosidase [122] as well as phenoloxidases such as

laccase [123]. Thus, a comparison between the two diverse types of cells strains was performed to evaluate their electron transfer after the polymerization of pyrrole within the cell culture at standard submerged cell cultivation conditions.

Previously, the research group had studied cell modification upon pyrrole addition in filamentous bacteria cultures during submerged fermentation (SmF) [94] (method section 2.7). The conditions applied for *Aspergillus niger* and *Rhizoctonia* sp. cell modification with Py were similar: the monomer was added during the 6th day of submerged cultivation and within 48 h the formation of Ppy became clearly visible due to the darkening of the culture media. But some aspects of the behavior of two different cultures after pyrrole addition during submerged fermentation differed. It was common that submerged cultures of fungi lead to a formation of three-dimensional structures, which tended to rearrange into mycelium-based macroscopic pellets. The formation of such pellets was thoroughly investigated for filamentous fungi of *Aspergillus niger* [124] being affected by aggregation of vegetative hyphae, dependent on a multitude of factors (available nutrients, pH, inoculum concentration, volume of culture medium etc.). Nonetheless, the production of various enzymes and metabolites proved to be dependent on the morphological forms attained by cultivation, mycelial conglomerates being characterized by specific metabolic activities [125,126]. Both culture mediums were placed in the pellet-containing environment, which became visibly darker after the incubation in pyrrole-containing solution. However, polypyrrole formation was more efficient in *Aspergillus niger* culture rather than in *Rhizoctonia* sp. culture containing solution.

3.3.1 Imaging of *Aspergilus niger* cells modified with polypyrrole

One of the main aims was to illustrate the improvement in the electrochemical performance of polypyrrole-modified cells of AN and RS cultures. After the addition of pyrrole monomers in the submerged culture, the pellets began to darken in contrast to the control group, this indicated the formation of Ppy in cultures, which were growing in pyrrole-containing media. Within 2 days after the addition of pyrrole, the polymerization in Aspergillus niger culture was noticeable and the Ppy modified culture was investigated using optical and SEM microscopy. Figure 20A illustrates the modification of Aspergillus niger culture with Ppy by coating the cell walls with polymer, leading to the formation of conglomerates. From the SEM

images, various sizes of polypyrrole particles, which formed on the surface of fungi/cell mycelia, are visible (Fig. 20B).
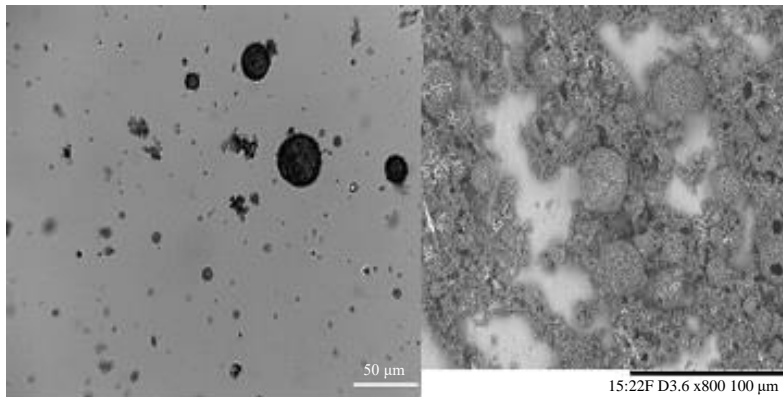

Fig. 20. (A) Optical microscopy and (B) SEM images of *Aspergillus niger* strain modified by Py.

Ppy was formed both in culture liquid and on the mycelium surface coating the bio-pellets. However, due to lower polymerization progress within *Rhizoctonia* sp. culture, the coating with Ppy in this culture was not well observable by the optical microscopy investigations. This could be explained by results obtained in previous research [91,94]: the polymerization of pyrrole in the growth medium and in the cell walls and/or periplasm was observed due to the presence of oxidoreductases within the cell's membrane. After 4 days of *Aspergillus niger* cells cultivation in the presence of pyrrole color of biomass fully changed from white to black and the bio-pellets were largely surrounded by a Ppy matrix (Fig. 21).
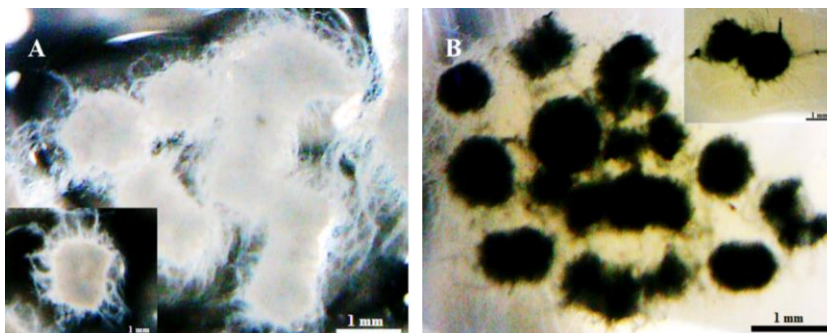

Figure 21. *Aspergilius. niger* culture optical microscope images **A** prior to pyrrole addition and **B** within 4 days after the addition of pyrrole.

3.3.2 Amperometric measurements of *Aspergillus niger* and *Rhizoctonia* sp. cells modified with polypyrrole

A double redox mediator system was applied for the amperometric measurements, one of them was a hydrophilic redox mediator – KF and the other one – a lipophilic redox mediator PD. The double redox mediator system acted as a charge transfer system in a series of chain-reactions because it linked intracellular redox activity of microorganisms with the electrode's surface. Such 'interconnection' of cells via the electron shuttle resulted in the formation of an electrical current, which was registered amperometrically (Fig. 22). For the amperometric measurements with the graphite rod, PD was chosen as a lipophilic redox mediator because in previous research [120], amperometric biosensors based on PD showed better charge transfer efficiency in comparison to the ones observed with other redox mediators (e.g. with PQ) [120].
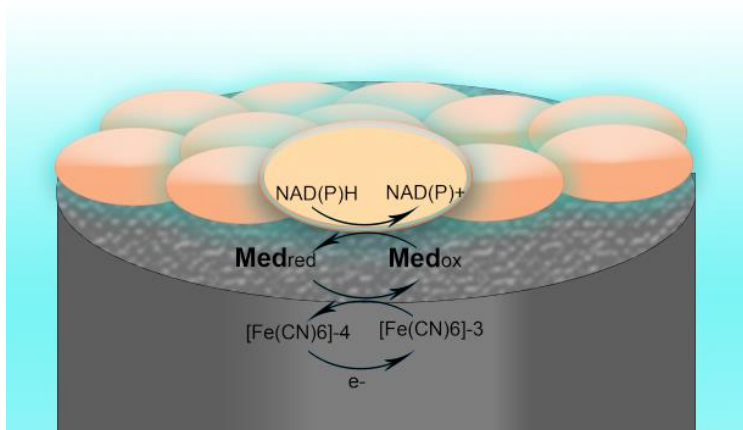
Fig. 22. Schematic representation of the electron transfer in amperometric measurements on a graphite rod electrode.

Amperometric measurements of GR/PD electrodes modified with two strains of cells (AN and RS) were performed (Fig. 23) (method section 2.8). It was determined that without Ppy both strains showed comparable results (Fig. 23 curves 3,4) and that the presence of Ppy influenced the amperometric signal (Fig. 23 curves 1,2). Living cells modified with Py showed higher amperometric currents in comparison to those registered in the control group

of unmodified cells. GR/ PD electrodes with immobilized *Aspergillus niger* strain cells, which were modified with Py (GR/PD/[AN:Py]) (Fig. 23 curve 1), at glucose concentrations of 300mM amperometrically registered currents $\Delta I(AN:Ppy) = 1.82$ µA and the electrodes with the immobilized cells from the control group of non-modified *Aspergillus niger* (GR/PD/AN) $\Delta I(An) = 0.18$ µA (Fig. 23 curve 3). Whereas amperometrically registered currents of GR/PD electrodes modified with Ppy-modified *Rhizoctonia* sp. (RS) strain cells (GR/PD/[RS:Py]) $\Delta I(RS:Py) = 0.88$ µA (Fig. 20 curve 2) in comparison to the electrodes modified with the control group of the same cells, which were not modified with Py (GR/PD/ RS) $\Delta I(AN) = 0.20$ µA (Fig. 23 curve 4).
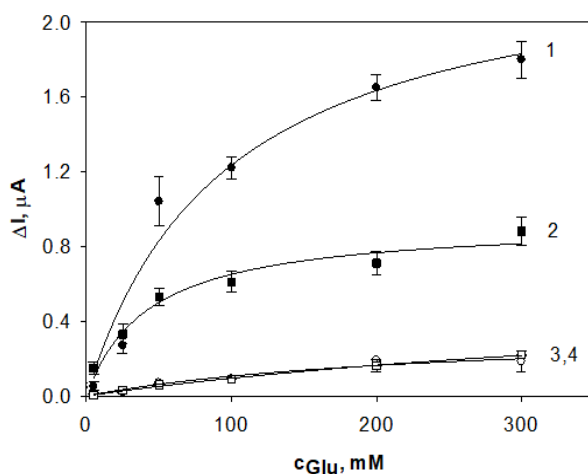

Fig. 23. Calibration plots of GR/PD electrodes with the immobilized cells: *Aspergillus niger* (1, 3 curves, ●, ○) and *Rhizoctonia* sp. (2, 4 curves, ■, □). The points denote experimental results obtained with polypyrrole (1, 2,●,■) and without polypyrrole (3, 4, ○,□); Changes in the anodic current are presented as a function of the glucose concentration.

Polypyrrole was used to increase the performance of biofuel cells from our earlier experiments (Fig.19). In several studies mostly polypyrrole or polyaniline conducting polymers were used for the modification of bioanodes before the deposition of cultured cells on the surface of the electrode [83,127–130] or for the modification of the bioanode, which was placed in the solution of the stirred cell culture [131]. The enhancement of biofuel cell performance by this technique could be related to the increased effective surface area of the anode, increased interface roughness and/or the electrostatic attraction between formed polymer layer and the negatively charged cells, because all

mentioned factors increase the cell adhesion to the surface of the electrode [128,132]. In our case, the advanced electrochemical activity of Py modified cells was based on the action of polypyrrole, which was formed on/within the cell walls and/or periplasm. Therefore, the Ppy could act as a redox mediator itself and could intercept electrons from the metabolic pathway to the electrode [130]. It was a critical aspect because the charge transfer is the rate-limiting process during the operation of MFC. In addition, it was already known that some conducting polymers including Ppy have been improving the compatibility between living cells and the electrode, which is important for the increase of MFC operational durability [81]. The sigmoidal dependence of the amperometric signal to the addition of the increasing glucose concentration was observed for both GR/PD/[AN:Py] and GR/PD/[RS:Py] electrodes (Fig. 23) (Table 4). From the calculated results (method section 2.16), it was observed that the highest electrode current (I_{max}) was attained with GR/PD/[AN:Py] electrodes and it was 2.41 µA, accordingly the K_{Mapp}. was 95.41 mM. For the GR/PD [RS:Py] electrode the I_{max}(RS:Py) = 0.93 µA and the K_{Mapp} – 43.03 mM. In the case where working electrodes were designed without any Ppy the I_{max} was much lower −0.36 and 0.62 µA, respectively for GR/PD/[AN:Py] and GR/PD/[RS:Py] electrodes. Whereas the K_{Mapp}. for GR/PD/AN and GR/PD/RS electrodes was 238.75 and 551.42 mM, respectively. Such a decrease of K_{Mapp} values and an increase of I_{max} values was described in an investigation of yeast cells immobilized in the Ppy matrix in comparison to the K_{Mapp} and I_{max} values registered with free yeast cells [133]. These changes of increased electrical current can be affected by the increased charge transfer rate. Higher I_{max} values for modified cells are responsible for the increased current density, which is directly related to the power density of biofuel cells and/or sensitivity of amperometric biosensors [82].

Table 4. Estimated kinetic parameters for GR/PD/[AN:Py] and (GR/PD/[RS:Py] electrodes

The type of electrode	I_{max}, µA	$K_{Mapp.}$, mM	R
GR/PD/[AR:Py]	2.41	95.41	0.9794
GR/PD/AR	0.36	238.75	0.9763
GR/PD/[RS:Py]	0.93	43.03	0.9810
GR/PD/RS	0.62	551.42	0.9980

As it was concluded from the previous amperometric measurements, the strain *A. niger* showed a more enhanced current signal by the modification of the cells with pyrrole. Thus, the differences in electrochemical behavior of the two different types of cells were assigned to the amount/activity of redox enzymes, which were present in the cell's wall and/or inside of the cells. For the fungi of *Aspergillus niger*, it has been identified that glucose oxidase is an intracellular component [134], while the phenoloxidases, which were secreted by *Rhizoctonia* sp. - extracellular. For instance, in the case of *Aspergillus niger* strain, the biosynthesis of glucose oxidase in the cell walls and/or periplasm renders the facilitated formation of Ppy. In situ polymerization of pyrrole due to the intracellular oxidative enzymes represented an attractive and a promising way for the cell coating. Moreover, this method allowed to simplify the preparation of the MFC anode, excluding the necessity of pre-modification of anode by redox mediators before the deposition of cells. However, for *Rhizoctonia* sp. strain, the polymerization of Py occurs predominantly in the liquid phase of the culture due to oxidoreductases secreted into the extracellular environment. Therefore, it lead to poor cell coating by the Ppy, thus diminished the registered electrical signal of the GR/PD/[RS:Py] electrode in comparison to that of the GR/PD/[AN:Py] electrode. For this reason, in further investigations of Py-modified cell cultures scanning electrochemical microscopy (SECM) was applied to the *Aspergillus niger* cell culture.

3.3.3   Scanning electrochemical microscopy investigation of modified *Aspergillus niger* cells

The double redox mediator system with PQ (100 μm) and KF (5 mM) was used for the evaluation of the electrochemical activity of A. niger cells by SECM, the same as in our previous experiments [Figure 8, 9, 13] for SECM measurements of yeast cell bioelectrochemical activity. The double redox mediator system converted the redox activity of intracellular enzymes of the Aspergillus niger cells into the current of the electrode, which was registered by the UME. Firstly, an approach curve was registered (Fig. 24A) while the UME approached the surface of the immobilized cells (0 μm), the registered current signal increased to its maximum value, which was associated with the higher concentration of the electroactive species on the surface of the immobilized cells (Fig. 24B). As was seen from the approaching curves, the SECM experiments allowed to distinguish the difference between the modified cell group (AN:Py) (Imax(An:Py) = 0.86 nA) and the control AN cell group (Imax(AN) = 0.30 nA). The cells modified with pyrrole showed a

higher registered current, which was nearly 3 times higher in comparison to the control cells.
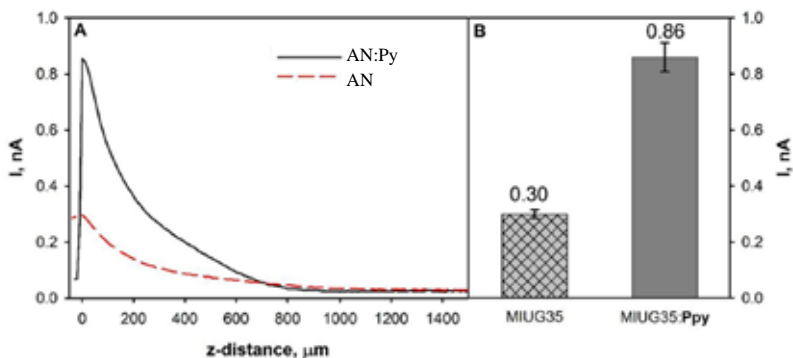

Fig. 24 A. The registered approaching curve to the immobilized control cell group and the pyrrole (Py) modified *Aspergillus niger* cell **B.** The maximum current values at the surface.

Further investigations were performed to observe the current value dependency by horizontal scans over the immobilized cells with different UME height values. Figure 25A shows the horizontal scans over the control group of the unmodified cells, while Fig. 25B shows horizontal scans over the polypyrrole modified *A. niger* cells. Fig. 25C displays a histogram with differences in the metabolic activity of the two types of AN cells. When the same height values were compared, it could be seen that the polypyrrole-modified cells were more active and displayed higher current values, than the control cell group. When the scanning by SCEM was performed at higher distances from the sample's surface, then the current signal decreased and the difference between the cell groups faded. It was determined that at 20 μm distance of the UME over the immobilized cells the current ($\Delta i(AN:Py) = 0.44$ nA) is more than 1.5 times higher over Py-modified cells compared to the registered over the control group cells ($\Delta i(AN) = 0.26$ nA). Increasing the distance from the cells' surface, the registered signal decreased due to the longer diffusion distance and the decreasing concentration of KF_{red} redox mediator.
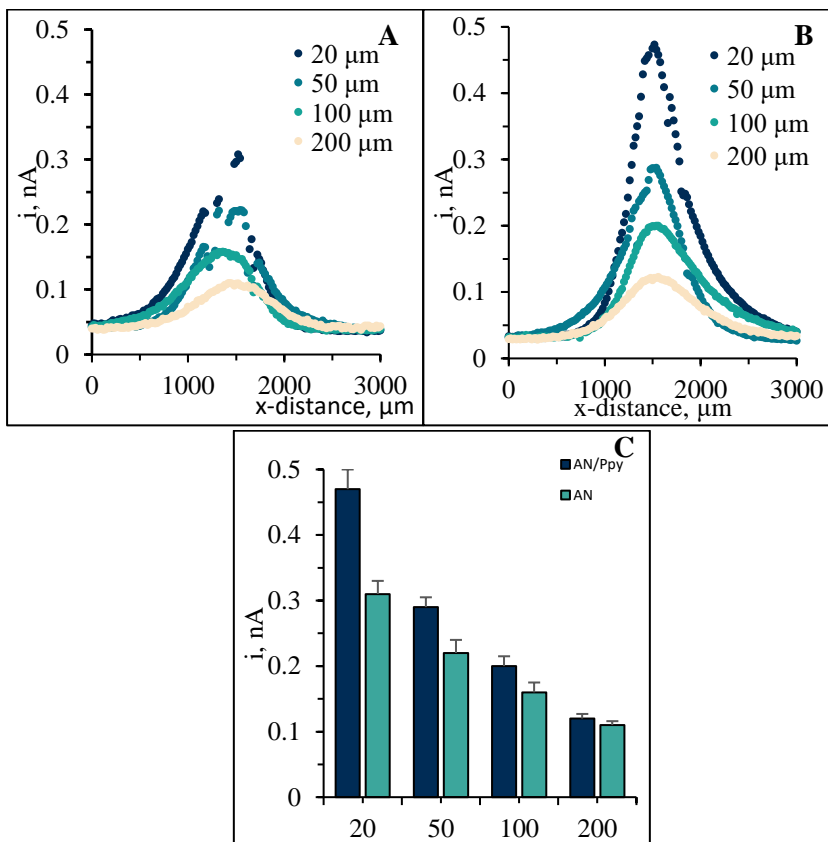
Fig. 25. Horizontal scans over the surface of immobilized cells **A** *Aspergillus niger* control (AN) cell group; **B** - the modified *Aspergillus niger* with pyrrole(An/Py) cell group. **C** histogram of the registered maximum values during the horizontal scans at various heights. Scans were performed with varying heights of 20/50/100/200 μm from the cells' surface.

The data registered by both the SECM and the amperometric measurements showed compatible results. The modification of *A. niger* fungi cells by Py increased the charge transfer efficiency, which was reflected by the increased registered current values after the glucose addition to the solution, compared to the observed in the control group of non-modified cells. Therefore, an enhanced biofuel cell performance could be achieved by the formation of the conducting polymer Py within the cell's wall/periplasm/ membrane with *Aspergillus niger*.

3.4 Scanning Electrochemical Microscopy for the human growth hormone detection

The applicability of the SECM to biological components is wide: ranging from enzymes, cells even to living organisms [4]. To expand the application of the SECM, a method was developed to detect the antigen of interest using the sandwich immunoassay format and detecting the antibody-GOx conjugate by the SECM.

As a model system, the human growth hormone (hGH) and two specific antibodies – monoclonal (m-anti-hGH) and polyclonal labelled with GOx (p-anti-hGH-GOx) were selected. After the hGH interaction with the immobilized antibodies, p-anti-hGH-GOx were specifically bound and the immune complex was formed (m-anti-hGH/hGH/p-anti-hGH-GOx). This way localized enzyme activity could be detected with the SECM, and the registered current depended on the hGH concentration in the sample. The enzyme GOx for the SECM immunoassay was used for the first time. The hGH is responsible for the body's structure and metabolism, including helping keep normal blood glucose levels[133]. The findings of this research could be adapted for the detection of many antigens of interest.

Firstly, the electrodes and the ECC were prepared: a double electrode system consisting of the UME as the WE and a silver wire coated with AgCl acting as a pseudo reference electrode were positioned in the ECC well (Fig.26A) (method section 2.2). The samples were prepared on vaporized Au micro-discs which were 50 μm in diameter and 300 μm apart from each other (Fig 26B) (method section 2.18). These micro-discs served as an immobilization platform to localize the electrochemical activity of the samples, by forming gold-sulphur (thiolate) bonds between the gold micro-discs and the self-assembled monolayer, onto which either the antigens or antibodies were attached.
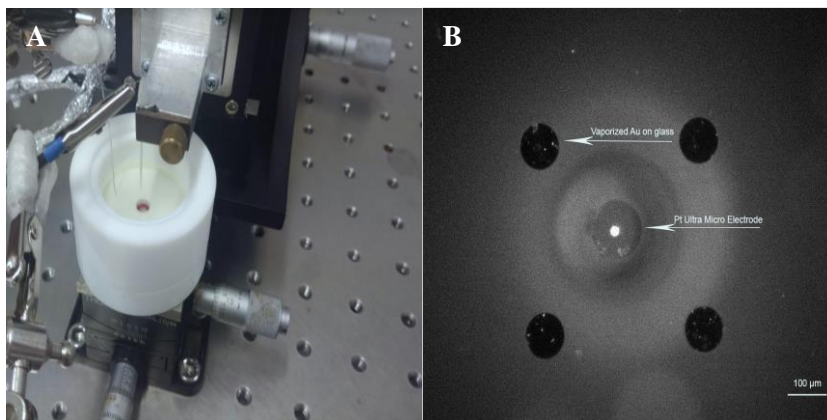
Fig. 26. A Electrochemical cell of a double electrode system **B** Optical microscope image in the dark field of the gold micro-discs on the glass surface, micro-disc diameter d≈ 50 μm, l≈ 300 μm apart from each other.

3.4.1 Ferrocenemethanol as the redox mediator for the detection of the antibody labeled with glucose oxidase

The first experiments were carried out using the feedback mode with ferrocene methanol (FeMeOH). which is commonly used in biosensing (79-81) due to good solubility in water-based solutions and efficient electron transfer. In the presence of glucose in the solution, the antibody-GOx conjugates catalyzed the oxidation of glucose (Fig. 27). During this enzymatic reaction FeMeOH(red) was formed. The reduced form of the redox mediator diffused from the active center of the GOx into the solution where it was detected by an ultra-microelectrode at a +0.45 V potential. The registered current i_T correlated to the concentrations of the reduced form of ferrocene methanol where higher currents indicated that the UME was above higher concentrations of the redox mediator (a more active area because of higher concentrations of the active GOx enzyme).
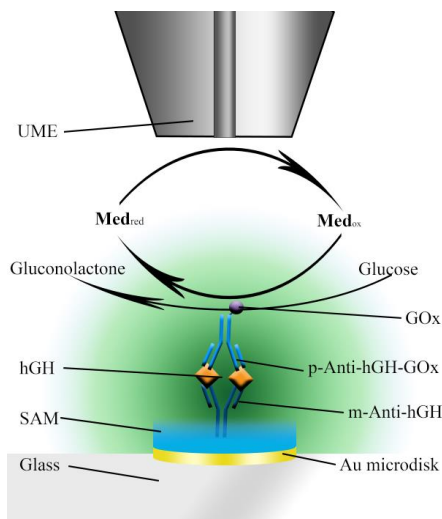
Fig.27. Schematic representation of the enzyme-labeled antibody detection with the SECM;

The samples were prepared by the methods described in method section 2.17-2.22 (Fig. 28) and by using the SECM, an indirect measurement of the antibody surface concentration was performed, as it was proportional to the concentration of the reduced form of the redox mediator and the registered current by the UME. The insulating surrounding area of the glass disregarded the positive feedback contribution in these experiments. A slightly increasing background current could be observed in some experiments due to the increasing concentration of the reduced redox mediator form, which diffused into the bulk after the addition of glucose and the enzymatic reactions. To accentuate the signal, resulting from the additional flux over the enzymatically active area, the background current was corrected by a linear plane fit to x axis by using both margins and subtracting a first-order polynomial background.
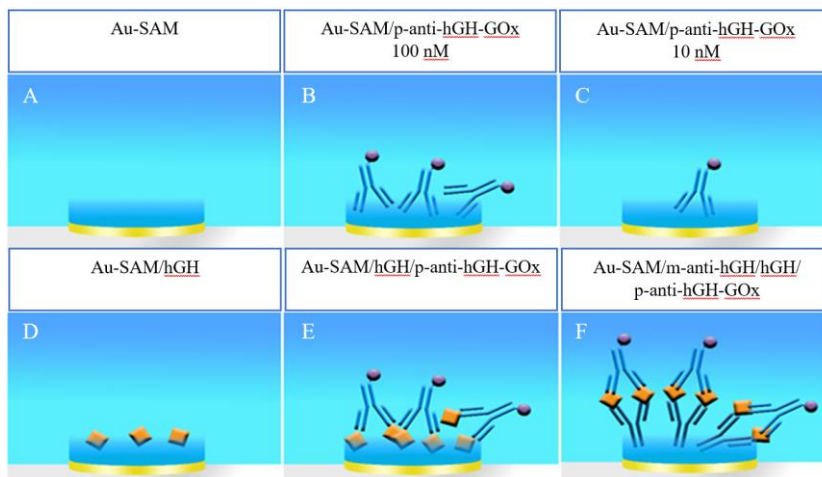
Fig. 28. Schematic representation of the different surfaces used for the analysis. **A** - Au micro-disc with SAM layer; **B** - Au micro-disc with SAM layer with covalently bound 100 nM of p-anti-hGH-GOx; **C** - Au micro-disc with SAM layer with covalently bound 10 nM of p-anti-hGH-GOx; **D** - Au micro-disc with SAM layer with covalently bound hGH; **E** - Au micro-disc with SAM layer with covalently bound hGH and specifically bound p-anti-hGH-GOx; **F** - Au micro-disc with SAM layer with covalently bound m-anti-hGH, specifically bound hGH and specifically bound p-anti-hGH-GOx.

To start the investigation of the immune complex formation, control experiments were performed to define the optimal SECM parameters and to analyze the surface. Firstly, scans of the surface of plain Au micro-discs were recorded (Fig. 29). From the results, it was noticed that the area with the Au micro-disc was clearly visible with the FeMeOH redox mediator. The UME registered a similar current when hovered over the gold regardless of the glucose present in the solution $\Delta i(A) \approx 3.08$ nA and $\Delta i(B) \approx 2.89$ nA. This was important in order to evaluate the differences when immobilizing other substrates onto the gold layer.

Fig. 29. The electrochemical activity over Au micro-discs, in a solution **A** without glucose, **B** in a solution with 5 mM glucose;

Secondly, a self-assembled monolayer based on 11-Mercaptoundecanoic-acid was formed on the surface of gold coated micro-discs via the Au-thiolate bond (Fig. 28A). The $\Delta i(A) \approx 2.12$ nA and $\Delta i(B) \approx 2.56$ nA theoretically should have been similar, because no enzyme was present (Fig. 30). The i_{max} currents were lower by around 0.6 nA compared to Fig. 29, because the SAM acted as an insulating layer between the gold.

Fig. 30. The electrochemical activity over Au-SAM micro-discs, in a solution A without glucose, **B** in a solution with 5 mM glucose;

Thirdly, the hGH was covalently immobilized onto the Au-SAM layer (Fig. 28D). From the images (Fig. 31) it was observed that the electric current values decreased even more compared to the Au-SAM layer (1.5 nA), due to the Au-micro-disc being covered even more. As in the previous experiments,

the addition of glucose into the solution should not have changed the current values $\Delta i_{max}(A) \approx 1.68$ nA and $i_{max}(B) \approx 1.16$ nA as there was no activated enzyme, however the resulting current slightly differed .
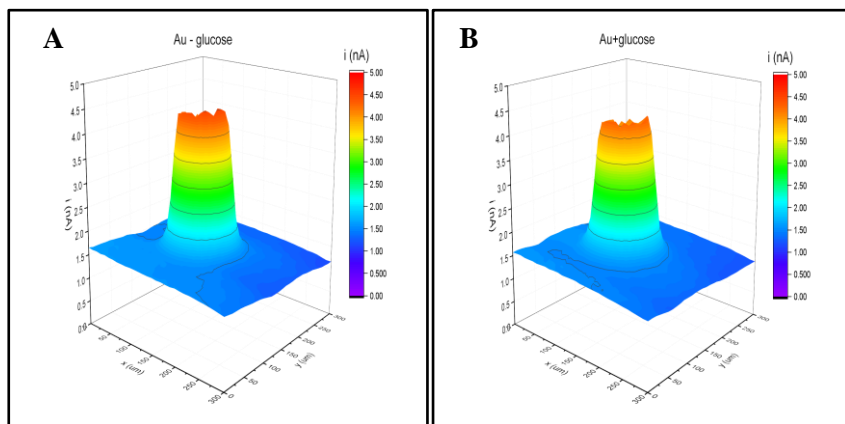

Fig. 31. The electrochemical activity over Au-SAM/hGH micro-discs, in a solution **A** without glucose, **B** in a solution with 5 mM glucose;

Fourthly, the Anti-hGH-GOx were covalently immobilized onto the Au-SAM layer (Fig. 28B). From the images (Fig. 32) it was recognized that the electric current values were slightly lower compared to the Au-SAM (Fig. 29) layer (about 1 nA), due to the Au-micro-disc being covered-up more. In this test, the addition of glucose into the solution had to change the registered UME values, as there was the glucose oxidase attached to the antibodies. However the change was low compared to the previous experiments $\Delta i(A) \approx 2.17$ nA and $\Delta i(B) \approx 2.50$ nA.
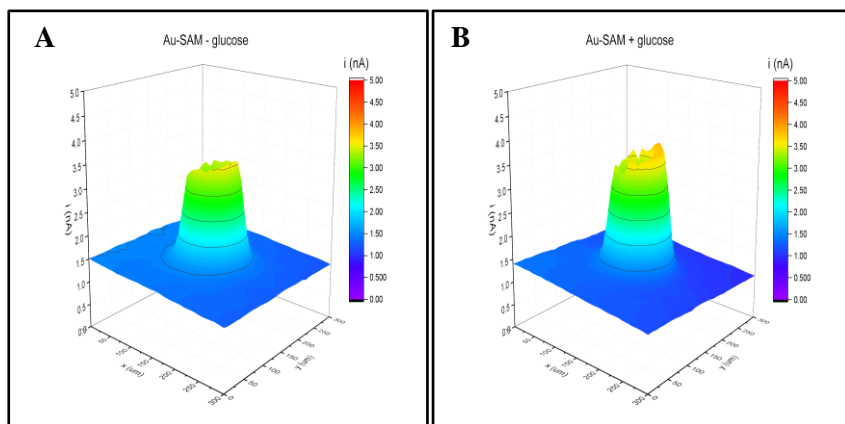

Fig. 32 The electrochemical activity over Au-SAM/Anti-hGH-GOx micro-discs, in a solution **A** without glucose, **B** in a solution with 5 mM glucose;

Lastly, the human growth hormone was covalently immobilized onto the Au-SAM layer and the antibodies against human growth hormone were attached by specific interactions (Fig. 28E). From the images (Fig. 33) it could be evaluated that the current signal from the gold was the lowest out of all the measurements, due to the Au-micro-disc being insulated the most (about 1.8 nA). What is more, the addition of glucose into the solution increased the registered UME values $\Delta i(A) \approx 1.42$ nA and $\Delta i(B) \approx 2.22$ nA as there was the glucose oxidase attached to the antibodies. These observations were optimistic for the human growth hormone detection with the scanning electrochemical microscopy using glucose oxidase as the signal amplifier toward immunoassay formation as the electrochemical differences could be registered. These were the first steps for improving the system, however, moving forward some improvements needed to be made (e.g. the elimination of the signal coming from the gold).
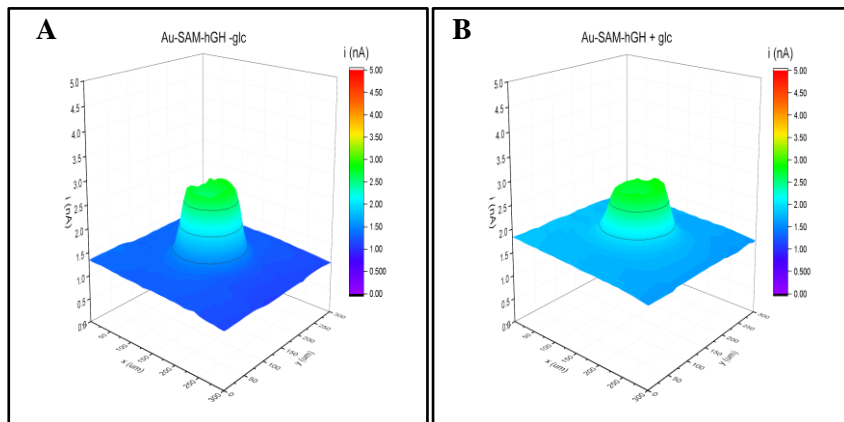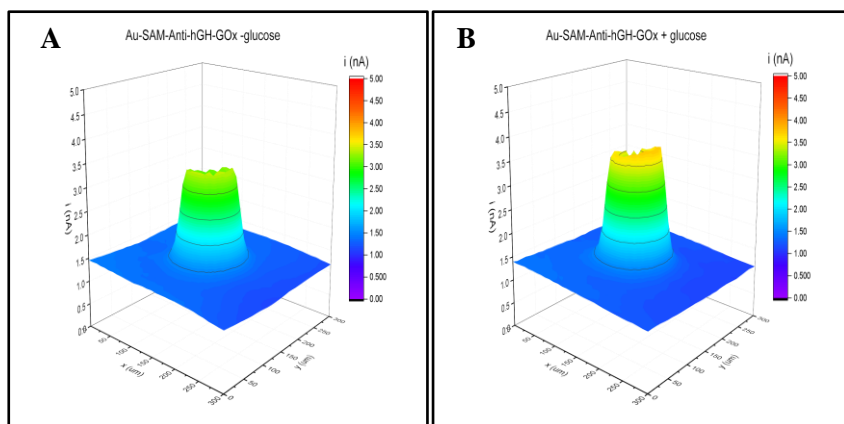

Fig. 33. The electrochemical activity over Au-SAM/hGH/Anti-hGH-GOx micro-discs, in a solution **A** without glucose, **B** in a solution with 5 mM glucose;

3.4.2 Potassium ferricyanide as the redox mediator for the detection of the antibody labeled with glucose oxidase

The earlier set of experiments was the start for the detection of the human growth hormone using the Anti-hGH-GOx with the SECM. In the second line of tests, improvements for the detection of hGH were made by decreasing the size of the Au micro-discs (Fig. 34), setting them farther apart, using a different redox mediator – KF and a more precise SECM with a mounted inverted optical microscope. This time the experiments were carried out using

the substrate generation – tip collection (SG-TC) mode using the hydrophilic redox mediator potassium ferricyanide. KF is known to be a suitable redox mediator for the evaluation of enzymatic reactions from the previous studies and literature [135], due to the good solubility in water-based solutions and efficient electron transfer between the GOx redox center and the electrode. In the presence of glucose in the solution, the antibody-GOx conjugates catalyzed the oxidation of glucose. During this enzymatic reaction, the reduced GOx redox center was re-oxidized by the redox mediator and ferrocyanide ions were formed. The ferrocyanide ions diffused from the active center of GOx into the solution where they were detected by an ultra-microelectrode at a +0.3 V potential. The registered current i_T correlated to the concentrations of KF(red) where higher currents indicated that the UME was above higher concentrations of the redox mediator (a more active area because of higher concentrations of the active enzyme) (Fig.27).
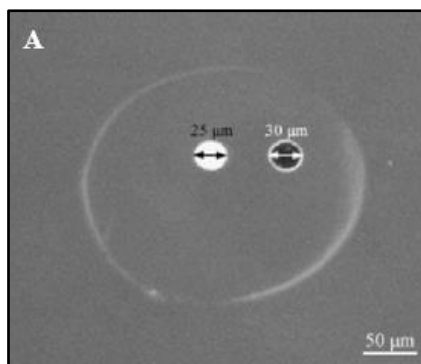
Fig. 34. Optical image x10 magnitude in the dark field of an UME Pt tip ∅ = 25 μm (white) near a gold micro-disc ∅=30 μm (black)

For the next set of experiments, after the control experiments were performed to check whether there was any interference from the gold surface (in our earlier experiments section 3.41 it was concluded that with ferrocenemethanol the interference from Au was visible). At first, the Au-SAM surface was prepared (Fig. 28A) and upon careful examination, it was seen that the background signal did not change when the UME was hovering over the Au micro-disc with the SAM, with and without the addition of glucose in the solution (Fig. 35). The differences in currents over the glass compared to the currents above the microdisc Δi for the same surface pre-modified with SAM were less than 1 pA for the solutions without and with glucose. These control results were very positive as the gold was not visible and the background was flat, meaning better detection of electrochemically

active substrates. It is also notable, that SECM combined with the micro-discs proved to be superior compared to spectroscopy or ellipsometry due to not just being able to evaluate the enzymes, but also to determine their location and bioelectrochemical activity [136].
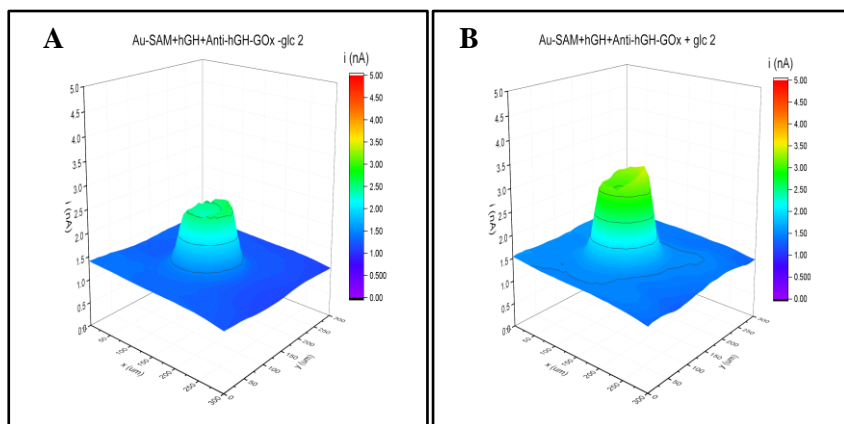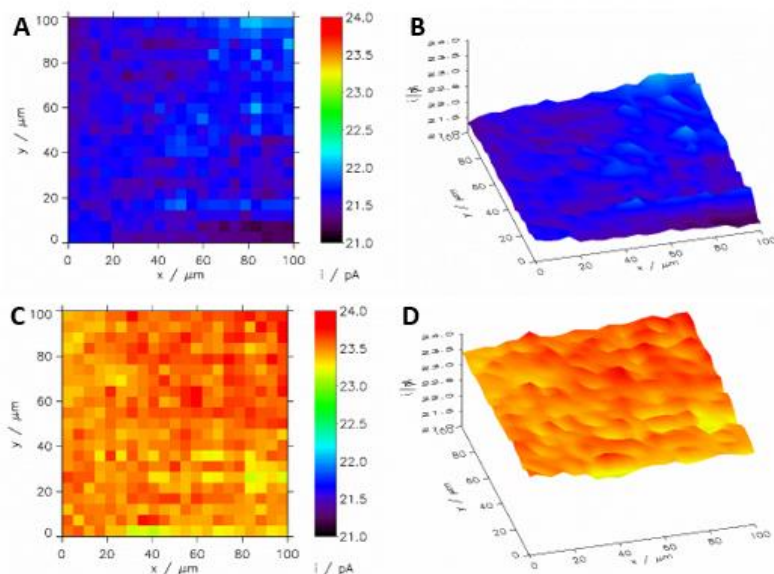

Fig. 35. The electrochemical activity over Au-SAM micro-discs, **A, B** in a solution without glucose, **C, D** in a solution with 5 mM glucose.

After the control experiments, p-anti-hGH-GOx with 100 nM concentration solution was covalently attached to the surface as described in the methodology (section 2.19) (Fig.28B) and the array scan was performed to evaluate the conjugate immobilization efficiency and the electrochemical activity of the surface. The images depicted in Figure 36 show the results of the investigation: the UME registered the reduced form of the redox mediator due to enzymatic activity of the GOx, which was attached to the p-anti-hGH, when glucose was added to the solution. From the results, it was observed that the highest GOx activity was visible around the edges of the micro-disc, probably because more of the substrate attaches around the edges. For the surface modified with p-anti-hGH-GOx in the solution without glucose the $\Delta i(A) \approx 5$ pA and for the solution with glucose $\Delta i(C) \approx 10$ pA.

Fig. 36. The electrochemical activity over Au-SAM/p-anti-hGH-GOx micro-discs (100 nM p-anti-hGH-GOx); **A, B** in a solution without glucose, **C, D** in a solution with 5 mM glucose

The same experiment was repeated with a 10 times lower concentration of the p-anti-hGH-GOx (10 nM) (Fig.28C) to check if it could be detectable. From the results regarded in Figure 37, the micro-disc area was still visible, although the difference in the change of the current was reduced due to lower surface concentration of the immobilized p-anti-hGH-GOx as well as GOx. The current differences compared to Figure 36 were not 10 times lower but around 4 times lower for the solution containing glucose ($\Delta i(C) \approx 2$ pA). It may be due to many reasons, i.e., surface coverage with the p-anti-hGH-GOx conjugate, steric hindrances between the antibodies, environmental changes, the quality of the electrode's tip etc. The system was tested for qualitative purposes and the parameters studied for the methodology to proceed further with the investigation.
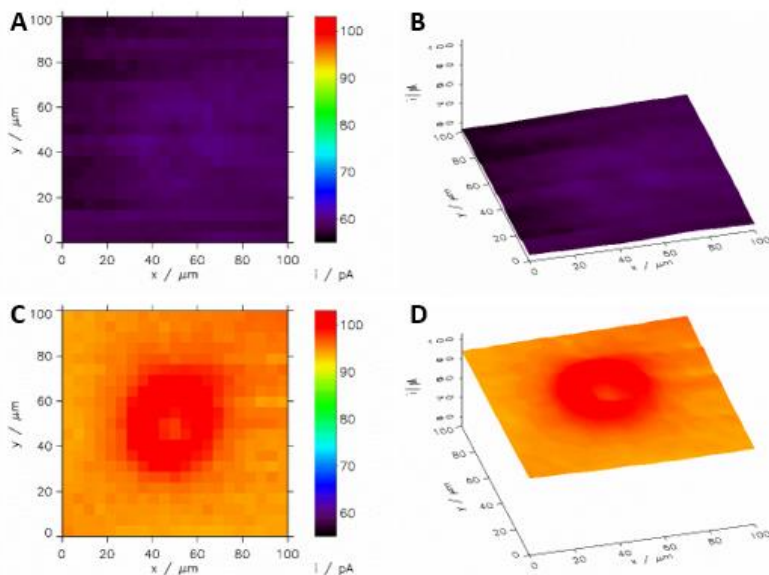
Fig. 37. The electrochemical activity over Au-SAM/p-anti-hGH-GOx microdiscs (10 nM p-anti-hGH-GOx); **A, B** − in a solution without glucose; **C, D** − in a solution with 5 mM glucose.

Due to the fact that the GOx labelled antibodies could be electrochemically detected, it was decided to use them for the hGH detection using the sandwich immunoassay format. Firstly, 40 nM hGH was covalently immobilized on the SAM layer (Fig. 28D). In theory, no active areas should have been seen, only the background signal. The miniscule changes in the currents were registered as follows: for the solution with and without glucose $\Delta i \approx 1$ pA (Fig. 38). An alternative current range was chosen to show that the presence of glucose did not make a difference.

Fig. 38. The electrochemical activity over Au-SAM/hGH micro-discs, **A, B –** in a solution without glucose, **C, D –** in a solution with 5 mM glucose.

Secondly, the Au-SAM/hGH surface was exposed to a 100 nM solution of p-anti-hGH-GOx and after the affinity interaction of hGH with p-anti-hGH-GOx, the surface of Au-SAM/hGH/p-anti-hGH-GOx was formed (Fig. 28E). The layers were visible by the SECM due to the presence of GOx and enzymatic activity in the solution containing glucose. The current range varied: for the solution without glucose $\Delta i(A) \approx 3$ pA and for the solution with glucose $\Delta i(C) \approx 10$ pA (Fig. 39).
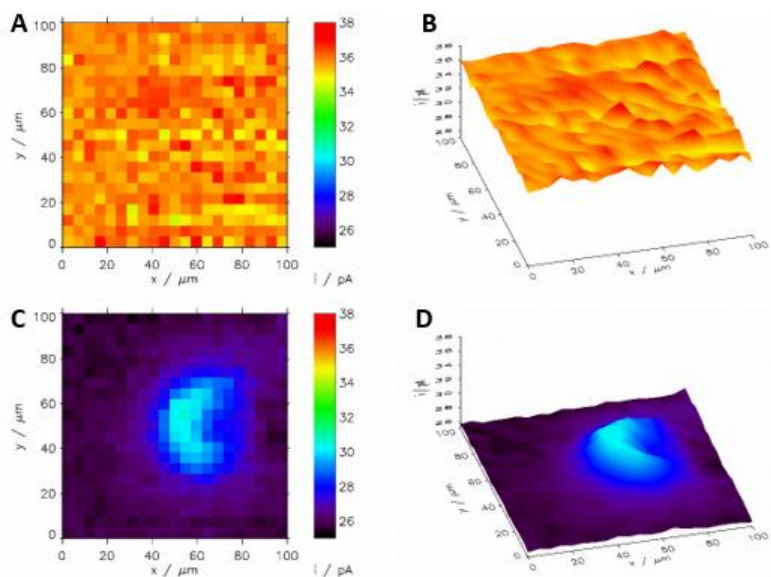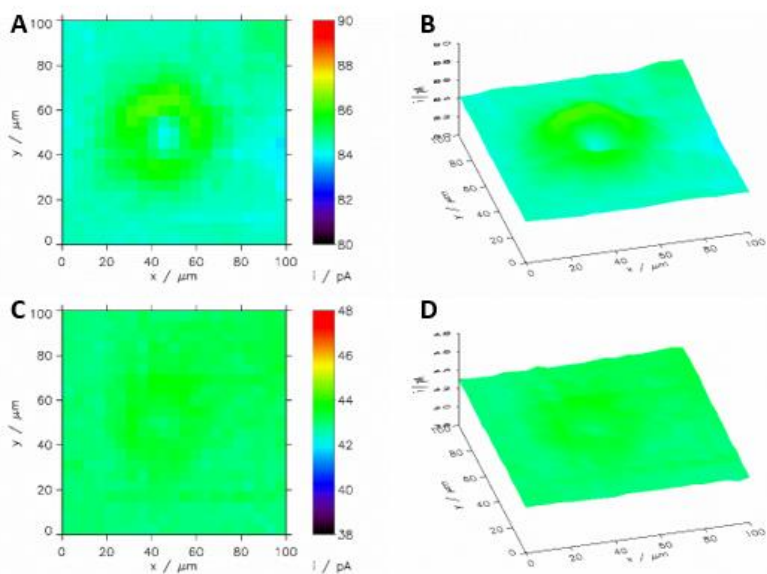
Fig. 39. The electrochemical activity over Au-SAM/hGH/anti-hGH-GOx micro-discs, **A, B** in a solution without glucose, **C, D** in a solution with 5 mM glucose.

Lastly, measurements for 40 nM hGH detection using the sandwich immunoassay format (Au-SAM/m-anti-hGH/hGH/p-anti-hGH-GOx) were made (Fig. 28F). The difference in the registered currents using different solutions was clearly visible: for the solution without glucose $\Delta i(A) \approx 1$ pA and by adding glucose to the solution $\Delta i(C) \approx 5$ pA (Fig. 40). These experiments confirmed that the methodology could be employed for the hGH electrochemical detection with the SECM in the sandwich immunoassay format and by using GOx labeled detection antibodies (p-anti-hGH-GOx). With further improvement in the immobilization techniques and the electrochemical parameters of SECM, a sensitive electrochemical immunoassay for hGH detection can be developed. Our system could report $1 \ \mu g \ mL^{-1}$ of hGH with the GOx label and KF on gold micro-discs, it is a concept that has not been reported before. The micro-discs are an advantage because they are visible with an optical microscope, so you could always know where the covalent binding takes place with no nonspecific adsorption observed on the glass. What is more, since a large number of the micro-discs are in a small area, it is a possibility to prepare samples in close proximity and to evaluate different samples in one SECM image for multianalysis.
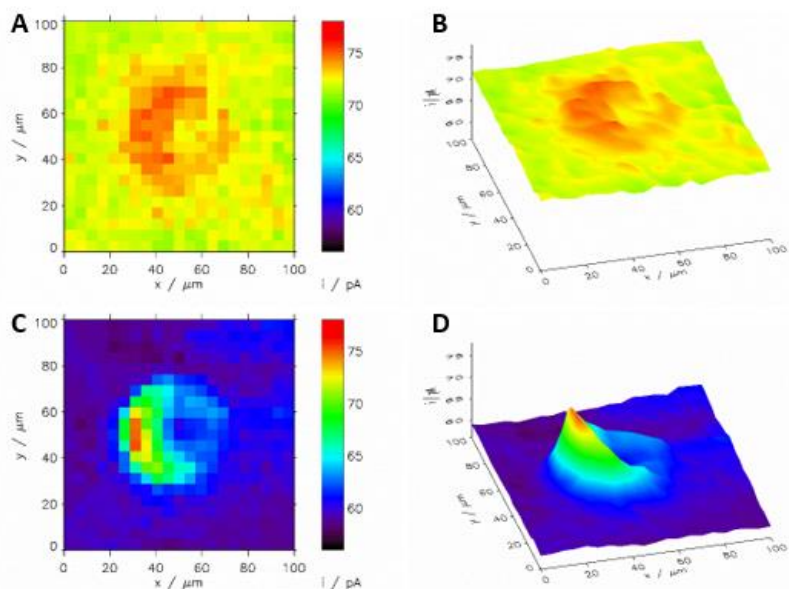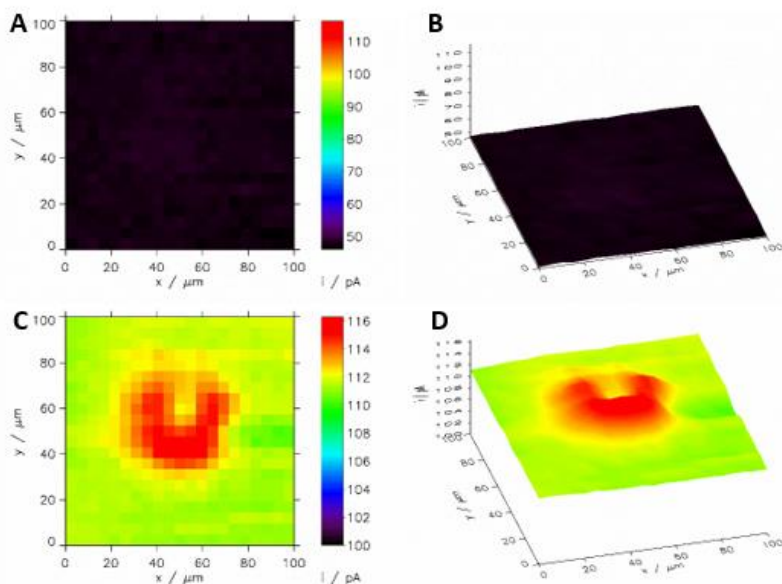
Fig. 40. The electrochemical activity over Au-SAM/m-anti-hGH/hGH/anti-hGH-GOx micro-discs, **A, B** − in a solution without glucose, **C, D** − in a solution with 5 mM glucose.

Lastly, after the area scan of the immune complex was completed, several horizontal scans were made over the same micro-disc at varying heights 5/10/25/50 μm (Fig. 41). These horizontal scans showed the dependency of the registered current according to the distance to the surface. At the height of 5 and 10 μm the recorded currents are similar in shape and value. However, if the distance was greater than 10 μm, then the background signal was also high and the electrochemical activity of the GOx could not be detected.
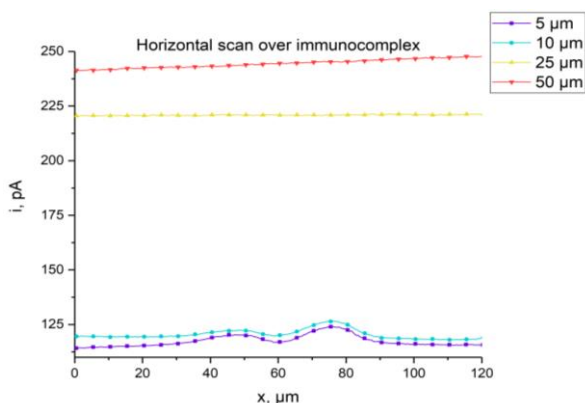
Fig 41. horizontal scans over an immune-complex at varying distances of 5/10/25/50 μm.

3.4.3   Evaluation of the immune complex formation by a mathematical model

The SECM operated in the SG-TC mode thus quantification of the additional flux of potassium ferrocyanide diffusing from the immobilized and active GOx could be achieved. The redox mediator in the solution initially was in its oxidized form $K_3[Fe(CN)_6]$, however, due to the occurring enzymatic reactions, it was reduced to $K_4[Fe(CN)_6]$ and formed a diffusion profile around the GOx. $K_4[Fe(CN)_6]$ could be detected by the ultramicroelectrode at +0.3V where it provided the electrode with one electron after oxidation of every molecule (eq. 5).

$$K_4[Fe(CN)_6] \rightarrow K_3[Fe(CN)_6] + e^- \tag{5}$$
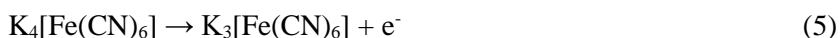
The height of the whole immune complex shouldn't have been higher than ~30nM [137], that is why topographical effects were negligible considering that the distance to the electrode was around 5 µm. The control at each experiment eliminated any topographic effects or electrochemical activity when the solution contained no glucose. The line of experiments showed a qualitative method for the detection of the human growth hormone as there were significant differences compared to the control experiments.
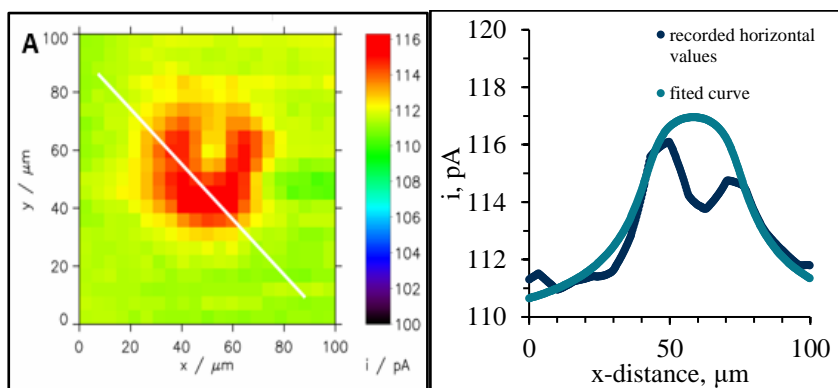
Fig. 42 A – Cross-section of the flux of $K_4[Fe(CN)_6]$ over the immune complex. **B** – Fitted curve over the immune complex; The flux values of $K_4[Fe(CN)_6]$ were obtained from the extracted profile along the white line over the sandwich type immune complex.

From the fitted and calculated results (method section 2.24), a tendency could be identified. The highest flux of the ferrocyanide was observed with the Au-SAM/p-anti-hGH-GOx (Fig. 4-1) at the surface with the highest

concentration of 100 nM. The least flux was seen with the Au-SAM/p-anti-hGH-GOx at a lower concentration of 10 nM (Fig. 43-2) and the immune complex formation using 40 nM concentration of hGH (Fig. 40-4). It was also noticed that by the additional layers of immune complex formation, the $[Fe(CN)_6]^{4-}$ flux decreased. This correlates to the theory: layering components of the immune complex decreases the chance of immobilization due to hindered interaction, antibody orientation, immobilization quality etc [138]. The generation rate was a helpful tool to determine surface activity, immobilization quality.
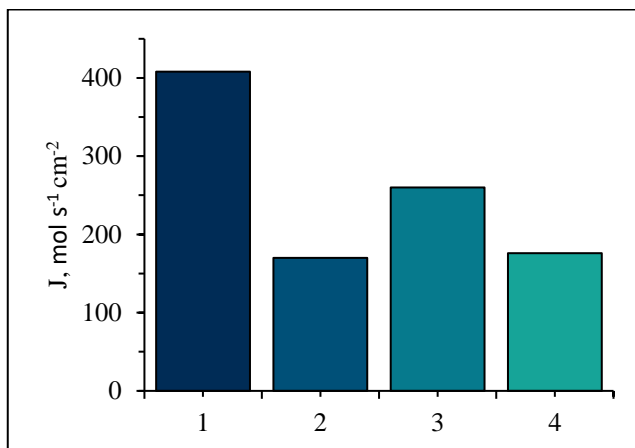
Fig. 43. Generation rate over varying surface modifications: **1** - Au-SAM/p-anti-hGH-GOx 100 nM, **2** – AU-SAM/p-anti-hGH-GOx 10 nM, **3** - Au-SAM/hGH/p-anti-hGH-GOx, **4** – Au-SAM/m-anti-hGH/hGH/p-anti-hGH-GOx.

There is a continuation of studies examining various strategies for the development of immunoassays, one of which are the electrochemical immunoassays. The advantages of which are faster, more economical, simpler testing and possibility to adapt for various analytes. Our research demonstrated a viable methodology for studying the aspects of an immunoassay: labeling, immobilization, conditions for electrochemical visualization. The SECM SG-TC amperometric system with the potassium ferricyanide as the redox mediator for the detection of human growth antigen in a non-competitive sandwich mode with the labeled human growth antibody determined qualitative and quantitative results. Developments in this area will further enhance the degree of sensitivity achievable in analysis. What is more, quantification could also be achieved but would need further investigation and improvement for such a technique.

CONCLUSIONS

1. It was determined that phenanthrenequinone (100 µM) in a double redox mediator system with potassium ferricyanide (5 mM) registered the highest electric current values (8.1 nA) of the bioelectrochemical activity of *Saccharomyces cerevisiae* cells compared to other redox mediators: menadione (6.65 nA), 1,4-benzoquinone (3.46 nA), 2,6-dichlorophenolindophenol sodium salt hidrate (1.01 nA), 1,10-Phenanthroline-5,6-dione (0.07nA), phenazine methosulfate (0.03 nA).

2. The modification of *Saccharomyces cerevisiae* cells with 0.1/0.3/0.5 M concentration of pyrrole in the incubation solution for 24 hours showed lower electron transfer (0.17/0.12/0.04 nA) than the control group (0.34 nA) after being immobilized on a Petri dish by the measurements of SECM with the double redox mediator system of PQ (100 µM) and KF (5 mM).

3. *Saccharomyces cerevisiae* cells entrapped in a CFE and modified with MWCNT (0.5 mg 10 mL^{-1}) showed similar electron transfer rates (1.85 mA) as the cells modified with 0.3 M Py (1.62 mA) and it was about 3 higher compared to the control group (0.63 mA) in the double redox mediator system of PQ (100 µM) and KF (5 mM).

4. The microorganism-assisted formation of polypyrrole (0.03 M) with the *Aspergillus niger* cells and *Rhizoctonia* sp. cells developed several times enhanced electron transfer by amperometric measurements (x10 for *A. niger* (1.82 µA) and x4 for *Rhizoctonia* sp. (0.88 µA)) compared to the control cell group (0.18 and 0.020 µA respectively) at glucose concentrations of 300 mM with PD (4.5 µL) and KF (10 mM). In addition, during SECM experiments, *A. niger* cells that were modified, recorded a 3 times larger UME current than the control group.

5. The SECM in the SG-TC mode could be used for the detection of the human growth antigen on gold microdisks in a non-competitive sandwich mode with the GOx labelled human growth antibody with the KF as the redox mediator and record 1 µg mL^{-1} concentrations of $\Delta i(hGH) = 5$ pA. The results obtained with the GC-SECM mode with the human growth antigen in a non-competitive sandwich mode with the GOx labelled human growth antibody was studied quantitatively by fiting a mathematical formula and calculating the rate flux of the redox mediator coming from the active enzyme area (about 400 mol/s cm^2).

REFERENCES

[1]   A.J. Bard, F.R.F. Fan, J. Kwak, O. Lev, Scanning Electrochemical Microscopy. Introduction and Principles, Anal. Chem. 61 (1989) 132–138. https://doi.org/10.1021/AC00177A011.

[2]   I. Beaulieu, S. Kuss, J. Mauzeroll, M. Geissler, Biological Scanning Electrochemical Microscopy and Its Application to Live Cell Studies, Anal. Chem. 83 (2011) 1485–1492. https://doi.org/10.1021/AC101906A.

[3]   T. Yasukawa, T. Kaya, T. Matsue, Characterization and Imaging of Single Cells with Scanning Electrochemical Microscopy, https://doi.org/10.1002/1521-4109(200005)12:9.

[4]   S. Bergner, P. Vatsyayan, F.M.-Matysik, Recent advances in high resolution scanning electrochemical microscopy of living cells–a review, Analytica chimica acta 775 (2013): 1-13.

[5]   G. Wittstock, Formation and imaging of microscopic enzymatically active spots on an alkanethiolate-covered gold electrode by scanning electrochemical microscopy, Anal. Chem. 69 (1997) 5059–5066. https://doi.org/10.1021/AC970504O.

[6]   D.T. Pierce, P.R. Unwin, A.J. Bard, Scanning electrochemical microscopy. 17. Studies of enzyme-mediator kinetics for membrane- and surface-immobilized glucose oxidase, Anal. Chem. 64 (1992) 1795–1804. https://doi.org/10.1021/AC00041A011.

[7]   S.E. Pust, W. Maier, G. Wittstock, Investigation of Localized Catalytic and Electrocatalytic Processes and Corrosion Reactions with Scanning Electrochemical Microscopy (SECM), Zeitschrift Für Phys. Chemie. 222 (2008) 1463–1517.
https://doi.org/10.1524/ZPCH.2008.5426.

[8]   Paolo Bertoncello, Advances on scanning electrochemical microscopy (SECM) for energy, Energy Environ. Sci. 3 (2010) 1620–1633. https://doi.org/10.1039/C0EE00046A.

[9]   L. Stoica, S. Neugebauer, W. Schuhmann, Scanning Electrochemical Microscopy (SECM) as a tool in biosensor research, Adv. Biochem. Eng. Biotechnol. 109 (2007) 455–492. https://doi.org/10.1007/10_2007_082.

[10]   A. Ramanavicius, A. Kausaite-Minkstimiene, I. Morkvenaite-Vilkonciene, P. Genys, R. Mikhailova, T. Semashko, J. Voronovic, A. Ramanaviciene, Biofuel cell based on glucose oxidase from Penicillium funiculosum 46.1 and horseradish peroxidase, Chem. Eng. J. 264 (2015) 165–173. https://doi.org/10.1016/J.CEJ.2014.11.011.

[11]   T. Yasukawa, Y. Hirano, N. Motochi, H. Shiku, T. Matsue, Enzyme immunosensing of pepsinogens 1 and 2 by scanning electrochemical microscopy, Biosens. Bioelectron. 22 (2007) 3099–3104. https://doi.org/10.1016/J.BIOS.2007.01.015.

[12]   S.F. D'Souza, Microbial biosensors, Biosens. Bioelectron. 16 (2001)

337–353. https://doi.org/10.1016/S0956-5663(01)00125-7.

[13] A.S. Mathuriya, J. V. Yakhmi, Microbial fuel cells to recover heavy metals, Environ. Chem. Lett. 2014 124. 12 (2014) 483–494. https://doi.org/10.1007/S10311-014-0474-2.

[14] A.J. Bard, M. V Mirkin, Scanning Electrochemical Microscopy, Scanning Electrochem. Microsc. (2001). https://doi.org/10.1201/9780203910771.

[15] G. Binnig, C.F. Quate, C. Gerber, Atomic Force Microscope, Phys. Rev. Lett. 56 (1986) 930. https://doi.org/10.1103/PhysRevLett.56.930.

[16] X. Pei, B. Zhang, J. Tang, B. Liu, W. Lai, D. Tang, Sandwich-type immunosensors and immunoassays exploiting nanostructure labels: A review, Anal. Chim. Acta. 758 (2013) 1–18. https://doi.org/10.1016/J.ACA.2012.10.060.

[17] G. Binnig, H. Rohrer, Scanning tunneling microscopy, Surf. Sci. 126 (1983) 236–244. https://doi.org/10.1016/0039-6028(83)90716-1.

[18] W.S. Roberts, D.J. Lonsdale, J. Griffiths, S.P.J. Higson, Advances in the application of scanning electrochemical microscopy to bioanalytical systems, Biosens. Bioelectron. 23 (2007) 301–318. https://doi.org/10.1016/J.BIOS.2007.06.020.

[19] S. Pons, M. Fleischmann, The Behavior of Microelectrodes, Anal. Chem. 59 (1987) 2021. https://doi.org/10.1021/AC00151A001.

[20] Peng Sun, Zhiquan Zhang, and Jidong Guo, Y. Shao, Fabrication of Nanometer-Sized Electrodes and Tips for Scanning Electrochemical Microscopy, Anal. Chem. 73 (2001) 5346–5351. https://doi.org/10.1021/AC010474W.

[21] B.D. Bath, E.R. Scott, J Bradley Phipps, H.S. White, Scanning Electrochemical Microscopy of Iontophoretic Transport in Hairless Mouse Skin. Analysis of the Relative Contributions of Diffusion, Migration, and Electroosmosis to Transport in Hair Follicles, (2000). https://doi.org/10.1002/1520-6017.

[22] S. Kuss, D. Trinh, J. Mauzeroll, High-Speed Scanning Electrochemical Microscopy Method for Substrate Kinetic Determination: Application to Live Cell Imaging in Human Cancer, Anal. Chem. 87 (2015) 8102–8106. https://doi.org/10.1021/ACS.ANALCHEM.5B01269.

[23] M. Tsionsky, Z.G. Cardon, A.J. Bard, R.B. Jackson, Photosynthetic Electron Transport in Single Guard Cells as Measured by Scanning Electrochemical Microscopy, Plant Physiol. 113 (1997) 895–901. https://doi.org/10.1104/PP.113.3.895.

[24] A. Kueng, C. Kranz, A. Lugstein, E. Bertagnolli, B. Mizaikoff, Integrated AFM-SECM in tapping mode: Simultaneous topographical and electrochemical imaging of enzyme activity, Angew. Chemie - Int. Ed. 42 (2003) 3238–3240. https://doi.org/10.1002/anie.200351111.

[25] I. Morkvenaite-Vilkonciene, A. Valiūnienė, J. Petroniene, A. Ramanavicius, Hybrid system based on fast Fourier transform electrochemical impedance spectroscopy combined with scanning

electrochemical microscopy, Electrochem. Commun. 83 (2017) 110–112. https://doi.org/10.1016/J.ELECOM.2017.08.020.

[26] A. Bard, F. Fan, D. Pierce, P.U., Chemical imaging of surfaces with the scanning electrochemical microscope, Science 254.5028 (1991): 68-74.

[27] D.O. Wipf, R.M. Wightman, Rapid Cleavage Reactions of Haloaromatic Radical Anions Measured with Fast-Scan Cyclic Voltammetry, J. Phys. Chem. 93 (1989) 4286–4291.

[28] C. Kranz, G. Wittstock, H. Wohlschläger, W.S., Imaging of microstructured biochemically active surfaces by means of scanning electrochemical microscopy, Electrochimica acta 42.20-22 (1997): 3105-3111.

[29] F. Zhou, P.R. Unwin, A.J. Bard, Scanning electrochemical microscopy. 16. Study of second-order homogeneous chemical reactions via the feedback and generation/collection modes, J. Phys. Chem. 96 (2002) 4917–4924. https://doi.org/10.1021/J100191A036.

[30] M. Etienne, A. Schulte, W.S., High resolution constant-distance mode alternating current scanning electrochemical microscopy (AC-SECM), Electrochimica acta 42.20-22 (1997): 3105-3111

[31] R. Yotter, D.W.-I.S. Journal, Sensor technologies for monitoring metabolic activity in single cells-part II: nonoptical methods and applications, IEEE Sensors Journal 4.4 (2004): 412-429. https://doi.org/10.1109/JSEN.2004.830954.

[32] C. Lee, J. Kwak, A.B. Application of scanning electrochemical microscopy to biological samples, Proceedings of the National Academy of Sciences 87.5 (1990): 1740-1743.

[33] F. Rawson, A. Downard, K.B. Electrochemical detection of intracellular and cell membrane redox systems in Saccharomyces cerevisiae, Scientific reports 4.1 (2014): 1-9.

[34] Wojciech Nogala, Katarzyna Szot, Malte Burchardt, Folkert Roelfs, Jerzy Rogalski, Marcin Opallo, Gunther Wittstock, Feedback mode SECM study of laccase and bilirubin oxidase immobilised in a sol–gel processed silicate film, Analyst. 135 (2010) 2051–2058. https://doi.org/10.1039/C0AN00068J.

[35] B. Nagel, H. Dellweg, L.M. Gierasch, Glossary for chemists of terms used in biotechnology (IUPAC Recommendations 1992), Pure Appl. Chem. 64 (1992) 143–168. https://doi.org/10.1351/PAC199264010143.

[36] D.R. Thévenot, K. Toth, R.A. Durst, G.S. Wilson, Electrochemical biosensors: recommended definitions and classification, Biosens. Bioelectron. 16 (2001) 121–131. https://doi.org/10.1016/S0956-5663(01)00115-4.

[37] J.D. Rabinowitz, J.F. Vacchino, C. Beeson, H.M. McConnell, Potentiometric measurement of intracellular redox activity, J. Am. Chem. Soc. 120 (1998) 2464–2473.

https://doi.org/10.1021/JA973560F.

[38]   S. Subrahmanyam, A. Balakrishnan, R. Viswanathan, Development of a Cytosensor for the Detection of Fusarium Oxysporum-A Functional Approach Towards Bioanalytical Applications, Core.Ac.Uk. 14 (2018) 1857–7881. https://doi.org/10.19044/esj.2018.v14n21p42.

[39]   K. Baronian, A. Downard, R. Lowen, N.P. 2, Detection of two distinct substrate-dependent catabolic responses in yeast cells using a mediated electrochemical method, Springer. 60 (2002) 108–113. https://doi.org/10.1007/s00253-002-1108-3.

[40]   T.C. Tan, F. Li, K.G. Neoh, Y.K. Lee, Microbial membrane-modified dissolved oxygen probe for rapid biochemical oxygen demand measurement, Sensors Actuators B Chem. 8 (1992) 167–172. https://doi.org/10.1016/0925-4005(92)80175-W.

[41]   D.R. Omstead, G. Georgiou, J. Aiche, W. Crueger, A. Crueger, K.B. Biotechnology ; Andersen, K.J. Von Meyenburg, I.L. Sun, F.L. Crane, R.B. Gennis, V. Stewart, F.C. Niedhardt, M.G. Sturr, T.A. Krulwich, D.B.J. Hicks, P.C. Bacteriol ; Loewen, B. Hu, J. Strutinsky, R. Sparling, Ferricyanide Reduction by Escherichia coli: Kinetics, Mechanism, and Application to the Optimization of Recombinant Fermentations, ACS Publ. 34 (1990) 4949–4956. https://doi.org/10.1021/ac000358d.

[42]   K. Baronian, A. Downard, R. Lowen, N.P, Detection of two distinct substrate-dependent catabolic responses in yeast cells using a mediated electrochemical method, Springer. 60 (2002) 108–113. https://doi.org/10.1007/s00253-002-1108-3.

[43]   K. Morris, K. Catterall, H. Zhao, N. Pasco, R.J., Ferricyanide mediated biochemical oxygen demand–development of a rapid biochemical oxygen demand assay, Analytica chimica acta 442.1 (2001): 129-139.

[44]   Y. Yashiki, S. Yamashoji, Extracellular reduction of menadione and ferricyanide in yeast cell suspension, J. Ferment. Bioeng. 82 (1996) 319–321. https://doi.org/10.1016/0922-338X(96)88828-3.

[45]   E. Akyilmaz, E. Dinçkaya, An amperometric microbial biosensor development based on Candida tropicalis yeast cells for sensitive determination of ethanol, Biosens. Bioelectron. 20 (2005) 1263–1269. https://doi.org/10.1016/J.BIOS.2004.04.010.

[46]   L. Rotariu, C. Bala, V. Magearu, Yeast cells sucrose biosensor based on a potentiometric oxygen electrode, Anal. Chim. Acta. 458 (2002) 215–222. https://doi.org/10.1016/S0003-2670(01)01529-X.

[47]   R. Verho, J. Londesborough, M.P., Engineering Redox Cofactor Regeneration for Improved Pentose Fermentation in Saccharomyces cerevisiae, Applied and environmental microbiology 69.10 (2003): 5892-5897 https://doi.org/10.1128/AEM.69.10.5892-5897.2003.

[48]   E. Nevoigt, Progress in Metabolic Engineering of Saccharomyces cerevisiae , Microbiol. Mol. Biol. Rev. 72 (2008) 379–412. https://doi.org/10.1128/MMBR.00025-07.

[49] L.A. Hazelwood, J.M. Daran, A.J.A. Van Maris, J.T. Pronk, J.R. Dickinson, The Ehrlich pathway for fusel alcohol production: A century of research on Saccharomyces cerevisiae metabolism, Appl. Environ. Microbiol. 74 (2008) 2259–2266. https://doi.org/10.1128/AEM.02625-07.

[50] F.S. Collins, Medical and Societal Consequences of the Human Genome Project, N. Engl. J. Med. 341 (1999) 28–37. https://doi.org/10.1056/NEJM199907013410106.

[51] J. Cui, J. Kaandorp, P. Sloot, C.L., Calcium homeostasis and signaling in yeast cells and cardiac myocytes, FEMS yeast research 9.8 (2009): 1137-1147.

[52] C.E. Rodriguez, M. Shinyashiki, J. Froines, R.C. Yu, J.M. Fukuto, A.K. Cho, An examination of quinone toxicity using the yeast Saccharomyces cerevisiae model system, Toxicology. 201 (2004) 185–196. https://doi.org/10.1016/J.TOX.2004.04.016.

[53] C. Rodriguez, Z. Sobol, R.S., 9, 10-Phenanthrenequinone induces DNA deletions and forward mutations via oxidative mechanisms in the yeast Saccharomyces cerevisiae, Toxicology in Vitro 22.2 (2008): 296-300.

[54] J. Weyermann, D. Lochmann, A. Zimmer, A practical note on the use of cytotoxicity assays, Int. J. Pharm. 288 (2005) 369–376. https://doi.org/10.1016/J.IJPHARM.2004.09.018.

[55] A. Chamas, H.T.M. Pham, M. Jähne, K. Hettwer, S. Uhlig, K. Simon, A. Einspanier, K. Baronian, G. Kunze, Simultaneous detection of three sex steroid hormone classes using a novel yeast-based biosensor, Biotechnol. Bioeng. 114 (2017) 1539–1549. https://doi.org/10.1002/BIT.26249.

[56] J. Racek, A yeast biosensor for glucose determination, Appl. Microbiol. Biotechnol. 1991 344. 34 (1991) 473–477. https://doi.org/10.1007/BF00180573.

[57] L. Campanella, G. Favero, M. Tomassetti, Immobilised yeast cells biosensor for total toxicity testing, Sci. Total Environ. 171 (1995) 227–234. https://doi.org/10.1016/0048-9697(95)04673-0.

[58] A. Heiskanen, C. Spégel, N. Kostesha, S. Lindahl, T. Ruzgas, J. Emnéus, Mediator-assisted simultaneous probing of cytosolic and mitochondrial redox activity in living cells, Anal. Biochem. 384 (2009) 11–19. https://doi.org/10.1016/J.AB.2008.08.030.

[59] I. Morkvenaite-Vilkonciene, A. Ramanaviciene, A. Ramanavicius, 9,10-Phenanthrenequinone as a redox mediator for the imaging of yeast cells by scanning electrochemical microscopy, Sensors Actuators B Chem. 228 (2016) 200–206. https://doi.org/10.1016/J.SNB.2015.12.102.

[60] B. Liu, S. Rotenberg, M.M., Scanning electrochemical microscopy of living cells: Different redox activities of nonmetastatic and metastatic human breast cells, Proceedings of the National Academy of Sciences

97.18 (2000): 9855-9860.

[61] J.W. Gallaway, S.A.C. Barton, Kinetics of Redox Polymer-Mediated Enzyme Electrodes, J. Am. Chem. Soc. 130 (2008) 8527–8536. https://doi.org/10.1021/JA0781543.

[62] J. Zhao, M. Wang, Z. Yang, Z. Wang, H. Wang, Z.Y. The different behaviors of three oxidative mediators in probing the redox activities of the yeast Saccharomyces cerevisiae, Analytica chimica acta 597.1 (2007): 67-74.

[63] T. Roukas, Citric and gluconic acid production from fig by Aspergillus niger using solid-state fermentation, J. Ind. Microbiol. Biotechnol. 2000 256. 25 (2000) 298–304. https://doi.org/10.1038/SJ.JIM.7000101.

[64] M. Papagianni, Advances in citric acid fermentation by Aspergillus niger: Biochemical aspects, membrane transport and modeling, Biotechnol. Adv. 25 (2007) 244–263. https://doi.org/10.1016/J.BIOTECHADV.2007.01.002.

[65] S. Solís-Pereira, E. Favela-Torres, G. Viniegra-González, M. Gutiérrez-Rojas, Effects of different carbon sources on the synthesis of pectinase by Aspergillus niger in submerged and solid state fermentations, Appl. Microbiol. Biotechnol. 1993 391. 39 (1993) 36–41. https://doi.org/10.1007/BF00166845.

[66] H. Tsuge, O. Natsuaki, K. Ohashi, Purification, Properties, and Molecular Features of Glucose Oxidase from Aspergillus niger, J. Biochem. 78 (1975) 835–843. https://doi.org/10.1093/OXFORDJOURNALS.JBCHEM.A130974.

[67] A. Ogoshi, Introduction — The Genus Rhizoctonia Rhizoctonia Species Taxon. Mol. Biol. Ecol. Pathol. Dis. Control. (1996) 1–9. https://doi.org/10.1007/978-94-017-2901-7_1.

[68] L. Tsror, Biology, Epidemiology and Management of Rhizoctonia solani on Potato, J. Phytopathol. 158 (2010) 649–658. https://doi.org/10.1111/J.1439-0434.2010.01671.X.

[69] M. Gerard, A. Chaubey, B.D. Malhotra, Application of conducting polymers to biosensors, Biosens. Bioelectron. 17 (2002) 345–359. https://doi.org/10.1016/S0956-5663(01)00312-8.

[70] X. Luo, A. Morrin, A.J. Killard, M.R. Smyth, Application of Nanoparticles in Electrochemical Sensors and Biosensors, Electroanalysis. 18 (2006) 319–326. https://doi.org/10.1002/ELAN.200503415.

[71] R.H. Newman, M.D. Fosbrink, J. Zhang, Genetically Encodable Fluorescent Biosensors for Tracking Signaling Dynamics in Living Cells, Chem. Rev. 111 (2011) 3614–3666. https://doi.org/10.1021/CR100002U.

[72] R. Jain, N. Jadon, A. Pawaiya, Polypyrrole based next generation electrochemical sensors and biosensors: A review, TrAC Trends Anal. Chem. 97 (2017) 363–373.

https://doi.org/10.1016/J.TRAC.2017.10.009.

[73]   H. Su, S. Li, Y. Jin, Z. Xian, D. Yang Wenxia Zhou, F. Mangaran, F. Leung, G. Sithamparanathan, K. Kerman, Advanced Health Care Technologies, (2017) 3–19. https://doi.org/10.2147/AHCT.S94025.

[74]   BardMiguel A. Correa-Duarte, , Nicholas Wagner, José Rojas-Chapana, Christian Morsczeck, and Michael Thie, Michael Giersig, Fabrication and Biocompatibility of Carbon Nanotube-Based 3D Networks as Scaffolds for Cell Seeding and Growth, Nano Lett. 4 (2004) 2233–2236. https://doi.org/10.1021/NL048574F.

[75]   J. Lian, X. Tian, Z. Li, J. Guo, Y. Guo, L. Yue, J. Ping, L. Duan, The effects of different electron donors and electron acceptors on perchlorate reduction and bioelectricity generation in a microbial fuel cell, Int. J. Hydrogen Energy. 42 (2017) 544–552. https://doi.org/10.1016/J.IJHYDENE.2016.11.027.

[76]   A.A. Yazdi, L. D'Angelo, N. Omer, G. Windiasti, X. Lu, J. Xu, Carbon nanotube modification of microbial fuel cell electrodes, Biosens. Bioelectron. 85 (2016) 536–552. https://doi.org/10.1016/J.BIOS.2016.05.033.

[77]   R.A. Bullen, T.C. Arnot, J.B. Lakeman, F.C. Walsh, Biofuel cells and their development, Biosens. Bioelectron. 21 (2006) 2015–2045. https://doi.org/10.1016/J.BIOS.2006.01.030.

[78]   G.G. Kumar, V.G.S. Sarathi, K.S. Nahm, Recent advances and challenges in the anode architecture and their modifications for the applications of microbial fuel cells, Biosens. Bioelectron. 43 (2013) 461–475. https://doi.org/10.1016/J.BIOS.2012.12.048.

[79]   G. Bagdžiūnas, Š. Žukauskas, A. Ramanavičius, Insights into a hole transfer mechanism between glucose oxidase and a p-type organic semiconductor, Biosens. Bioelectron. 102 (2018) 449–455. https://doi.org/10.1016/J.BIOS.2017.11.053.

[80]   F. Pillet, C. Formosa-Dague, H. Baaziz, E.D., Cell wall as a target for bacteria inactivation by pulsed electric fields, Scientific reports 6.1 (2016): 1-8.

[81]   M. Lu, Y. Qian, L. Huang, X. Xie, W. Huang, Improving the Performance of Microbial Fuel Cells through Anode Manipulation, Chempluschem. 80 (2015) 1216–1225. https://doi.org/10.1002/CPLU.201500200.

[82]   A. Zebda, S. Tingry, C. Innocent, S. Cosnier, C. Forano, C. Mousty, Hybrid layered double hydroxides-polypyrrole composites for construction of glucose/O2 biofuel cell, Electrochim. Acta. 56 (2011) 10378–10384. https://doi.org/10.1016/J.ELECTACTA.2011.01.101.

[83]   M. Mashkour, M. Rahimnejad, M. Mashkour, Bacterial cellulose-polyaniline nano-biocomposite: A porous media hydrogel bioanode enhancing the performance of microbial fuel cell, J. Power Sources. 325 (2016) 322–328. https://doi.org/10.1016/J.JPOWSOUR.2016.06.063.

[84] M. Ammam, J. Fransaer, Glucose/O2 biofuel cell based on enzymes, redox mediators, and Multiple-walled carbon nanotubes deposited by AC-electrophoresis then stabilized by electropolymerized polypyrrole, Biotechnol. Bioeng. 109 (2012) 1601–1609. https://doi.org/10.1002/BIT.24438.

[85] S. Cosnier, Biomolecule immobilization on electrode surfaces by entrapment or attachment to electrochemically polymerized films. A review, Biosens. Bioelectron. 14 (1999) 443–456. https://doi.org/10.1016/S0956-5663(99)00024-X.

[86] Y. Zou, C. Xiang, L. Yang, L.X. Sun, F. Xu, Z. Cao, A mediatorless microbial fuel cell using polypyrrole coated carbon nanotubes composite as anode material, Int. J. Hydrogen Energy. 33 (2008) 4856–4862. https://doi.org/10.1016/J.IJHYDENE.2008.06.061.

[87] A. Ramanaviciene, A. Kausaite, S.T., Biocompatibility of polypyrrole particles: an in-vivo study in mice, Journal of pharmacy and pharmacology 59.2 (2007): 311-315. https://doi.org/10.1211/jpp.59.2.0017.

[88] A. Vaitkuviene, V. Kaseta, J. Voronovic, G. Ramanauskaite, G. Biziuleviciene, A. Ramanaviciene, A. Ramanavicius, Evaluation of cytotoxicity of polypyrrole nanoparticles synthesized by oxidative polymerization, J. Hazard. Mater. 250–251 (2013) 167–174. https://doi.org/10.1016/J.JHAZMAT.2013.01.038.

[89] A. Vaitkuviene, V. Ratautaite, L. Mikoliunaite, V. Kaseta, G. Ramanauskaite, G. Biziuleviciene, A. Ramanaviciene, A. Ramanavicius, Some biocompatibility aspects of conducting polymer polypyrrole evaluated with bone marrow-derived stem cells, Colloids Surfaces A Physicochem. Eng. Asp. 442 (2014) 152–156. https://doi.org/10.1016/J.COLSURFA.2013.06.030.

[90] R. Apetrei, G. Carac, G. Bahrim, A.R.-, Modification of Aspergillus niger by conducting polymer, Polypyrrole, and the evaluation of electrochemical properties of modified cells, Bioelectrochemistry 121 (2018): 46-55

[91] A. Ramanavicius, E. Andriukonis, A. Stirke, L. Mikoliunaite, Z. Balevicius, A. Ramanaviciene, Synthesis of polypyrrole within the cell wall of yeast by redox-cycling of [Fe(CN)6]3−/[Fe(CN)6]4−, Enzyme Microb. Technol. 83 (2016) 40–47. https://doi.org/10.1016/J.ENZMICTEC.2015.11.009.

[92] X. Xin, G. Huang, C. An, C. Huang, H. Weger, S. Zhao, Y. Zhou, S. Rosendahl, Insights into the Toxicity of Triclosan to Green Microalga Chlorococcum sp. Using Synchrotron-Based Fourier Transform Infrared Spectromicroscopy: Biophysiological Analyses and Roles of Environmental Factors, Environ. Sci. Technol. 52 (2018) 2295–2306. https://doi.org/10.1021/ACS.EST.7B05533.

[93] P.J. Reeve, H.J. Fallowfield, The toxicity of cationic surfactant HDTMA-Br, desorbed from surfactant modified zeolite, towards

faecal indicator and environmental microorganisms, J. Hazard. Mater. 339 (2017) 208–215. https://doi.org/10.1016/J.JHAZMAT.2017.06.022.

[94] A. Stirke, R.M. Apetrei, M. Kirsnyte, L. Dedelaite, V. Bondarenka, V. Jasulaitiene, M. Pucetaite, A. Selskis, G. Carac, G. Bahrim, A. Ramanavicius, Synthesis of polypyrrole microspheres by Streptomyces spp., Polymer (Guildf). 84 (2016) 99–106. https://doi.org/10.1016/J.POLYMER.2015.12.029.

[95] I. Morkvenaite-Vilkonciene, A. Ramanaviciene, A. Kisieliute, V. Bucinskas, A. Ramanavicius, Scanning electrochemical microscopy in the development of enzymatic sensors and immunosensors, Biosens. Bioelectron. 141 (2019) 111411. https://doi.org/10.1016/J.BIOS.2019.111411.

[96] F. Conzuelo, S. Grützke, L. Stratmann, J.M. Pingarrón, W. Schuhmann, Interrogation of immunoassay platforms by SERS and SECM after enzyme-catalyzed deposition of silver nanoparticles, (n.d.). https://doi.org/10.1007/s00604-015-1654-x.

[97] W. Song, Z. Yan, K. Hu, Electrochemical immunoassay for CD10 antigen using scanning electrochemical microscopy, Biosens. Bioelectron. 38 (2012) 425–429. https://doi.org/10.1016/J.BIOS.2012.06.002.

[98] S. Kasai, H. Shiku, Y. suke Torisawa, K. Nagamine, T. Yasukawa, T. Watanabe, T. Matsue, Cytokine assay on a cellular chip by combining collagen gel embedded culture with scanning electrochemical microscopy, Anal. Chim. Acta. 566 (2006) 55–59. https://doi.org/10.1016/J.ACA.2006.02.061.

[99] F. Conzuelo, L. Stratmann, S. Grützke, J.M. Pingarrón, W. Schuhmann, Detection and Quantification of Sulfonamide Antibiotic Residues in Milk Using Scanning Electrochemical Microscopy, Electroanalysis. 26 (2014) 481–487. https://doi.org/10.1002/ELAN.201300577.

[100] G. Wittstock, K. jia Yu, H.B. Halsall, T.H. Ridgway, W.R. Heineman, Imaging of Immobilized Antibody Layers with Scanning Electrochemical Microscopy, Anal. Chem. 67 (1995) 3578–3582. https://doi.org/10.1021/AC00115A030.

[101] C.A. Wijayawardhana, G. Wittstock, + H Brian Halsall, W.R. Heineman, Electrochemical Immunoassay with Microscopic Immunomagnetic Bead Domains and Scanning Electrochemical Microscopy, (n.d.). https://doi.org/10.1002/1521-4109(200005)12:9.

[102] D.T. Pierce, P.R. Unwin, A.J. Bard, Enzyme-Mediator Kinetics for Membrane-and Surface-Immobilized Glucose Oxidase, Anal. Chem. 64 (1992) 1795–1804. https://pubs.acs.org/sharingguidelines (accessed September 11, 2021).

[103] E. Engvall, P. Perlmann, Enzyme-Linked Immunosorbent Assay, Elisa, J. Immunol. 109 (1972).

[104] I. Morkvenaite-Vilkonciene, A. Ramanaviciene, P. Genys, A. Ramanavicius, Evaluation of Enzymatic Kinetics of GOx-based Electrodes by Scanning Electrochemical Microscopy at Redox Competition Mode, Electroanalysis. 29 (2017) 1532–1542. https://doi.org/10.1002/ELAN.201700022.

[105] H. Shiku, Y. Hara, T. Matsue, I. Uchida, T. Yamauchi, Dual immunoassay of human chorionic gonadotropin and human placental lactogen at a miocrofabricated substrate by scanning electrochemical microscopy, J. Electroanal. Chem. 438 (1997) 187–190. https://doi.org/10.1016/S0022-0728(96)04979-0.

[106] X. Ning, Q. Xiong, F. Zhang, P. He, Simultaneous detection of tumor markers in lung cancer using scanning electrochemical microscopy, (2018). https://doi.org/10.1016/j.jelechem.2018.01.061.

[107] A. Zinovicius, I. Morkvenaite-Vilkonciene, A. Ramanaviciene, J. Rozene, A. Popov, A. Ramanavicius, Scanning Electrochemical Impedance Microscopy in Redox-Competition Mode for the Investigation of Antibodies Labelled with Horseradish Peroxidase, Mater. 2021, Vol. 14, Page 4301. 14 (2021) 4301. https://doi.org/10.3390/MA14154301.

[108] E.R. Scott, H.S. White, J.B. Phipps, Iontophoretic Transport through Porous Membranes Using Scanning Electrochemical Microscopy: Application to in Vitro Studies of Ion Fluxes through Skin, Anal. Chem. 65 (1993) 1537–1545. https://pubs.acs.org/sharingguidelines (accessed September 20, 2021).

[109] B.D. Bath, R.D. Lee, H.S. White, E.R. Scott, Imaging Molecular Transport in Porous Membranes. Observation and Analysis of Electroosmotic Flow in Individual Pores Using the Scanning Electrochemical Microscope, Anal. Chem. 70 (1998) 1047–1058. https://doi.org/10.1021/AC971213I.

[110] S. Wilkinson, J. Klar, S.A., Optimizing biofuel cell performance using a targeted mixed mediator combination, Electroanalysis: An International Journal Devoted to Fundamental and Practical Aspects of Electroanalysis 18.19-20 (2006): 2001-2007. https://doi.org/10.1002/elan.200603621.

[111] K. Habermüller, M. Mosbach, W. Schuhmann, Electron-transfer mechanisms in amperometric biosensors, Fresenius. J. Anal. Chem. 366 (2000) 560–568. https://doi.org/10.1007/S002160051551.

[112] J. Mauzeroll, A.B., Scanning electrochemical microscopy of menadione-glutathione conjugate export from yeast cells Proceedings of the National Academy of Sciences 101.21 (2004): 7862-7867.

[113] A. Heiskanen, J. Yakovleva, C.S. Amperometric monitoring of redox activity in living yeast cells: comparison of menadione and menadione sodium bisulfite as electron transfer mediators, Electrochemistry communications 6.2 (2004): 219-224

[114] E. Andriukonis, A. Stirke, A.G., Yeast-assisted synthesis of

polypyrrole: Quantification and influence on the mechanical properties of the cell wall, Colloids and Surfaces B: Biointerfaces 164 (2018): 224-231

[115] Guang Jia, Haifang Wang, Lei Yan, Xiang Wang, Rongjuan Pei, Tao Yan, ,‡, and Yuliang Zhao, Xinbiao Guo, Cytotoxicity of Carbon Nanomaterials: Single-Wall Nanotube, Multi-Wall Nanotube, and Fullerene, Environ. Sci. Technol. 39 (2005) 1378–1383. https://doi.org/10.1021/ES048729L.

[116] J.J. Gooding, R. Wibowo, J. Liu, W. Yang, D. Losic, S. Orbons, F.J. Mearns, J.G. Shapter, D.B. Hibbert, Protein electrochemistry using aligned carbon nanotube arrays, J. Am. Chem. Soc. 125 (2003) 9006–9007. https://doi.org/10.1021/JA035722F.

[117] Y. Hindatu, M. Annuar, A.G., Mini-review: Anode modification for improved performance of microbial fuel cell, Renewable and Sustainable Energy Reviews 73 (2017): 236-248

[118] R.A. Sheldon, Enzyme immobilization: the quest for optimum performance, Advanced Synthesis & Catalysis 349.8-9 (2007): 1289-1307. https://doi.org/10.1002/adsc.200700082.

[119] L. Zhou, H. Forman, Y. Ge, J.L., Multi-walled carbon nanotubes: a cytotoxicity study in relation to functionalization, dose and dispersion, Toxicology In Vitro 42 (2017): 292-298

[120] E. Zor, Y. Oztekin, L. Mikoliunaite, J.V, 1, 10-Phenanthroline-5, 6-dione and 9, 10-phenanthrenequinone as redox mediators for amperometric glucose biosensors, Journal of Solid State Electrochemistry 18.6 (2014): 1529-1536.

[121] V. Leskovac, S. Trivić, G. Wohlfahrt, J.K., Glucose oxidase from Aspergillus niger: the mechanism of action with molecular oxygen, quinones, and one-electron acceptors, The international journal of biochemistry & cell biology 37.4 (2005): 731-750

[122] C. Bonciu, O.C., Screening of biotechnological parameters for fructofuranosidases production by a newly isolated fungal strain using plackett-burman design, Notulae Botanicae Horti Agrobotanici Cluj-Napoca 39.2 (2011): 271-275.

[123] J.D. Crowe, S. Olsson, Induction of Laccase Activity in Rhizoctonia solani by Antagonistic Pseudomonas fluorescens Strains and a Range of Chemical Treatments, Appl. Environ. Microbiol. 67 (2001) 2088–2094. https://doi.org/10.1128/AEM.67.5.2088-2094.2001.

[124] A.Pometto, A.D., Technologies Used for Microbial Production of Food Ingredients, Functional Foods and Biotechnology. CRC Press, 2006. 541-552.

[125] M.Papagianni, Fungal morphology and metabolite production in submerged mycelial processes, Biotechnology advances 22.3 (2004): 189-259.

[126] S. Kelly, L.H. Grimm, J. Hengstler, E. Schultheis, R. Krull, D.C. Hempel, Agitation effects on submerged growth and product

formation of Aspergillus niger, Bioprocess Biosyst. Eng. 26 (2004) 315–323. https://doi.org/10.1007/S00449-004-0368-Y.

[127] Y. Han, Y.F, Conducting polyaniline and biofuel cell, International journal of green energy 3.1 (2006): 17-23.. https://doi.org/10.1080/01971520500198684.

[128] C. Feng, L. Ma, F. Li, H. Mai, X. Lang, S.F., A polypyrrole/anthraquinone-2, 6-disulphonic disodium salt (PPy/AQDS)-modified anode to improve performance of microbial fuel cells, Biosensors and Bioelectronics 25.6 (2010): 1516-1520

[129] M. Kizling, K. Stolarczyk, P. Tammela, Z.W., Bioelectrodes based on pseudocapacitive cellulose/polypyrrole composite improve performance of biofuel cell, Bioelectrochemistry 112 (2016): 184-190.

[130] Y. Yuan, S.K., Polypyrrole-coated reticulated vitreous carbon as anode in microbial fuel cell for higher energy output, Bulletin of the Korean Chemical Society 29.1 (2008): 168-172.

[131] Y. Qiao, C.M. Li, S.J. Bao, Q.L. Bao, Carbon nanotube/polyaniline composite as anode material for microbial fuel cells, J. Power Sources. 170 (2007) 79–84. https://doi.org/10.1016/J.JPOWSOUR.2007.03.048.

[132] S. Cheng, B.E. Logan, Ammonia treatment of carbon cloth anodes to enhance power generation of microbial fuel cells, Electrochem. Commun. 9 (2007) 492–496. https://doi.org/10.1016/J.ELECOM.2006.10.023.

[133] E. Corpas, S.M. Harman, M.R. Blackman, Human Growth Hormone and Human Aging, Endocr. Rev. 14 (1993) 20–39. https://doi.org/10.1210/EDRV-14-1-20.

[134] C.F.B. Witteveen, M. Veenhuis, J. Visser, Localization of glucose oxidase and catalase activities in Aspergillus niger, Appl. Environ. Microbiol. 58 (1992) 1190–1194. https://doi.org/10.1128/AEM.58.4.1190-1194.1992.

[135] L. Wei, H. Han, J.S., Effects of cathodic electron acceptors and potassium ferricyanide concentrations on the performance of microbial fuel cell, International journal of hydrogen energy 37.17 (2012): 12980-12986.

[136] G. Wittstock, K. Yu, H. Brian Halsall, T.H. Ridgway, W.R. Heineman, Adhesion and Adsorption of Polymers, J. Polym. Sci. Technol. 67 (1995) 47. https://pubs.acs.org/sharingguidelines (accessed September 11, 2021).

[137] N. German, A. Kausaite-Minkstimiene, J.K., Determination of antibodies against human growth hormone using a direct immunoassay format and different electrochemical methods, Analyst 138.5 (2013): 1427-1433.

[138] A. Makaraviciute, A. Ramanaviciene, Site-directed antibody immobilization techniques for immunosensors, Biosens. Bioelectron. 50 (2013) 460–471. https://doi.org/10.1016/J.BIOS.2013.06.060.

SANTRAUKA

ĮVADAS

Skenuojanti elektrocheminė mikroskopija (SECM) yra technika, kuria galima vizualizuoti įvairių paviršių vietinį elektrocheminį aktyvumą. SECM veikimo principas pagrįstas ultramikroelektrodu (UME), galinčiu užregistruoti 3D erdvinį elektrocheminį paviršiaus aktyvumą, kuriame vyktų katalizės/ redokso ar kitos elektrocheminės reakcijos. Šiuose eksperimentuose UME dažniausiai būna prijungtas kaip darbinis elektrodas elektrocheminėje sistemoje, o išmatuota srovė priklauso nuo elektroaktyviųjų medžiagų vietinės koncentracijos ir elektrodui suteikto potencialo. Pagrindinis SECM pranašumas yra tas, kad ši technika gali būti taikoma in situ tyrimams, nepažeidžiant dominančios sistemos paviršiaus. Be to, SECM gali būti naudojama didelės skiriamosios gebos vietinių cheminių reakcijų vaizdavimui ir ląstelių topografijai, biojutikliams, fermentams ir fermentų pagrindu suformuotoms sistemoms imunologiniuose tyrimuose ir kitiems tyrimams. SECM yra vertingas įrankis paviršių, modifikuotų biomedžiagomis, tyrimams, ir kuris galėtų būti pritaikytas kuriant ir tiriant biojutiklius ir biokuro elementus.

Mikrobiologiniai biokuro elementai (MFC) pastaruoju metu pasirodė kaip labai patrauklūs elektros energijos šaltiniai, galintys paversti cheminę energiją elektros srove ir gaminti elektros energiją biocheminiais redokso procesais net iš praskiestų biokuro tirpalų. Šis pranašumas atveria galimybes taikyti MFC elektros srovės generavimui ir nuotekų valymui tuo pačiu metu. Tačiau pagrindinė MFC efektyvumo problema vis dar išlieka dėl krūvio pernašos, todėl daugumą tyrimų siekia sukurti naujus metodus, pagerinančius MFC našumą. Kai kurių laidžių medžiagų (pvz., anglies nanovamzdelių, laidžių polimerų ir kt.) taikymas ir (arba) ląstelių imobilizavimas sudėtingose matricose gali pagerinti krūvio pernašą MFC. Taip pat, siekiant padidinti MFC stabilumą ir efektyvumą, galima naudoti efektyvesnius redokso tarpininkus, kurie būtų mažiau toksiški, ir ląstelių apgaubimą biologiškai suderinamą elektrai laidžią polimerine matrica.

Taip pat padidėjęs susidomėjimas elektrocheminių imunologinių tyrimų kūrimu, nes šie metodai gali būti sėkmingai naudojami kaip alternatyva gerai žinomam ir plačiai taikomam su fermentais susijusiam imunosorbentiniam tyrimui (ELISA). Sluoksniuotojo ELISA formato metu, fermentas, esantis ant paviršiaus, yra antikūno ir fermento konjugato pavidalu, ir aptinkamas naudojant skenuojantį elektrocheminį mikroskopą.

Redokso ir fermentinės reakcijos gali būti sėkmingai pritaikytos antigenams aptikti po giminingos sąveikos su antikūnais, pažymėtais fermentais lokalizuotose paviršiaus vietose, o antikūno-fermento konjugato kiekį galima įvertinti elektrocheminiu būdu. Didėjantis dėmesys elektrocheminiams metodams kyla dėl: mažesnio cheminių reagentų sunaudojimo, greitesnės analizės, gebėjimo jautriai nustatyti analizuojamą medžiagą ir galimybę miniatiūrizuoti elektrochemines sistemas.

Šio darbo tikslas buvo ištirti įvairiai modifikuotų biojutiklių ir imuninių-jutiklių bioelektrocheminį aktyvumą ir pagerinti krūvio pernašą. Įvertinti laidžių medžiagų, imobilizacijos metodų, ląstelių kultūrų, elekronų pernašos tarpininkų, elektrocheminių sistemų parametrų modifikavimo įtaką.

Darbo uždaviniai:
1. Ištirti redokso tarpininkų įtaką elektrocheminiam atsakui ir parinkti optimalius parametrus krūvio pernašai iš *Saccharomyces cerevisiae* ląstelių amperometriniams ir skenuojančios elektrocheminės mikroskopijos eksperimentams.
2. Įvertinti in situ polimerizuoto polipirolo įtaką *Saccharomyces cerevisiae* ląstelių bioelektrocheminiam atsakui naudojant skenuojančią elektrocheminę mikroskopiją.
3. Išanalizuoti daugiasienių nanovamzdelių ir/ar polipirolo įtaką *Saccharomyces cerevisiae* ląstelių bioelektrocheminiam atsakui ciklinės voltamperometrijos metodu.
4. Išnagrinėti in situ polimerizuoto polipirolo įtaką *Aspergillus niger* ir *Rhizoctonia species* ląstelių bioelektrocheminiam atsakui.
5. Surasti optimalius parametrus imuninio-jutiklio su gliukozės oksidazės žyme susiformavimo detekcijai su skenuojančia elektrochemine mikroskopija. Įvertinti imuninio komplekso su antikūnais prieš žmogaus augimo hormoną, pažymėtais gliukozės oksidaze, susiformavimą matematiniu modeliu.

Mokslinis naujumas
In situ mikroorganizmų padedama polipirolo polimerizacija yra naujas gyvų ląstelių modifikavimo laidžioje medžiagoje metodas, kurio elektrocheminės savybės turėtų būti atidžiai ištirtos. Mikroorganizmų padedamas polipirolo susidarymas galėtų būti naudojamas siekiant pagerinti mikrobiologinių biokuro elementų ir (arba) ląstelių pagrindu veikiančių biojutiklių elektrocheminį veikimą. Šiame tyrime mes išbandėme minėto tipo modifikacijas su gyvomis *Aspergillus niger*, *Rhizoctonia* sp. ir

Saccharomyces cerevisae ląstelėmis elektrocheminiais metodais: amperometriniais ir voltamperometriniais modifikuoto elektrodo matavimais ir amperometriniais paviršiaus matavimais skenuojančia elektrochemine mikroskopija.

Pastaruoju metu populiarėja tyrimai, nagrinėjantys įvairias imuninių tyrimų kūrimo strategijas, iš kurių vieni yra elektrocheminiai imuniniai tyrimai. Šių metodų pranašumai: jie gali būti greitesni, ekonomiškesni ir paprastesni. Šis tyrimas pademonstravo perspektyvią imunologinio tyrimo aspektų nagrinėjimo metodiką: antikūno ženklinimą fermentu, imobilizavimą, elektrocheminio aktyvumo vaizdinimo sąlygas. SECM substrato generacijos ir elektrodo surinkimo režimu (angl. SG-TC), esant tirpale kalio fericianidui - redokso tarpininkui, galima aptikti žmogaus augimo antigeną nekonkurenciniu sluoksniuotosios imunofermentinės analizės metodu su GOx pažymėtu žmogaus augimo antikūnu ir apskaičiuoti kokybinius ir kiekybinius rezultatus. Šio metodo tobulinimas neabejotinai dar labiau padidins analizės metu pasiekiamą jautrumą, taip pat kiekybinį įvertinimą.

Ginamieji teiginiai:

1. Naudojant 9,10-Fenantrenchinoną dviguboje elektronų pernašos sistemoje, galima užregistruoti didesnes *Saccharomyces cerevisiae* ląstelių bioelektrocheminio aktyvumo srovės stiprio vertes negu su kitais redokso tarpininkais ar vienguba sistema.

2. Naudojant skirtingas pirolo koncentracijas inkubaciniame tirpale 24 val. su imobilizuotomis *Saccharomyces cerevisiae* ląstėmis galima užregistruoti žemesnės krūvio pernašos vertės negu su kontrole, tiriant skenuojančiu elektrocheminiu mikroskopu ir taikant dvigubą 9,10-fenantrenchinono ir kalio fericianido redokso tarpininkų sistemą.

3. *Saccharomyces cerevisiae* ląstelės, imobilizuotos ant anglies veltinio elektrodo ir modifikuotos daugiasieniais anglies nanovamzdeliais arba polipirolu, pasižymi tarpusavyje panašiomis elektronų krūvio pernašos vertėmis ir didesnėmis negu kontrolė.

4. Polipirolo sintezė, panaudojant mikroorganizmus *Aspergillus niger* ir *Rhizoctonia species* ląsteles, kelis kartus padidina srovės stiprį, registruojant amperometriškai ir skenuojančiu elektrocheminiu mikroskopu, lyginant su kontrole.

5. Skenuojančio elektrocheminio mikroskopo substrato generacijos - elektrodo surinkimo režimas gali būti taikomas nustatyti žmogaus augimo hormoną nekonkurenciniu sluoksniuotosios imunofermentinės analizės metodu, naudojant antikūnus prieš žmogaus augimo hormoną, žymėtus

gliukozės oksidaze, su kalio fericianidu. Registruoti rezultatai, gali būti kiekybiškai įvertinti naudojant matematinį modelį.

EKSPERIMENTŲ METODIKA

Saccharomyces cerevisiae ląstelių kultūra buvo laikoma ant mitybinės terpės su agaru Petri lėkštelėje šaldytuve iki tyrimų. Prieš tyrimus, viena kolonija buvo perkeliama į kolbą su auginimo terpė, kurioje buvo inkubuojama 30°C apie 24 valandas. Po paros tirpalas buvo centrifuguojamas 3000 aps min^{-1} 3 minutes, plaunamas 3 kartus su fosfatiniu buferiu ir praskiedžiamos iki 0,33 arba 0,5 g mL^{-1} suspensijos.

Chronoamperometriniams matavimams buvo paruošta trijų elektrodų sistema: 25 μm skermens platinos UME – darbinis, Ag/AgCl(KCl$_{3M}$) – palyginamasis, platinos viela – pagalbinis elektrodas. Elektrodai buvo įmerkti į elektrocheminės celės (angl. ECC) buferio tirpalą ir įjungtas maišymas, bei nustatytas potencialas +0,4 V palyginus su Ag/AgCl(KCl$_{3M}$). Priklausomai nuo tyrimo, buvo išvirkščiami tirpalai į ECC specifiniu laiku iki galutinės koncentracijos: redokso tarpininkų (5 mM hidrofilinio ir 100 μM lipofilinio), mielių suspensijos (6,7 mg mL^{-1}), 10 mM gliukozės (Glc).

SECM eksperimentams buvo imobilizuojamos mielės ant Petri lėkštelės paviršiaus. Pradžioje paviršius buvo nuvalomas etanoliu, po to paeiliui užlašinamas 0,5 μL poli-L-lizino lašelis, palaukima, kol nudžius, tada užlašinama 0,5 μL mielių suspensijos lašelis, ir taip pat palaukiama, kol nudžius, prieš pradedant eksperimentus. SECM tyrimams buvo paruošta ta pati trijų elektrodų sistema (kaip ir chronoamperometriniuose tyrimuose) Petri lėkštelėje ir vykdomi tyrimai dviguboje redokso tarpininkų sistemoje su 5 mM kalio fericianidu (angl. KF) ir 100 μM 9,10-fenantrenchinonu (angl. PQ). Priartėjimo kreivėms UME judėjo 1 μm/s greičiu 0,5 μm/s link mielių paviršiaus ir 10 μm s^{-1} 10 μm žingsniais horizontaliuose skenavimuose.

Vėlesniems tyrimams ląstelės buvo modifikuojamos su pirolu (angl. Py) ir/arba daugiasieniais nanovamzdeliais (angl. MWCNT), jas inkubuojant tirpaluose (lentelė 1) ir maišant 24 valandoms 30°C termostate. Po inkubacijos, buvo centrifuguojamos, plaunamos, pagal aukščiau aprašytą metodiką ir paruošiamos 0,5 g mL^{-1} suspensijos. Šios ląstelės buvo imobilizuojamos ant Petri lėkštelės ir tiriamos SECM pagal aukščiau aprašytus metodus. Ciklinės voltamperometrijos (angl. CV) atveju, ląstelės buvo imobilizuojamos anglies veltinio elektrode (angl. CFE) $\varnothing = 1,5$ cm, praleidžiant 1 mL mielių suspensijos vakuuminiame aparate. Vėliau trijų elektrodų sistemoje, susidedančioje iš CFE, Kalomelio elektrodo ir plieno lazdelės, modifikuotos ląstelės buvo tiriamos 5 mV s^{-1} greičiu CV būdu,

įšvirkščiant paeiliui redokso tarpininkus: 50 μM PQ, 2,5 mM KF ir 10 mM gliukozės ir pateikiant trečio ciklo rezultatus.

Aspergillus niger ir *Rhizoctonia* ląstelės buvo auginamos specialioje mitybinėje terpėje 6 dienas, 27°C temperatūroje pastoviai maišant, po to buvo įpilta Py ir toliau inkubuojama 4 dienas, kad įvyktų modifikacija. Šios ląstelės buvo tiriamos amperometriškai, imobilizuojant ant ⌀ = 3 mm grafitinio strypo elektrodo 0,5 mg suspensijos, kartu su 4,5 μL 0,05 M išdžiūvusio 1,10-fenantrolin-5,6-dionu (angl. PD) trijų elektrodų sistemoje su Ag/AgCl(KCl$_{3M}$) ir platinos viela. Chronoamperometriniai tyrimai buvo vykdomi maišomoje ECC, su nustatytu +0,3 V potencialu, 10 μM KF, paeiliui didinant Glc koncentraciją 5-300 mM. Po to buvo vykdomi *Aspergillus niger* SECM tyrimai su prieš tai aprašyta imobilizavimo ir SECM tyrimo metodika.

Auksiniai mikrodiskai ⌀ = 30/50 μm 1 mm atstumu ant stiklinio lusto buvo pagaminti ir naudoti prijungiant kovalentiškai savitvarkį monosluoksnį (angl. SAM). Ant šio sluoksnio buvo paeiliui imobilizuojami sluoksniuotosios imunofermentinės analizės antigenai ir antikūnai prieš žmogaus augimo hormoną (28 pav.). SECM tyrimams buvo paruošta 2 elektrodų sistema susidedančia iš: UME ir sidabrinės vielos (veikiančios kaip pseudo-palyginamsis elektrodas), kurie buvo įmerkti į ECC su imobilizuotu ant aukso paviršiaus imuninio komplekso (ar jo dalies) mėginiu, esant tirpale 5 mM ferocenmetanolio arba KF, veikiančius kaip redokso tarpininkus. Pradžioje UME buvo atliekami priartėjimai prie nelaidžios stiklo paviršiaus dalies, su nustatytu 0,3 V potencialu. Vėliau, nustačius atstumą iki paviršiaus, UME buvo atitraukiamas 5 μm atstumu ir skenuojamas paviršius.

REZULTATŲ APTARIMAS

Bioelektrocheminis *Saccharomyces cerevisiae* aktyvumas

Amperometriniuose *Saccharomyces cerevisiae* ląstelių tyrimuose buvo taikyta dviguba redokso tarpininko sistema, o jos veikimo schema parodyta 5 pav. Redokso tarpininkai perneša elektronus reakcijų grandinėje, kuri jungia tarpląstelinį aktyvumą su terpe, už ląstelės ribų, todėl susidaro elektronų srovė, kuri gali būti užregistruojama ultramikroelektrodu (angl. UME). Lipofilinis redokso tarpininkas įsiskverbia į ląstelės membraną ir perneša elektronus į fericianido/ferocianido pagrindu veikiančią užląstelinę sistemą iš NAD$^+$ ir NADP$^+$ priklausomų flavoproteinų, sieros-geležies turinčių baltymų, chinonų, citochromų ir kai kurių kitų junginių, dalyvaujančių su metabolizmu susijusiuose ląstelės redokso procesuose. Kiekybinei analizei buvo naudojama dviguba redokso tarpininko sistema, kurią sudarė lipofilinis redokso

tarpininkas ir hidrofilinis redokso tarpininkas – kalio fericianidas (ang. KF), kuris veikė kaip užląstelinis elektronų akceptorius. Šio tipo sistemos gali vadintis "antrosios kartos biojutikliais", kuriuose naudojami dirbtiniai redokso tarpininkai, pasižymintys grįžtamomis elektronų perdavimo savybėmis, ir kurie buvo naudojami kaip laisvai difunduojantys elektronų perdavimo kompleksai. Mikroorganizmų sukaupta redukuoto redokso tarpininko koncentracija buvo tiesiogiai proporcinga ląstelių metabolizmo greičiui. Mikroorganizmo redokso aktyvumas susietas su ląstelės kvėpavimu per elektronų pernašos grandinę, todėl, analizuojant gyvos ląstelės metabolinę būseną, tai gali būti naudojama toksiškumo lygio nustatymui.

Amperometriniai matavimai

Pirmiausiai, siekiant nustatyti efektyviausią redokso tarpininką, buvo lyginama šešių skirtingų lipofilinių junginių elektronų pernaša (6A pav). Buvo išmatuoti srovės stipriai: didžiausiu pasižymėjo PQ $i_T(PQ) = 8,10$ nA, antroje vietoje - menadionas (angl. MD) $i_T(MD) = 6,65$ nA, mažiausiu - PD $i_T(PD) = 0,07$ nA ir fenazinmetasulfatas (angl. PMS) i_T (PMS) $= 0,03$ nA. Tolimesniems eksperimentams buvo pasirinktas PQ kaip lipofilinis redokso tarpininkas, nes jis užfiksavo didžiausias UME srovės stiprio vertes.

Taip pat, tyrimuose buvo išmatuota krūvio pernaša skirtingose redokso tarpininkų sistemose (vienguboje/dviguboje). Buvo išmatuota hidrofilinio redokso tarpininko sistema: $i_T(KF) = 0,20$ nA ir $i_T(KF+Glc) = 0,21$ nA, taip pat dviguba redokso tarpininko sistema: $i_T(KF+PQ) = 3,53$ nA ir $i_T(KF+PQ+Glc) = 6,61$ nA (6B pav.). Dėl didesnio užregistruojamo srovės stiprio, buvo pasirinkta dviguba redokso tarpininko sistema su gliukoze.

Vėlesniuose eksperimentuose buvo užregistruotas *S. cerevisiae* ląstelių bioelektrocheminis aktyvumas poros valandų periode, kuriame srovės stiprio nusistovėjimas pasiektas aplink 15 minutę, po 30 minučių pradėjo kristi, o po 2 valandų nukrito beveik trečdaliu. (7B pav.).

Tolimesniems *Saccharomyces cerevisiae* ląstelių tyrimams buvo pasirinkta dviguba redokso tarpininkų sistema su KF ir PQ, gliukoze, nes tokioje sistemoje buvo užregistruota didžiausia elektronų pernaša.

SECM matavimai

SECM tyrimams elektrocheminė celė buvo su imobilizuotomis *S. cerevisiae* ląstelėmis ant Petri lėkštelės kaip aprašyta metodų skiltyje. Pirmiausiai, buvo atliktos priartėjimo kreivės virš ląstelių paviršiaus, kad būtų įvertintas atstumas iki jų. Iš priartėjimo kreivių buvo pastebėta, kad srovės stipris didėja, kol buvo pasiektas $i_T(max)$ = 3,03 nA arti ląstelių paviršiaus (5A pav.). Vėliau, UME buvo atitrauktas 20/50/100 μm atstumu nuo paviršiaus ir buvo atlikti horizontalūs skenavimai. Buvo pastebėta, kad, tolstant nuo paviršiaus, srovės pokytis (nuo foninės srovės) mažėja: $\Delta i(20\mu m)$ = 0,13 nA, $\Delta i(50\mu m)$ = 0,12 nA, $\Delta i(100\mu m)$ = 0,10 nA) (8B pav.).

Vėliau buvo atlikti imobilizuotų ląstelių paviršiaus metabolinio aktyvumo skenavimai. Pradžioje buvo atlikti priartėjimai prie paviršiaus, tada buvo registruota horizontalaus skenavimo kreivė $\Delta i(2D)$ = 0,55 nA (9A pav.) ir galiausiai, 3D paviršiaus vaizdinimas (6B pav.) $\Delta i(3D)$ = 0,41 nA.

Tolimesniems ląstelių tyrimams buvo pasirinkta imobilizavimo technika ant poli-L-lizino ir pasirinktas 20 μm atstumas eksperimentams su SECM, nes buvo fiksuotas didžiausias srovės pokytis ir nebuvo rizikos apteršti elektrodo.

Popipirolu ir nanovamzdeliais modifikuotų *Saccharomyces cerevisiae* ląstelių tyrimas

Norint pagerinti bioelektrocheminius prietaisus kaip biojutiklius ar mikrobinius kuro elementus (ang. MFC), buvo išbandyta nauja technika elektronų pernašai – ląstelės buvo modifikuojamos pirolu arba daugiasieniais nanovamzdeliais (10 pav.).

Skirtumams pastebėti tarp pirolu modifikuotų ir nemodifikuotų ląstelių buvo pasitelktas optinis mikroskopas (11 pav). Kontrolinės ląstelės mikrografose atrodė vienodos formos ir beveik peršviečiamos. Tuo tarpu Py modifikuotos ląstelės buvo išskirtinės: jų sienelės buvo storesnės ir tamsesnės su polipirolo aglomeratais tarp jų.

Dėl detalesnio įvertinimo buvo pasitelktas atominių jėgų mikroskopas, kuriuo buvo įvertintas paviršiaus šiurkštumas ir padarytos aukštesnės rezoliucijos nuotraukos (12 pav). Šiurkštumo vertės buvo apskaičiuotos ir pateiktos 3 lentelėje. Iš jų buvo nustatyta, kad ląstelės, modifikuotos didesne pirolo koncentracija, pasižymėjo didesniu šiurkštumu: $R_a(0M)$ = 0,48, $R_a(0,05M)$ = 0,21, $R_a(0,1M)$ = 0,22, $R_a(0,3M)$ = 0,70, ($R_a(0,5M)$ = 1,19. Buvo padaryta išvada, kad didėjanti pirolo koncentracija inkubaciniame tirpale, sudarydavo ląstelių sienelėse didesnes ir tankesnes polipirolo

struktūras, kurios varijuodavo savo forma ir išsidėstymu, palyginus su kontrolinėmis ląstelėmis, kurių ląstelių paviršius buvo plokščias ir lygus.

Buvo ištirta pirolo modifikavimo įtaka imobilizuotų ant Petri lėkštelės ląstelių elektronų pernašai su SECM. Pirmiausiai, buvo įvykdyti priartėjimai prie ląstelių paviršiaus ir užregistruoti srovės stipriai: $i_T(C) = 0,34$ nA, $i_T(0,1M) = 0,17$ nA, $i_T(0,3M) = 0,12$ nA, $i_T(0,5M) = 0,04$ nA (13A pav.). Vėliau buvo užregistruoti horizontalūs skenavimai esant 20 µm virš ląstelių paviršiaus: $\Delta i(C) = 0,19$ nA, $\Delta i(0,1M) = 0,15$ nA, $\Delta i(0,3M) = 0,06$ nA, $\Delta i(0,5M) = 0,02$ nA (13B pav). Iš šių rezultatų buvo pastebėta, kad pirolas darė įtaką ląstelių gyvybingumui, galėjo būti apsunkinta pernaša pro ląstelės sienelę arba pasireiškė pirolo toksiškumas.

Ląstelės, modifikuotos Py ir MWCNT, buvo ištirtos ciklinės voltamperometrijos metodu, jas imobilizavus ant anglies veltinio elektrodo (16-18 pav.). Esant tirpale lipofilinio redokso tarpininko, aukščiausiu oksidaciniu aktyvumu pasižymėjo ląstelės, modifikuotos I tirpalu $i_T(I) = 0.10$ mA (19A pav.). Dviguboje redokso tarpininkų sistemoje didžiausia oksidacinė smailė buvo pasiekta su ląstelėmis, modifikuotomis 0,5 mg mL^{-1} MWCNT ($i_T(0.5) = 1.85$ mA) ir 0,3 M Py ($i_T(0.3Py) = 1.62$ mA) (19B pav.).

Iš šių eksperimentų buvo pastebėta, kad polipirolu modifikuotos ląstelės, kurios turėjo artimą sąlytį su elektrodu, pasižymėjo didesne elektronų pernaša, nei kontrolės ląstelės, todėl tolimesniuose eksperimentuose buvo toliau plėtojami tyrimai su polipirolu.

Polipirolu modifikuotų *Aspergillus niger* ir *Rhizoctonia* species ląstelių tyrimai

Vienas iš uždavinių buvo ištirti pirolu modifikuotų *Aspergillus niger* (angl. AN) ir *Rhizoctonia* species (RS) ląstelių kultūrų elektrochemines savybes. Buvo įvertinti AN ląstelių pokyčiai optiniu ir skenuojančiu elektroniniu mikroskopu (20,21 pav.). Iš mikrografų buvo nustatyta, kad po 2 dienų inkubaciniame tirpale su pirolu, polipirolas susidarė daugiausiai aplink ląstelių/grybienos sieneles, tačiau buvo pastebėtas ir kultivavimo terpėje.

Dviguba redokso tarpininkų sistema buvo pritaikyta amperometriniams modifikuoto grafitinio strypo (angl. GR) elektrodo ir SECM matavimams. Atlikti GR/PD elektrodų, modifikuotų ląstelėmis (AN ir RS), amperometriniai matavimai, priklausomi nuo gliukozės koncentracijos (23 pav.). Buvo nustatyti amperometriniai signalai 300 mM gliukozės koncentracijai: $\Delta I(AN:Py) = 1,82$ µA, $\Delta I(AN) = 0,18$ µA, $\Delta I(RS:Py) = 0.88$ µA, $\Delta I(RS) = 0.20$ µA. Iš šių rezultatų buvo matyti, kad nemodifikuotų ląstelių

amperometrinė srovė tarpusavyje buvo panaši, tačiau po modifikavimo su pirolu, RS ląstelių krūvio pernaša pakilo 4 kartais, o AN net 10 kartų.

Tolimesniems tyrimams buvo naudotos AN ląstelės, kadangi su jomis buvo užregistruota didesnė elektronų pernaša. Ląstelės buvo tirtos su SECM esant dvigubai redokso tarpininkų sistemai su PQ. Pradžioje buvo atlikti priartėjimai prie ląstelių paviršiaus, kurių metu nustatyta: i_T(An:Ppy) = 0,86 nA) ir i_T(AN) = 0,30 nA (24 pav.). Vėliau buvo užregistruotos horizontalaus skenavimo kreivės virš modifikuotų ir nemodifikuotų AN ląstelių, varijuojant atstumą 20/50/100/200 µm (25A,B pav). Rezultatai palyginimui buvo pavaizduoti histogramoje (22C pav.), iš jos buvo matyti, kad polipirolu modifikuotų ląstelių elektronų pernaša esant 20 µm atstumui buvo didesnė apie 1,5 karto: i_T(AN:Py) = 0,47 nA i_T(AN) = 0,31 nA. Didėjant atstumui nuo ląstelių paviršiaus, srovės pokytis mažėjo ir susilygino tarpusavyje ties 200 µm.

Iš šių eksperimentų buvo padaryta išvada, kad in situ pirolo modifikacija *Aspergillus niger* ir *Rhizoctonia* ląstelėse padidino elektronų pernašą amperometriniuose tyrimuose su modifikuotu grafitinio strypo elektrodu ir SECM. Šis modifikavimo metodas gali būti pritaikomas biojutiklių ar mikrobinių kuro elementų vystimui.

Skenuojančio elektrocheminio mikroskopo taikymas žmogaus augimo hormono detekcijai

Siekiant išplėsti SECM pritaikomumą, buvo kuriamas elektrocheminis metodas, dominančiam antigenui aptikti, naudojant nekonkurencinį sluoksniuotosios imunofermentinės analizės metodą ir nustatant antikūno-gliukozės oksidazės (angl. GOx) konjugatą. Kaip modelinė sistema buvo pasirinktas žmogaus augimo hormonas (angl. hGH) ir 2 specifiniai antikūnai: monokloniniai (angl. m-anti-hGH) ir polikloniniai su gliukozės oksidazės žyme (angl. p-anti-hGH-GOx).

Po hGH sąveikos su imobilizuotais antikūnais (m-anti-hGH), p-anti-hGH-GOx specifiškai susijungia su hGH ir susidaro imuninis kompleksas (m-anti-hGH/hGH/p-anti-hGH-GOx) (24 pav.). Tokiu būdu aptiktamas lokalizuotas GOx fermento aktyvumas, naudojant SECM generacijos detekcijos (angl. GC) režimą, o registruota srovė priklauso nuo hGH koncentracijos mėginyje. GOx fermentas yra naudojamas pirmą kartą SECM imuninių jutiklių tyrimuose. Antikūnų-GOx konjugatai katalizuoja gliukozės oksidaciją, kai tirpale yra gliukozės. Šios fermentinės reakcijos metu susidaro redukuota (red) redokso tarpininko forma, kuri iš aktyvaus GOx centro patenka į tirpalo terpę ir užregistruoja UME.

Imunofermentinės analizės sluoksniai buvo imobilizuojami pagal (28 pav.) schemą ant aukso (angl. Au) taškų paviršiaus su savitvarkiu monosluoksniu (angl. SAM). Pirmuosiuose eksperimentuose buvo naudojamas dažnas imunojutiklių redokso tarpininkas - ferocenmetanolis (FeMeOH), tirpalai be gliukozės buvo pažymėti A raide, o su gliukoze - B raide. Kontroliniuose bandymuose, virš aukso taškų buvo užregistruoti srovės pokyčiai: (Au) $i_{max}(A) \approx 4,3$ nA ir $i_{max}(B) \approx 4,2$ nA (29 pav.). Aukštas signalas buvo užregistruotas dėl aukso taškų paviršiaus įtakos, imobilizavus imunojutiklio sluoksnius, šis signalas mažėjo, nes jie veikdavo kaip izoliaciniai sluoksniai. Srovės pokyčiai virš skirtingų paviršių buvo užregistruoti: (Au-SAM) $i_{max}(A) \approx 3,4$ nA ir $i_{max}(B) \approx 3,6$ nA, (Au-SAM/hGH) $i_{max}(A) \approx 2,8$ nA ir $i_{max}(B) \approx 2,8$ nA, (Au-SAM/Anti-hGH-GOx) $i_{max}(A) \approx 3,3$ nA ir $i_{max}(B) \approx 3,6$ nA, (Au-SAM/hGH/Anti-hGH-GOx) $i_{max}(A) \approx 2,5$ nA ir $i_{max}(B) \approx 3,5$ nA (30-33 pav). Atlikti eksperimentai parodė, kad šiuo metodu buvo galima aptikti žmogaus augimo hormoną, esantį imuno komplekse, nes buvo užregistruoti srovės pokyčiai, į tirpalą įpylus gliukozės. Tačiau, aukso signalas buvo nepageidaujamas šalutinis efektas, ir nors jis mažėjo didinant imunofermentinės analizės sluoksnius, vėlesni tyrimai buvo planuojami, kad jo būtų išvengta.

Antroje eksperimentų serijoje, buvo atlikti keli sistemos pakeitimai, iš kurių vienas: pakeistas redokso tarpininkas į kalio fericianidą. Kontroliniai eksperimentai parodė, kad šiuose ekperimentuose neliko dėl aukso skleidžiamo signalo: (Au-SAM) tirpale be gliukozės (A) $\Delta i(A)$ ir tirpale esant gliukozei (C) $\Delta i(C)$ srovės stiprio pokyčiai buvo mažesni nei 1 pA (35 pav.). Virš kitų paviršių užregistruoti srovės pokyčiai: (Au-SAM/p-anti-hGH-GOx 100 nM) $\Delta i(A) \approx 5$ pA ir $\Delta i(C) \approx 10$ pA, (Au-SAM/p-anti-hGH-GOx 10 nM) ($\Delta i(C) \approx 2$ pA), (Au-SAM/hGH) $\Delta i(A) \approx 1$ pA ir $\Delta i(C) \approx 1$ pA, (Au-SAM/hGH/anti-hGH-GOx) $\Delta i(A) \approx 3$ pA ir $\Delta i(C) \approx 10$ pA, (Au-SAM/m-anti-hGH/hGH/anti-hGH-GOx) $\Delta i(A) \approx 1$ pA ir $\Delta i(C) \approx 5$ pA (36-40 pav.). Šie eksperimentai patvirtino, kad aukščiau aprašyta metodika gali būti naudojama hGH elektrocheminiam aptikimui, naudojant SECM nekonkurencinį sluoksniuotosios imunofermentinės analizės metodą ir GOx pažymėtus aptikimo antikūnus (p-anti-hGH-GOx). Toliau tobulinant imobilizacijos metodus ir SECM elektrocheminius parametrus, turėtų būti įmanoma sukurti jautrų elektrocheminį imuninį tyrimą hGH aptikimui. Mūsų sistema galėjo aptikti apie 1 μg mL^{-1} hGH su GOx žymėtais anti-hGH ant aukso taškų ir KF.

Galiausiai imunofermentinis kompleksas buvo įvertintas kiekybiškai, naudojant matematinį modelį, kurio rezultatai pateikti histogramoje (43 pav.). Didžiausias KF generavimo greitis (J) buvo pastebėtas paviršiuje - Au-SAM/p-anti-hGH-GOx 100 nM $J(1) = 408$ mol s^{-1} cm^2, kitų paviršių srautas:

(2 – Au-SAM/p-anti-hGH-GOx 10 nM) J(2) = 170 mol s^{-1} cm^2, (3 – Au-SAM/hGH/p-anti-hGH-GOx) J(3) = 260 mol s^{-1} cm^{2}J (4 – Au-SAM/m-anti-hGH/hGH/p-anti-hGH-GOx) (4) = 176 mol s^{-1} cm^2. Šie KF generavimo greičio skaičiavimai buvo naudinga priemonė paviršiaus aktyvumui, imobilizacijos kokybei ir hGH koncentracijai nustatyti.

Šiuo tyrimu buvo parodyta perspektyvi imunojutiklio aspektų tyrimo metodika: ženklinimas, imobilizavimas, SECM elektrocheminės vizualizacijos sąlygos. SECM SG-TC sistema su KF buvo gauti kokybiniai ir apskaičiuoti kiekybiniai rezultatai žmogaus augimo antigenui aptikti, naudojant paženklintą žmogaus augimo antikūną su GOx. Šio tyrimo metodika gali būti pritaikyta daugeliui dominančių antigenų aptikimui.

IŠVADOS

1. Naudojant 25 μm UME ir 9,10-fenantrenchinoną (100 μM) dviguboje elektronų pernašos sistemoje su kalio fericianidu (5 mM) užregistruojamos didžiausios *Saccharomyces cerevisiae* ląstelių bioelektrocheminio aktyvumo srovės stiprio vertės (8.10 nA), negu naudojant kitus redokso tarpininkus: menadioną (6,65 nA), 1,4-benzochinoną (3,46 nA), 2,6-dichlorofenolindo-fenolio natrio druskos hidratą (1,01 nA), 1,10-fenantrolin 5,6-dioną (0,07 nA), fenazin metasulfatą (0,03 nA) ar viengubą sistemą su kalio fericianidu (0,20 nA).

2. Naudojant skirtingas pirolo koncentracijas (0,1/0,3/0,5 M) inkubaciniame tirpale 24 val. su imobilizuotomis *Saccharomyces cerevisiae* ląstelėmis ant Petri lėkštelės, registruojamos žemesnės elektros krūvio pernašos vertės (0,17/0,12/0,04 nA) negu su kontrole (0,34 nA), tiriant skenuojančiu elektrocheminiu mikroskopu ir taikant dvigubą 9,10-fenantrenchinono (100 μM) ir kalio fericianido (5 mM) redokso tarpininkų sistemą.

3. *Saccharomyces cerevisiae* ląstelės, imobilizuotos ant anglies veltinio elektrodo ir modifikuotos anglies nanovamzdeliais (0,5 mg 10 mL^{-1}) (1,85 mA) arba su polipirolu (0,3 M) (1,62 mA), pasižymi didesnėmis ir tarpusavyje panašiomis elektronų krūvio pernašos vertėmis, naudojant dvigubą redokso tarpininkų sistemą 9,10-fenantrenchinoną (100 μM) ir kalio fericianidą (5 mM), negu kontrolė (0,63 mA).

4. Polipirolo sintezė (0,03 M 4 dienas), panaudojant mikroorganizmus, padidina elektronų pernašą *Aspergillus niger* ląstelėse apie 10 kartų (nuo 0,18 μA iki 1,82 μA) ir *Rhizoctonia* species apie 4 kartus (nuo 0,02 μA iki 0,88 μA), tiriant amperometriškai, esant 300 mM gliukozės koncentracijai, 4,5 μL PD ant grafitinio strypo elektrodo ir 10 mM KF tirpale, palyginus su

kontrole; Tyrinėjant Skenuojančia elektrochemine mikroskopija, *Aspergillus niger* ląstelių registruotas srovės stipris pakyla 3 kartais: nuo 0,3 nA iki 0,86 nA, esant PQ (100 μM) ir KF (5 mM) tirpale, lyginant su kontrole.

5. Skenuojančios elektrocheminės mikroskopijos substrato generacijos – elektrodo detekcijos režimas gali būti naudojamas nustatyti žmogaus augimo hormoną (1 μg mL^{-1} Δi(hGH) = 5 pA) taikant nekonkurencinį sluoksniuotosios imunofermentinės analizės metodą , naudojant antikūnus prieš žmogaus augimo hormoną, žymėtus gliukozės oksidaze, kartu su kalio fericianidu, Registruoti re zultatai buvokiekybiškai įvertinti 400 mol s^{-1}cm^2 , naudojant matematinį modelį.

ACKNOWLEDGEMENT

Firstly, I would like to express my deep gratitude to my supervisor prof. habil. dr. Arūnas Ramanavičius and consultant dr. Inga Morkvėnaitė-Vilkončienė who have guided me through this challenging, yet fasacinating path and presented great scientific opportunities.

I am also grateful to my mentors: prof. (HP) dr. Almira Ramanavičienė, dr. Wojciech Nogala and dr. Etienne Mathieu who have provided me with knowledge and research opportunities.

I would like to thank all the members of the Physical Chemistry department, especially Lina, Urte, Vilma, Jūratė, Teresė, Šarūnas.

Also, I am blessed to have worked with many great colleagues, who I can now proudly call my friends: Inga, Tomas, Modestas, Ramūnas, Vilius, Katažyna and Antanas.

Finally, I am grateful for the love and support of my family and friends.

I appreciate each and everyone who has helped me in my journey.

Ačiū, kad padėjote man išpildyti svajonę.

CURRICULUM VITAE

Name, Surname	Aura Kisieliūtė
Date of birth	1991-06-08
E-mail	Aura.kisieliute@gmail.com

EDUCATION

2014-2016	M.Sc. Chemistry of Nanomaterials
	Vilnius Univesity
2010-2014	B.Sc. in Biochemistry
	Vilnius University

WORK EXPERIENCE

2021.01.04-04.30	Junior researcher
2020.03.19-11.30	„Glucose biofuel cells"
	Vilnius University
2019.08.01-11.26	Junior researcher
	„The development of sensor nanostructured coatings and sensor arrays"
	UAB ArsLab
2018.01.14-04.12	Junior researcher
	„Smart membranes for electrochemical devices"
	Center for Physical Sciences and technology
2017.10.01-	Senior specialist
2018.02.01	Vilnius University
2016.05.01-07.01	Chemistry teacher
	Vilnius Zemynos gymnasium
2015.01.19-06.19	Administrator
	UAB Ausila Skypark

TRAINING

2020.09.03-17	Internship in Institute of Physical Chemistry, Polish
2020.03.02-17	Academy of Sciences,
2019.07.06-09.08	Warsaw, Poland
2018.03.12-07.13	Internship in Laboratory of Physical Chemistry and Microbiology for the Environment, Lorraine University,
	Nancy, France
2017.10.08-15	Secondment to Canakkale Onsekiz Mart University, Canakkale, Turkey

ACADEMIC CONFERENCES

Author

1. A. Kisieliute, I. Morkvenaite Vilkonciene, A. Popov, B. Brasiunas, A. Ramanaviciene, A. Ramanavicius;
   "Structures of Human Growth Antibodies Studied by Scanning Electrochemical Microscopy"
   Advanced Materials and Technologies, Palanga 2020

2. A. Kisieliute , J. Petroniene, I. Morkvenaite -Vilkonciene, W. Nogala, A. Popov,B. Brasiunas, A. Ramanaviciene, A. Ramanavicius,
   "Scanning Electrochemical Microscopy for the Investigation of Layered Structures Based on Human Growth Hormone Antibodies labelled with Glucose Oxidase"
   SECM-10 Workshop, Prancūzija Paryžius, 2019

3. A. Kisieliute , J. Petroniene, I. Morkvenaite -Vilkonciene, W. Nogala, A. Popov,B. Brasiunas, A. Ramanaviciene, A. Ramanavicius,
   "Study of Human Growth Hormone Antibody Layered Structures with Scanning Electrochemical Microscopy"
   9th International Workshop on Surface Modification for Chemical and Biochemical Sensing, Lenkija Varšuva, 2019

4. A. Kisieliute , V. Aukscionis, A. Zinovicius, A. Ramanavicius
   "An Electrochemical Evaluation of Electron Transfer in Biocomposite Based on Polypyrrole, Carbon Nanotubes and Saccharomyces Cerevisiae"
   1st International Congress on Analytical and Bioanalytical Chemistry, Antalija Turkija, 2019

5. A. Kisieliute , V. Aukscionis, A. Zinovicius, A.Ramanavicius
   "Biocomposite with Polypyrrole, Carbon Nanotubes and Saccharomyces Cerevisiae Electrochemical Investigation"
   The 77th International Scientific Conference of the University of Latvia, Ryga Latvija, 2019

6. A Kisieliute, V. Aukscionis, A. Zinovicius, A.Ramanavicius
   "Atomic Force Microscopy and Scanning Electron Microscopy for Imaging Modified Saccharomyces Cerevisiae Cells with Polypyrrole and Carbon Nanotubes"
   Advanced Materials and Technologies, Palanga 2019

7. A. Kisieliute , V. Aukscionis, M. Etienne, A. Ramanavicius

"Saccharomyces Cerevisiae in Biocomposite Design for Anode Modification"
IV International Conference Oxygenalia, Vilnius 2018

8. A. Kisieliute , V. Aukscionis, A. Zinovicius, A.Ramanavicius
"Electrochemical Response of Biocomposites Consisting of Saccharomyces Cerevisiae, Carbon Nanotubes and Polypyrrole for Anode Modification"
Advanced Materials and Technologies 2018, Palanga 2018

9. A. Kisieliute , S. el Kirat Chatel, M. Etienne, A.Ramanavicius
"Biocomposites with Polypyrrole for Bio-electrochemical Devices"
ElecNano8, International Conference on Electrochemistry in Nanoscience, Nancy 2018

10. A. Kisieliute , I. Morkvenaite-Vilkonciene, A. Popov, R. M. Apetrei, G. Carac, A. Ramanaviciene, A. Ramanavicius
"Evaluation of Bioelectrochemical Activity of Modified Aspergillus Niger Cells for the Improvement of Bioelectrochemical Systems"
Pittcon, Orlando 2017

11. A. Kisieliute, J. Petroniene, I. Morkvenaite-Vilkonciene, Ramanavicius A.
"Cyclic Voltammetry for Probing Redox Activity of *Saccharomyces cerevisiae*"
Advanced Materials and Technologies, Palanga 2017

12. A. Kisieliute, I. Morkvenaite –Vilkonciene, J. Petroniene, A. Popov, A. Ramanaviciene, A. Valiuniene, R.M. Apetrei, G. Carac, A. Ramanavicius
"Polypyroole-Modified Aspergillus Niger Cells for Microbial Fuel Cell/biosensor Electrochemical Systems"
60-oji tarptautinė konferencija Open Readings, Vilnius, 2017

13. A. Kisieliute, A. Ramanvicius
"Evaluation of Polypyrrole-Modified Cells by Scanning Electrochemical Microscopy"
Jaunųjų chemikų konferencija "Inovatyvioji ir tvarioji chemija" Puvočiai 2016

14. A. Kisieliute, A. Ramanavicius, I. Morkvenaite-Vilkonciene, J. Petroniene, A. Ramanaviciene
"*Saccharomyces cerevisiae* Cell Viability Determination by Hill's Function"
9th Internationl Nanoconference ¨Advances in Bioelectrochemistry and Nanomaterials¨2016 Vilnius

Co-Author

1. A. Ramanavicius, E. Andriukonis, V. Ratautaite, I. Baleviciute, N. German, A. Kausaite-Minkstimiene, S. Zukauskas, A. Kisieliute, A. Ramanaviciene
"Formation of Conducting Polymer based Structures Suitable for Sensor Design"
2 nd ICABC, Antalija, Turkija 2020

2. A. Ramanavicius, M. Gicevicius, P. Genys, S. Zukauskas, L. Sinkevicius, V. Aukscionis, A. Zinovicius, I. Morkvenaite-Vilkonciene , A. Valiūnienė , L. Mikoliunaite, J. Petroniene, E. Andriukonis, A. Kausaite, A. Kisieliute, U. Bubnienė, A. Ramanaviciene
„Sensors and Biosensors based on Conducting Polymers"
1st International Congress on Analytical and Bioanalytical Chemistry, Antalija Turkija, 2019

3. A. Ramanavicius, P. Genys, J. Petroniene, E. Andriukonis, A. Kausaite, A. Kisieliute, U. Bubnienė, A. Ramanaviciene
„Conducting Polymers Based Sensors And Biosensors Biocomposite"
The 77th International Scientific Conference of the University of Latvia, Ryga Latvija, 2019

4. V. Aukščionis, A. Zinovičius, A. Kisieliūtė, A. Ramanavičius;
„The Behaviours Of Different Electron Transfer Mediators In Measuring The Redox Activity Of Saccharomyces Cerevisiae"
Open Readings 62nd, Vilnius, Lietuva 2019

5. A. Zinovicius, A. Kisieliute, V. Aukščionis, I. Morkvėnaitė-Vilkončienė, A. Ramanavičienė, A, Ramanavičius;
„Application of Scanning Electrochemical Microscope for Immunosensor Electrochemical Activity"
Open Readings 62nd, Vilnius, Lietuva 2019

6. A. Zinovicius , V. Aukscionis, I. Morkvenaite-Vilkonciene, J. J. Petroniene, A. Kisieliute, N. Petrasauskiene, A. Kirdeikiene, R. Ramanauskas, A. Ramanavicius;
„Treatment of Yeast Cells by Electric Field"
Open readings, Vilnius 2018

7. V. Aukscionis , A. Zinovicius, A. Kisieliute, J. Petroniene, L. Mikoliunaite, I. Vilkonciene-Morkvenaite, A. Ramanavicius;

"Electrochemical Activity of Polypyrrole Modified *Saccharomyces cerevisiae"*

Open readings.Vilnius 2018

8. K. Bagdonas , A. Kisieliute, A. Ramanavicius;

   "Scanning Electrochemical Microscopy Investigation of a Glucose Biosensor Based on Glucose Oxidase and Carbon Nanotubes Arranged on the Polycarbonate Membrane Filters"

   Current Trends in Electrochemistry and Material Sciences 2017, Vilnius, 2017

9. J. Petroniene, A. Kisieliute, I. Morkvenaite-Vilkonciene, A. Ramanavicius

   „Evaluation of Quinone Toxity for Yeast *Saccharomyces cerevisiae* by Scanning Electrochemical Microscopy"

   Advanced Materials and Technologies, Palanga 2017

10. Ramanavicius A., Morkvenaite-Vilkonciene I., Sareikaite R., Kisieliute A., Genys P., Petroniene J., Ramanaviciene A;

    „Imaging of Immobilized Enzymes and Yeast Cells by Scanning Electrochemical Microscopy"

    Pittcon Atlanta, Georgia, USA 2016

LIST OF PUBLICATIONS

ARTICLE I

Scanning electrochemical microscopy based evaluation of influence of pH on bioelectrochemical activity of yeast cells− *Saccharomyces cerevisiae*.

A. Ramanavicius, I. Morkvenaite-Vilkonciene, A. Kisieliute, J. Petroniene, A. Ramanaviciene

ARTICLE II

Towards microbial biofuel cells: Improvement of charge transfer by self-modification of microoganisms with conducting polymer–Polypyrrole

A. Kisieliute, A. Popov, R. M. Apetrei, G. Cârâc, I. Morkvenaite-Vilkonciene, A. Ramanaviciene, A. Ramanavicius

ARTICLE III

Scanning electrochemical microscopy in the development of enzymatic sensors and immunosensors

I. Morkvenaite-Vilkonciene, A. Ramanaviciene, A. Kisieliute, V. Bucinskas, A. Ramanavicius

NOTES

NOTES

NOTES